



Air Quality Modeling Technical Support Document
for the Final
Cross State Air Pollution Rule Update

Office of Air Quality Planning and Standards
United States Environmental Protection Agency
August 2016

This page intentionally left blank

1. Introduction

In this technical support document (TSD) we describe the air quality modeling performed to support the final Cross State Air Pollution Rule for the 2008 ozone National Ambient Air Quality Standards (NAAQS)¹. In this document, air quality modeling is used to project ozone concentrations at individual monitoring sites to 2017² and to estimate state-by-state contributions to those 2017 concentrations. The projected 2017 ozone concentrations are used to identify ozone monitoring sites that are projected to be nonattainment or have maintenance problems for the 2008 ozone NAAQS in 2017. Ozone contribution information is then used to quantify projected interstate contributions from emissions in each upwind state to ozone concentrations at projected 2017 nonattainment and maintenance sites in other states (i.e., in downwind states).³

The remaining sections of this TSD are as follows. Section 2 describes the air quality modeling platform and the evaluation of model predictions using measured concentrations. Section 3 defines the procedures for projecting ozone design value concentrations to 2017 and the approach for identifying monitoring sites with projected nonattainment and/or maintenance problems. Section 4 describes (1) the source contribution (i.e., apportionment) modeling and (2) the procedures for quantifying contributions to individual monitoring sites including nonattainment and/or maintenance sites. Section 5 includes an analysis of the contributions captured at alternative thresholds. For questions about the information in this TSD please contact Norm Possiel at possiel.norm@epa.gov or (919) 541-5692. An electronic copy of the 2009 – 2013 base period and projected 2017 ozone design values and 2017 ozone contributions based on the final rule modeling can be obtained from docket for this rule. Electronic copies of the ozone design values and contributions can also be obtained at www.epa.gov/airtransport.

¹ The EPA revised the levels of the primary and secondary 8-hour ozone standards to 0.075 parts per million (ppm). 40 CFR 50.15. [73 FR 16436 \(March 27, 2008\)](https://www.ecfr.gov/current/title-40/chapter-I/subchapter-C/part-50/subpart-15/section-50.15).

² 2017 was selected as the future year analytic base case because 2017 corresponds to the attainment date for ozone nonattainment areas classified as Moderate.

³ The 2011-based modeling platform used for the final rule air quality modeling reflects revisions based on comments on the proposal modeling.

2. Air Quality Modeling Platform

EPA has developed a 2011-based air quality modeling platform which includes emissions, meteorology and other inputs for 2011. The 2011 base year emissions were projected to a future year base case scenario, 2017. The 2011 modeling platform and projected 2017 emissions were used to drive the 2011 base year and 2017 base case air quality model simulations.⁴ The base year 2011 platform was chosen in part because it represents the most recent, complete set of base year emissions information currently available for national-scale air quality modeling. In addition, as described below, the meteorological conditions during the summer of 2011 were generally conducive for ozone formation across much of the U.S., particularly the eastern U.S.

2.1 Air Quality Model Configuration

The photochemical model simulations performed for this ozone transport assessment used the Comprehensive Air Quality Model with Extensions (CAMx version 6.20) (Ramboll Environ, 2015)⁵. CAMx is a three-dimensional grid-based Eulerian air quality model designed to simulate the formation and fate of oxidant precursors, primary and secondary particulate matter concentrations, and deposition over regional and urban spatial scales (e.g., the contiguous U.S.). Consideration of the different processes (e.g., transport and deposition) that affect primary (directly emitted) and secondary (formed by atmospheric processes) pollutants at the regional scale in different locations is fundamental to understanding and assessing the effects of emissions on air quality concentrations. CAMx was applied with the carbon-bond 6 revision 2 (CB6r2) gas-phase chemistry mechanism⁶ (Ruiz and Yarwood, 2013) and the Zhang dry deposition scheme (Zhang, et al., 2003).

⁴ EPA also used the 2011-based air quality modeling platform to perform a 2017 “illustrative” control case air quality model simulation to inform (1) the analysis to quantify upwind state emissions that significantly contribute to nonattainment or interfere with maintenance of the NAAQS in downwind states and (2) the analysis of the costs and benefits of this proposed rule. The 2017 illustrative control case emissions and air quality modeling results are described in the Ozone Transport Policy Analysis Final Rule TSD and in the Regulatory Impact Assessment for the final rule.

⁵ For the proposal modeling EPA had used CAMx v6.11. For the final rule air quality modeling EPA used CAMx version 6.20 which was the latest public release version of CAMx available at the time the air quality modeling was performed for the final rule. In response to comments on the proposal, EPA used the default value for the “HMAX” time step parameter, as specified by the CAMx model developer Ramboll Environ, in the final rule air quality modeling.

⁶ The “chemparam.2_CF” chemical parameter file was used in the CAMx model simulations.

Figure 2-1 shows the geographic extent of the modeling domain that was used for air quality modeling in this analysis. The domain covers the 48 contiguous states along with the southern portions of Canada and the northern portions of Mexico. This modeling domain contains 25 vertical layers with a top at about 17,550 meters, or 50 millibars (mb), and horizontal grid resolution of 12 km x 12 km. The model simulations produce hourly air quality concentrations for each 12 km grid cell across the modeling domain.

CAMx requires a variety of input files that contain information pertaining to the modeling domain and simulation period. These include gridded, hourly emissions estimates and meteorological data, and initial and boundary concentrations. Separate emissions inventories were prepared for the 2011 base year and the 2017 base case. All other inputs (i.e. meteorological fields, initial concentrations, and boundary concentrations) were specified for the 2011 base year model application and remained unchanged for the future-year model simulations⁷.



Figure 2-1. Map of the CAMx modeling domain used for transport modeling.

⁷ The CAMx annual simulations for 2011 and 2017 were each performed using two time segments (January 1 through April 30, 2011 with a 10-day ramp-up period at the end of December 2010 and May 1 through December 31, 2011 with a 10-day ramp-up period at the end of April 2011). The CAMx 2017 contribution modeling was performed for the period May 1 through September 30, 2011 with a 10-day ramp-up period at the end of April 2011.

2.2 Characterization of 2011 Summer Meteorology

Meteorological conditions including temperature, humidity, winds, solar radiation, and vertical mixing affect the formation and transport of ambient ozone concentrations. Ozone is more readily formed on warm, sunny days when the air is stagnant. Conversely, ozone production is more limited on days that are cloudy, cool, rainy, and windy (<http://www.epa.gov/airtrends/weather.html>). Statistical modeling analyses have shown that temperature and certain other meteorological variables are highly correlated with the magnitude of ozone concentrations (Camalier, et al., 2007).

In selecting a year for air quality modeling it is important to simulate a variety of meteorological conditions that are generally associated with elevated air quality (U.S. EPA, 2014a). Specifically for ozone, modeled time periods should reflect meteorological conditions that frequently correspond with observed 8-hour daily maximum concentrations greater than the NAAQS at monitoring sites in nonattainment areas (U.S. EPA, 2014a). However, because of inter-annual variability in weather patterns it may not always be possible to identify a single year that will be representative of “typical” meteorological conditions favorable for ozone formation within each region of the U.S.

As part of the development of the 2011 modeling platform we examined the “ozone season” (i.e., May through September) temperature and precipitation regimes across the U.S. in 2011 compared to long-term, climatological normal (i.e., average) conditions⁸. Table A-1 in Appendix A describes the observed 2011 surface temperature anomalies (i.e., departure from normal) for each of the nine National Oceanic and Atmospheric Administration (NOAA) climate regions shown in Figure 2-2. The aggregate temperature and precipitation anomalies by state for the core summer months, June through August, of 2011 are shown in Figures A-1 and A-2, respectively. Overall, temperatures were warmer than normal during the summer of 2011 in nearly all regions, except for the West and Northwest. Record warmth occurred in portions of the South and Southwest regions. The summer months experienced below average precipitation for much of the southern and southeastern U.S., whereas wetter conditions than average were

⁸ Note that because of the relatively large inter-annual variability in certain meteorological conditions such as temperature and precipitation, “average” conditions, usually referred to as “normal” are often the mathematical mean of extremes and thus, “average” or “normal” values of temperature or precipitation should not necessarily be considered as being “typical”.

experienced in California and in several northern tier states. Extensive drought conditions occurred in portions of the southern Great Plains states. The warmer and dryer conditions were associated with a strong upper air ridge over the central U.S during the summer of 2011.

In addition to the above characterization of the ozone season meteorology in 2011, we also compared the temperature and precipitation regimes in 2011 to those in other individual years from 2005 through 2016⁹ for the eastern U.S. (see Appendix A for climate region temperature anomaly tables and state temperature and precipitation anomaly maps for each year in from 2005 through 2016). While warmer than the long-term average, 2011 summer temperatures in the eastern U.S. were comparable to those in several other recent years. The tables and maps in Appendix A indicate that 2005, 2006, 2007, 2010, 2012, and 2016 also featured above normal or much above normal temperatures across broad areas of the East. Thus, on a regional basis, temperatures in the summer of 2011 and therefore the temperature-related meteorological conduciveness for ozone formation, was not “unusual” compared to other summers over the most recent 12-year time period. Also of note is that temperatures during the summer months in 2008, 2009, 2013, 2014, and to a more limited extent 2015, were cooler than normal across broad portions of the eastern U.S. indicating that these years were generally unfavorable for ozone formation in the East. This was most notable during July 2014 when most states in the East recorded below average summer temperatures. Examining the precipitation anomaly maps in Figure A-2 indicates that while 2011 may have featured record or near record drought in the South and portions of the Southeast, other recent years featured near record drought in other regions (i.e., the Southeast in 2007 and the Upper Midwest in 2012).

The inter-annual variability in summer temperatures can also be analyzed by examining temporal patterns in “cooling degree days”. This metric is calculated as the sum of the difference between the daily mean temperature and a reference temperature of 65 degrees, which is used as an indicator of indoor comfort. Cooling degree days provide a measure of how much (in degrees), and for how long (in days), the outside air temperature was *above* a certain level. That is, cooling degree days is an estimate of the energy needed to cool a residence to a comfortable temperature. Higher values indicate warm weather and result in higher energy demand for cooling. Figure A-3 contains charts showing the temporal pattern in cooling degree

⁹ The data for the ozone season in 2016 is limited to May through July since July is the most recent month for which data are available for consideration in this rulemaking.

days from 1990 through 2015 for each of the climate regions in the East (i.e., the Northeast, Ohio Valley, Upper Midwest, and Southeast, and South regions). These charts indicate that there is considerable inter-annual variability in the magnitude in cooling degree days. Although the summer 2011 was above average in each climate region in the East, 2011 was not “extreme” compared to a number of the other years during this long-term record. Specific examples that illustrate this finding include:

- Upper Midwest: 2010 and 2012 had a greater number of cooling degree days than 2011
- Northeast: 2005 and 2010 had a greater number of cooling degree days than 2011
- Ohio Valley and Southeast: 2010 had a greater number of cooling degree days than 2011

However, in the South region the magnitude of cooling degree days was greater in 2011 than other years. In contrast, the more recent summers of 2013, 2014, and 2015 had much fewer cooling degree days in most of the eastern climate regions compared to 2011. In addition, the Southeast region had a below average number of cooling degree days in the summer of 2012.

Thus, the results of the analysis of summer average temperatures (above) and the analysis of summer cooling degree days (which is based on temperature) demonstrate that, on balance, the summer of 2011 was an appropriate year to choose for the air quality modeling for this rule in view of the following considerations: (1) based on temperature indicators, 2011 was generally conducive to ozone formation in all of the climate regions in the East, (2) 2011 was not the warmest summer since 2005, except in one of the eastern climate regions, and (3) other years since 2005 have been either warmer than 2011 in multiple eastern climate regions (i.e., 2010) or cooler than 2011, and thus potentially unconducive for ozone formation in one or more of the eastern climate regions (i.e., 2009, 2012, 2013, 2014, and 2015).

U.S. Climate Regions

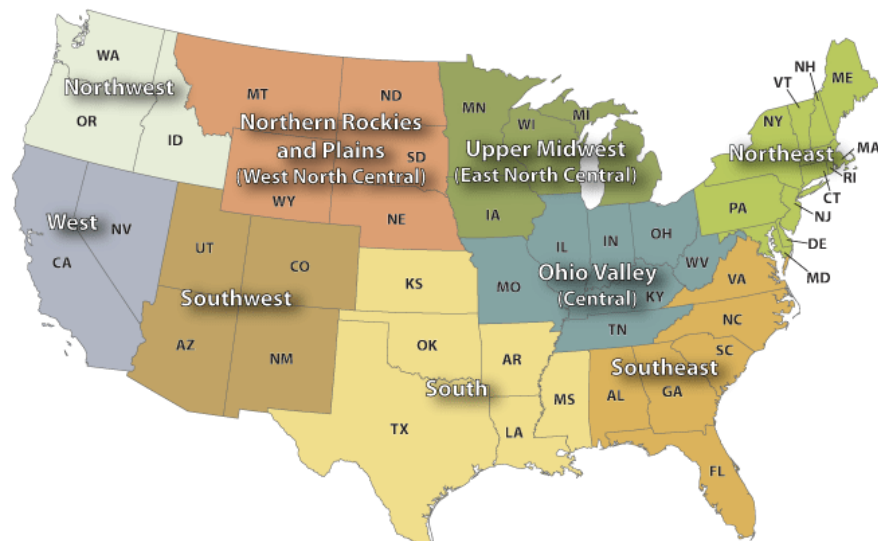


Figure 2-1. U.S. climate regions.

(<http://www.ncdc.noaa.gov/monitoring-references/maps/us-climate-regions.php>)

2.3 Meteorological Data for 2011

The meteorological data for air quality modeling of 2011 were derived from running Version 3.4 of the Weather Research Forecasting Model (WRF) (Skamarock, et al., 2008). The meteorological outputs from WRF include hourly-varying horizontal wind components (i.e., speed and direction), temperature, moisture, vertical diffusion rates, and rainfall rates for each grid cell in each vertical layer. Selected physics options used in the WRF simulation include Pleim-Xiu land surface model (Xiu and Pleim, 2001; Pleim and Xiu, 2003), Asymmetric Convective Model version 2 planetary boundary layer scheme (Pleim 2007a,b), Kain-Fritsch cumulus parameterization (Kain, 2004) utilizing the moisture-advection trigger (Ma and Tan, 2009), Morrison double moment microphysics (Morrison, et al., 2005; Morrison and Gettelman, 2008), and RRTMG longwave and shortwave radiation schemes (Iacono, et.al., 2008).

The WRF model simulation was initialized using the 12km North American Model (12NAM) analysis product provided by the National Climatic Data Center (NCDC). Where 12NAM data were unavailable, the 40km Eta Data Assimilation System (EDAS) analysis (ds609.2) from the National Center for Atmospheric Research (NCAR) was used. Analysis nudging for temperature, wind, and moisture was applied above the boundary layer only. The model simulations were conducted in 5.5 day blocks with soil moisture and temperature carried

from one block to the next via the “ipxwrf” program (Gilliam and Pleim, 2010). Landuse and land cover data were based on the 2006 National Land Cover Database (NLCD2006) data.¹⁰ Sea surface temperatures at 1 km resolution were obtained from the Group for High Resolution Sea Surface Temperatures (GHRSSST) (Stammer, et al., 2003). As shown in Table 2-2, the WRF simulations were performed with 35 vertical layers up to 50 mb, with the thinnest layers being nearest the surface to better resolve the planetary boundary layer (PBL). The WRF 35-layer structure was collapsed to 25 layers for the CAMx air quality model simulations, as shown in Table 2-2.

Table 2-2. WRF and CAMx layers and their approximate height above ground level.

CAMx Layers	WRF Layers	Sigma P	Pressure (mb)	Approximate Height (m AGL)
25	35	0.00	50.00	17,556
	34	0.05	97.50	14,780
24	33	0.10	145.00	12,822
	32	0.15	192.50	11,282
23	31	0.20	240.00	10,002
	30	0.25	287.50	8,901
22	29	0.30	335.00	7,932
	28	0.35	382.50	7,064
21	27	0.40	430.00	6,275
	26	0.45	477.50	5,553
20	25	0.50	525.00	4,885
	24	0.55	572.50	4,264
19	23	0.60	620.00	3,683
18	22	0.65	667.50	3,136
17	21	0.70	715.00	2,619
16	20	0.74	753.00	2,226
15	19	0.77	781.50	1,941
14	18	0.80	810.00	1,665
13	17	0.82	829.00	1,485
12	16	0.84	848.00	1,308
11	15	0.86	867.00	1,134
10	14	0.88	886.00	964
9	13	0.90	905.00	797

¹⁰ The 2006 NLCD data are available at http://www.mrlc.gov/nlcd06_data.php

CAMx Layers	WRF Layers	Sigma P	Pressure (mb)	Approximate Height (m AGL)
	12	0.91	914.50	714
8	11	0.92	924.00	632
	10	0.93	933.50	551
7	9	0.94	943.00	470
	8	0.95	952.50	390
6	7	0.96	962.00	311
5	6	0.97	971.50	232
4	5	0.98	981.00	154
	4	0.99	985.75	115
3	3	0.99	990.50	77
2	2	1.00	995.25	38
1	1	1.00	997.63	19

Details of the annual 2011 meteorological model simulation and evaluation are provided in a separate technical support document (US EPA, 2014b) which can be obtained at http://www.epa.gov/ttn/scram/reports/MET_TSD_2011_final_11-26-14.pdf

The meteorological data generated by the WRF simulations were processed using wrfcamx v4.3 (Ramboll Environ, 2014)¹¹ meteorological data processing program to create model-ready meteorological inputs to CAMx. In running wrfcamx, vertical eddy diffusivities (Kv) were calculated using the Yonsei University (YSU) (Hong and Dudhia, 2006) mixing scheme. We used a minimum Kv of 0.1 m²/sec except for urban grid cells where the minimum Kv was reset to 1.0 m²/sec within the lowest 200 m of the surface in order to enhance mixing associated with the nighttime “urban heat island” effect. In addition, we invoked the subgrid convection and subgrid stratoform cloud options in our wrfcamx run for 2011.

¹¹ For the proposal modeling EPA used wrfcamx version 4.0. For the final rule air quality modeling EPA used wrfcamx version 4.3 since this was the latest public release version of wrfcamx at the time the meteorological data were processed for the final rule air quality modeling.

2.4 Initial and Boundary Concentrations

The lateral boundary and initial species concentrations are provided by a three-dimensional global atmospheric chemistry model, GEOS-Chem (Yantosca, 2004) standard version 8-03-02 with 8-02-01 chemistry. The global GEOS-Chem model simulates atmospheric chemical and physical processes driven by assimilated meteorological observations from the NASA's Goddard Earth Observing System (GEOS-5; additional information available at: <http://gmao.gsfc.nasa.gov/GEOS/> and <http://wiki.seas.harvard.edu/geos-chem/index.php/GEOS-5>). This model was run for 2011 with a grid resolution of 2.0 degrees x 2.5 degrees (latitude-longitude). The predictions were used to provide one-way dynamic boundary concentrations at one-hour intervals and an initial concentration field for the CAMx simulations. The 2011 boundary concentrations from GEOS-Chem were used for the 2011 and 2017 model simulations. The procedures for translating GEOS-Chem predictions to initial and boundary concentrations are described elsewhere (Henderson, 2014). More information about the GEOS-Chem model and other applications using this tool is available at: <http://www-as.harvard.edu/chemistry/trop/geos>.

2.5 Emissions Inventories

CAMx requires detailed emissions inventories containing temporally allocated (i.e., hourly) emissions for each grid-cell in the modeling domain for a large number of chemical species that act as primary pollutants and precursors to secondary pollutants. Annual emission inventories for 2011 and 2017 were preprocessed into CAMx-ready inputs using the Sparse Matrix Operator Kernel Emissions (SMOKE) modeling system (Houyoux et al., 2000).¹² Information on the emissions inventories used as input to the CAMx model simulations can be found in the following emissions inventory technical support documents: Emissions Inventories for the Version 6.3, 2011 Emissions Modeling Platform (U.S. EPA, 2016) and 2011 National Emissions Inventory, version 2 (U.S. EPA, 2015).¹³

¹² The SMOKE output emissions case name for the 2011 base year is "2011ek_cb6v2_v6_11g" and the emissions case name for the 2017 base case is "2017ek_cb6v2_v6_11g".

¹³ Numerous revisions were made to the 2011 and 2017 emissions inventories for the final rule air quality modeling based on comments on the emissions data use for the proposal (see U.S. EPA, 2016).

2.6 Air Quality Model Evaluation

An operational model performance evaluation for ozone was conducted to examine the ability of the CAMx v6.20 modeling system to simulate 2011 measured concentrations. This evaluation focused on graphical analyses and statistical metrics of model predictions versus observations. Details on the evaluation methodology, the calculation of performance statistics, and results are provided in Appendix B. Overall, the ozone model performance statistics for the CAMx v6.20 2011 simulation are within or close to the ranges found in other recent peer-reviewed applications (e.g., Simon et al, 2012). As described in Appendix B, the predictions from the 2011 modeling platform correspond closely to observed concentrations in terms of the magnitude, temporal fluctuations, and geographic differences for 8-hour daily maximum ozone. Thus, the model performance results demonstrate the scientific credibility of our 2011 modeling platform. These results provide confidence in the ability of the modeling platform to provide a reasonable projection of expected future year ozone concentrations and contributions.

3. Identification of Future Nonattainment and Maintenance Receptors

3.1 Definition of Nonattainment and Maintenance Receptors

The approach in the final rule for identifying the 2017 nonattainment and maintenance receptors is described in the preamble. In brief, we are finalizing an approach for identifying nonattainment receptors in this rulemaking as those sites that are violating the NAAQS based on current measured air quality (i.e., 2013-2015 design values) and that also have projected 2017 average design values that exceed the NAAQS (i.e., 2017 average design values of 76 ppb or greater).¹⁴ We followed the approach in the CSAPR to identify sites that would have difficulty maintaining the 2008 ozone NAAQS in a scenario that takes into account historic variability in air quality at the monitoring site. In the CSAPR approach, monitoring sites with a 2017 maximum design value that exceeds the NAAQS, even if the 2017 average design value is below the NAAQS, are projected to have a maintenance problem in 2017. Monitoring sites with a 2017 average design value below the NAAQS, but with a maximum design value that exceeds the NAAQS, are considered maintenance-only sites. In addition, those sites that have projected 2017

¹⁴ In determining compliance with the NAAQS, ozone design values are truncated to integer values. For example, a design value of 75.9 ppb is truncated to 75 ppb which is attainment. In this manner, design values at or above 76.0 ppb are considered to be violations of the NAAQS.

average design values that exceed the NAAQS, but are currently measuring clean data based on 2013-2015 design values are also defined as maintenance-only receptors. Maintenance-only receptors therefore include both (1) those sites with projected average design values above the NAAQS that are currently measuring clean data and (2) those sites with projected average design values below the level of the NAAQS, but with projected maximum design values of 76 ppb or greater. In addition to the maintenance-only receptors, the 2017 ozone nonattainment receptors are also maintenance receptors because the maximum design values for each of these sites is always greater than or equal to the average design value. The procedures for calculating projected 2017 average and maximum design values are described below. The monitoring sites that we project to be nonattainment and maintenance receptors for the ozone NAAQS in the 2017 base case are used for assessing the contribution of emissions in upwind states to downwind nonattainment and maintenance of the 2008 ozone NAAQS as part of this final rule.

3.2 Approach for Projecting 2017 Ozone Design Values

The ozone predictions from the 2011 and 2017 CAMx model simulations were used to project ambient (i.e., measured) ozone design values (DVs) to 2017 following the approach described in EPA's current guidance for attainment demonstration modeling (US EPA, 2014a),¹⁵ as summarized here. The modeling guidance recommends using 5-year weighted average ambient design values¹⁶ centered on the base modeling year as the starting point for projecting average design values to the future. Because 2011 is the base emissions year, we used the average ambient 8-hour ozone design values for the period 2009 through 2013 (i.e., the average of design values for 2009-2011, 2010-2012 and 2011-2013) to calculate the 5-year weighted average design values. The 5-year weighted average ambient design value at each site was projected to 2017 using the Model Attainment Test Software program (Abt Associates, 2014). This program calculates the 5-year weighted average design value based on observed data and projects future year values using the relative response predicted by the model. Equation (3-1) describes the recommended model attainment test in its simplest form, as applied for monitoring site *i*:

¹⁵ EPA's ozone attainment demonstration modeling guidance is referred to as "the modeling guidance" in the remainder of this document.

¹⁶ The air quality design value for a site is the 3-year average of the annual fourth-highest daily maximum 8-hour average ozone concentration.

$$(DVF)_i = (RRF)_i * (DVB)_i \quad \text{Equation 3-1}$$

DVF_i is the estimated design value for the future year at monitoring site i ; RRF_i is the relative response factor for monitoring site i ; and DVB_i is the base period design value monitored at site i . The relative response factor for each monitoring site $(RRF)_i$ is the fractional change in 8-hour daily maximum ozone between the base and future year. The RRF is based on the average ozone on model-predicted “high” ozone days in grid cells in the vicinity of the monitoring site. The modeling guidance recommends calculating RRFs based on the highest 10 modeled ozone days in the base year simulation at each monitoring site. Specifically, the RRF was calculated based on the 10 highest days in the 2011 base year modeling in the vicinity of each monitor location.

As recommended by the modeling guidance, we considered model response in grid cells immediately surrounding the monitoring site along with the grid cell in which the monitor is located. The RRF was based on a 3 x 3 array of 12 km grid cells centered on the location of the grid cell containing the monitor. On each high ozone day, the grid cell with the highest base year ozone value in the 3 x 3 array surrounding the location of the monitoring site was used for both the base and future components of the RRF calculation (paired in space). In cases for which the base year model simulation did not have 10 days with ozone values greater than or equal to 60 ppb at a site, we used all days with ozone ≥ 60 ppb, as long as there were at least 5 days that meet that criteria. At monitor locations with less than 5 days with modeled 2011 base year ozone ≥ 60 ppb, no RRF or DVF was calculated for the site and the monitor in question was not included in this analysis.

The approach for calculating 2017 maximum design values is similar to the approach for calculating 2017 average design values. To calculate the 2017 maximum design value we start with the highest (i.e., maximum) ambient design value from the 2011-centered 5-year period (i.e., the maximum of design values from 2009-2011, 2010-2012, and 2011-2013). The base period maximum design value at each site was projected to 2017 using the site-specific RRFs, as determined using the procedures for calculating RRFs described above.

Table 3-1 contains the 2009-2013 base period average and maximum 8-hour ozone design values, the 2017 base case average and maximum design values, and the 2013-2015 design values for the 6 sites in the eastern U.S. projected to be 2017 nonattainment receptors. Table 3-2 contains this same information for the 13 maintenance-only sites in the eastern U.S.

The 2009-2013 base period and 2017 base case average and maximum design values for individual monitoring sites in the U.S. are provided in the docket.¹⁷

Table 3-1. Average and maximum 2009-2013 and 2017 base case 8-hour ozone design values and 2013-2015 design values (ppb) at projected nonattainment sites in the eastern U.S. (nonattainment receptors).

Monitor ID	State	County	Average Design Value 2009-2013	Maximum Design Value 2009-2013	Average Design Value 2017	Maximum Design Value 2017	2013-2015 Design Value
090019003	Connecticut	Fairfield	83.7	87	76.5	79.5	84
090099002	Connecticut	New Haven	85.7	89	76.2	79.2	78
480391004	Texas	Brazoria	88.0	89	79.9	80.8	80
484392003	Texas	Tarrant	87.3	90	77.3	79.7	76
484393009	Texas	Tarrant	86.0	86	76.4	76.4	78
551170006	Wisconsin	Sheboygan	84.3	87	76.2	78.7	77

¹⁷ There are 7 sites in 3 counties in the West that were excluded from this listing because the ambient design values at these sites were dominated by wintertime ozone episodes and not summer season conditions that are the focus of this transport assessment. High winter ozone concentrations that have been observed in certain parts of the Western U.S. are believed to result from the combination of strong wintertime inversions, large NO_x and VOC emissions from nearby oil and gas operations, increased UV intensity due to reflection off of snow surfaces and potentially still uncharacterized sources of free radicals. The 7 sites excluded from this analysis are in Rio Blanco County, CO (site ID 081030006), Fremont County, WY (site ID 560130099), and Sublette County, WY (site IDs 560350097, 560350099, 560350100, 560350101, and 560351002). Information on the analysis to identify these sites as influenced by wintertime ozone episodes can be found in Appendix 3A of the Regulatory Impact Analysis of the Proposed Revisions to the National Ambient Air Quality Standards for Ground-Level Ozone (EPA, 2014d) (<http://www.epa.gov/ttn/ecas/ria.html>)

Table 3-2. Average and maximum 2009-2013 and 2017 base case 8-hour ozone design values and 2013-2015 design values (ppb) at projected maintenance-only sites in the eastern U.S. (maintenance-only receptors).

Monitor ID	State	County	Average Design Value 2009-2013	Maximum Design Value 2009-2013	Average Design Value 2017	Maximum Design Value 2017	2013-2015 Design Value
090010017	Connecticut	Fairfield	80.3	83	74.1	76.6	81
090013007	Connecticut	Fairfield	84.3	89	75.5	79.7	83
211110067	Kentucky	Jefferson	85.0	85	76.9	76.9	N/A*
240251001	Maryland	Harford	90.0	93	78.8	81.4	71
260050003	Michigan	Allegan	82.7	86	74.7	77.7	75
360850067	New York	Richmond	81.3	83	75.8	77.4	74
361030002	New York	Suffolk	83.3	85	76.8	78.4	72
390610006	Ohio	Hamilton	82.0	85	74.6	77.4	70
421010024	Pennsylvania	Philadelphia	83.3	87	73.6	76.9	73
481210034	Texas	Denton	84.3	87	75.0	77.4	83
482010024	Texas	Harris	80.3	83	75.4	77.9	79
482011034	Texas	Harris	81.0	82	75.7	76.6	74
482011039	Texas	Harris	82.0	84	76.9	78.8	69

*The 2013-2015 design value at this site is not valid due to incomplete data for 2013. There are valid 4th high measured concentrations for 2014 and 2015 and therefore the site may have valid design value data when the 2014-2016 data are complete. The 2014 4th high value at this site was 70 ppb and the 2015 4th high value at this site was 76 ppb. In addition, there is one other monitoring site in Jefferson County, KY which has a valid 2013-2015 design value of 66 ppb. There is one other site in the Louisville CBSA which has a slightly higher 2013-2015 design value of 68 ppb (site 211850004 in Oldham County, KY). Since there are no valid design value data that indicate that the Jefferson County receptor or any other monitoring site in Jefferson County or the Louisville metropolitan area is currently exceeding the 2008 NAAQS, for the purposes of this final rule, the Jefferson County, KY receptor will be considered a maintenance receptor.

4. Ozone Contribution Modeling

4.1 Methodology

The EPA performed nationwide,¹⁸ state-level ozone source apportionment modeling using the CAMx OSAT/APCA technique¹⁹ (Ramboll Environ, 2015) to quantify the contribution of 2017 base case NO_x and VOC emissions from all sources in each state to projected 2017 ozone concentrations at ozone monitoring sites. In the source apportionment model run, we tracked the ozone formed from each of the following contribution categories (i.e., “tags”):

- States – anthropogenic NO_x and VOC emissions from each state tracked individually (emissions from all anthropogenic sectors in a given state were combined);

¹⁸ As shown in Figure 2-1, the EPA’s nationwide modeling includes the 48 contiguous states and the District of Columbia.

¹⁹ As part of this technique, ozone formed from reactions between biogenic VOC and NO_x with anthropogenic NO_x and VOC are assigned to the anthropogenic emissions.

- Biogenics – biogenic NO_x and VOC emissions domain-wide (i.e., not by state)²⁰;
- Boundary Concentrations – concentrations transported into the modeling domain;
- Tribes – the emissions from those tribal lands for which we have point source inventory data in the 2011 NEI (we did not model the contributions from individual tribes);
- Canada and Mexico – anthropogenic emissions from sources in the portions of Canada and Mexico included in the modeling domain (contributions from Canada and Mexico were not modeled separately);
- Fires – combined emissions from wild and prescribed fires domain-wide (i.e., not by state); and
- Offshore – combined emissions from offshore marine vessels and offshore drilling platforms (i.e., not by state).

The contribution modeling provided contributions to ozone from anthropogenic NO_x and VOC emissions in each state, individually. The contributions to ozone from chemical reactions between biogenic NO_x and VOC emissions were modeled and assigned to the “biogenic” category. The contributions from wild fire and prescribed fire NO_x and VOC emissions were modeled and assigned to the “fires” category. The contributions from the “biogenic”, “offshore”, and “fires” categories are not assigned to individual states nor are they included in the state contributions.

CAMx OSAT/APCA model run was performed for the period May 1 through September 30 using the projected 2017 base case emissions and 2011 meteorology for this time period. The hourly contributions²¹ from each tag were processed to calculate an 8-hour average contribution metric. The process for calculating the contribution metric uses the contribution modeling outputs in a “relative sense” to apportion the projected 2017 average design value at each monitoring location into contributions from each individual tag. This process is similar in concept to the approach described above for using model predictions to calculate 2017 ozone design values. The approach used to calculate the contribution metric is described by the following steps:

²⁰ Biogenic emissions and emissions from wild fires and prescribed fires were held constant between 2011 and 2017 since (1) these emissions are tied to the 2011 meteorological conditions and (2) the focus of this rule is on the contribution from anthropogenic emissions to projected ozone nonattainment and maintenance.

²¹ Contributions from anthropogenic emissions under “NO_x-limited” and “VOC-limited” chemical regimes were combined to obtain the net contribution from NO_x and VOC anthropogenic emissions in each state.

Step 1. Modeled hourly ozone concentrations are used to calculate the 8-hour daily maximum ozone (MDA8) concentration in each grid cell on each day.

Step 2. The gridded hourly ozone contributions from each tag are subtracted from the corresponding gridded hourly total ozone concentrations to create a “pseudo” hourly ozone value for each tag for each hour in each grid cell.

Step 3. The hourly “pseudo” concentrations from Step 2 are used to calculate 8-hour average “pseudo” concentrations for each tag for the time period that corresponds to the MDA8 concentration from Step 1. Step 3 results in spatial fields of 8-hour average “pseudo” concentrations for each grid cell for each tag on each day.

Step 4. The 8-hour average “pseudo” concentrations for each tag and the MDA8 concentrations are extracted for those grid cells containing ozone monitoring sites. We used the data for all days with 2017 MDA8 concentrations ≥ 76 ppb (i.e., projected 2017 exceedance days) in the downstream calculations. If there were fewer than five 2017 exceedance days at a particular monitoring site then the data from the top five 2017 MDA8 concentration days are extracted and used in the calculations.²²

Step 5. For each monitoring site and each tag, the 8-hour “pseudo” concentrations are then averaged across the days selected in Step 4 to create a multi-day average “pseudo” concentration for tag at each site. Similarly, the MDA8 concentrations were average across the days selected in Step 4.

Step 6. The multi-day average “pseudo” concentration and the corresponding multi-day average MDA8 concentration are used to create a Relative Contribution Factor (RCF) for each tag at each monitoring site. The RCF is the difference between the MDA8 concentration and the corresponding “pseudo” concentration, normalized by the MDA8 concentration.

Step 7. The RCF for each tag is multiplied by the 2017 average ozone design value to create the ozone contribution metrics for each tag at each site. Note that the sum of the contributions from each tag equals the 2017 average design value for that site.

Step 8. The contributions calculated from Step 7 are truncated to two digits to the right of the decimal (e.g., a calculated contribution of 0.78963... is truncated to 0.78 ppb). As a result of truncation the reported contributions may not always sum to the 2017 average design value.

²² If there were fewer than 5 days with a modeled 2017 MDA8 concentration ≥ 60 ppb for the location of a particular monitoring site, then contributions were not calculated at that monitor.

Table 4-1 provides an example of the calculation of contributions from two states (state A and state B) to a particular nonattainment site starting with Step 4, above. The table includes the daily “pseudo” concentrations for state A and state B and corresponding MDA8 ozone concentrations on those days with 2017 model-predicted exceedances at this site. The MDA8 ozone concentrations on these days are ranked-ordered in the table. The 2017 average design value for this example is 77.5 ppb. Using the data in Table 4-1, the RCF for state A and state B are calculated as:

$$(90.372 - 81.857) / 90.372 = 0.09422 \text{ for state A, and}$$

$$(90.372 - 90.163) / 90.372 = 0.00231 \text{ for state B}$$

The contributions from state A and state B to the 2017 average design value at this site are calculated as:

$$77.5 \times 0.09422 = 7.3020 \text{ which is truncated to 7.30 ppb for state A, and}$$

$$77.5 \times 0.00231 = 0.1790 \text{ which is truncated to 0.17 ppb for state B}$$

Table 4-1. Example calculation of ozone contributions (units are ppb).

Month	Day	Predicted MDA8 O3 on 2017 Modeled Exceedance Days	"Pseudo" 8-Hr O3 for State A	"Pseudo" 8-Hr O3 for State B
7	11	110.832	98.741	110.817
7	6	102.098	89.017	102.081
7	21	100.739	87.983	100.560
6	9	94.793	87.976	93.179
6	8	92.255	84.707	92.207
7	18	84.768	72.196	84.635
8	1	81.719	81.065	81.718
7	17	81.453	73.034	81.443
7	22	78.377	74.500	78.303
6	16	76.695	69.357	76.695
Multi-Day Average =>		90.372	81.857	90.163
2017 Average Design Value is 77.5 ppb		Relative Contribution Factors =>	0.09422	0.00231
		Contributions =>	7.3020	0.1790
		Truncated Contributions =>	7.30	0.17

The average contribution metric calculated in this manner is intended to provide a reasonable representation of the contribution from individual states to the projected 2017 design value, based on modeled transport patterns and other meteorological conditions generally associated with modeled high ozone concentrations in the vicinity of the monitoring site. This average contribution metric is beneficial since the magnitude of the contributions is directly related to the magnitude of the design value at each site.

4.2 Contribution Modeling Results

The contributions from each tag to individual nonattainment and maintenance-only sites in the East are provided in Appendix C. The largest contributions from each state to 2017 downwind nonattainment sites and to downwind maintenance-only sites are provided in Table 4-2. The 2017 contributions from each tag to individual monitoring sites across the U.S. are provided in the docket.

Table 4-2. Largest Contribution to Downwind 8-Hour Ozone Nonattainment and Maintenance Receptors for Each State in the Eastern U.S. (units are ppb).

Upwind State	Largest Downwind Contribution to Nonattainment Receptors	Largest Downwind Contribution to Maintenance Receptors
AL	0.99	0.73
AR	1.00	2.07
CT	0.00	0.46
DE	0.38	1.32
DC	0.07	0.86
FL	0.71	0.75
GA	0.60	0.62
IL	17.90	23.61
IN	6.49	12.32
IA	0.58	0.81
KS	1.13	1.22
KY	0.68	10.88
LA	3.01	3.20
ME	0.00	0.01
MD	2.12	5.22
MA	0.12	0.06
MI	2.62	1.27
MN	0.40	0.36

Upwind State	Largest Downwind Contribution to Nonattainment Receptors	Largest Downwind Contribution to Maintenance Receptors
MS	0.81	0.79
MO	1.67	3.78
NE	0.35	0.27
NH	0.02	0.02
NJ	9.52	11.90
NY	18.50	18.81
NC	0.51	0.50
ND	0.06	0.22
OH	1.83	3.78
OK	2.24	1.62
PA	9.28	14.61
RI	0.03	0.01
SC	0.15	0.30
SD	0.08	0.12
TN	0.50	1.82
TX	2.18	2.64
VT	0.01	0.01
VA	1.92	5.21
WV	1.04	3.31
WI	0.33	2.52

As discussed in the preamble, the EPA is establishing an air quality screening threshold calculated as one percent of the NAAQS. For this rule, the 8-hour ozone threshold is 0.75 ppb. This threshold is used to identify upwind states that contribute to downwind ozone concentrations in amounts sufficient to “link” them to these to downwind nonattainment and maintenance receptors.

States in the East whose contributions to a specific receptor meet or exceed the screening threshold are considered linked to that receptor; those states’ ozone contributions and emissions (and available emission reductions) are analyzed further, as described in the preamble, to determine whether and what emissions reductions might be required from each state. States in the East whose contribution to a specific receptor is below the screening threshold are not linked to that receptor and the EPA determines that such states do not significantly contribute to nonattainment or interfere with maintenance of the NAAQS at that downwind receptor.

Based on the maximum downwind contributions identified in Table 4-2, the following states contribute at or above the 0.75 ppb threshold to downwind nonattainment receptors: Alabama, Arkansas, Illinois, Indiana, Kansas, Louisiana, Maryland, Michigan, Mississippi, Missouri, New Jersey, New York, Ohio, Oklahoma, Pennsylvania, Texas, Virginia, and West Virginia. Based on the maximum downwind contributions in Table 4-2, the following states contribute at or above the 0.75 ppb threshold to downwind maintenance-only receptors: Arkansas, Delaware, District of Columbia, Florida, Illinois, Indiana, Iowa, Kansas, Kentucky, Louisiana, Maryland, Michigan, Mississippi, Missouri, New Jersey, New York, Ohio, Oklahoma, Pennsylvania, Tennessee, Texas, Virginia, West Virginia, and Wisconsin. The following states contribute below the threshold to all identified receptors: Connecticut, Georgia, Maine, Massachusetts, Minnesota, Nebraska, New Hampshire, North Carolina, North Dakota, Rhode Island, South Carolina, South Dakota, and Vermont.

4.4 Considerations for Florida

In the EPA's 2017 modeling for the final rule, Florida is modeled to have an average contribution at the 0.75 ppb threshold to the 2017 design values at two receptors in Houston (i.e., Harris County sites 482010024 and 482011034). However, a newer version of the CAMx chemical mechanism contains updated chemical reactions (halogen chemistry) which may have an impact on the estimated ozone contributions from Florida emissions to Houston receptors. In the final rule modeling, the EPA was not able to explicitly account for the updated chemistry because this chemistry had not yet been included by the model developer in the source apportionment tool in CAMx at the time the modeling was performed for this final rule. However, because Florida's maximum contribution to receptors in Houston is exactly at the 0.75 ppb threshold, the agency believes that if it had performed the final rule modeling with the updated halogen chemistry, Florida's contribution would likely be below this threshold. Therefore, the EPA is not including Florida in the final rule because it finds that Florida's contribution to downwind nonattainment and maintenance receptors is insignificant when this updated halogen chemistry is considered. More details and analysis of the impact of the CAMx halogen chemistry updates on the contributions from Florida and other Gulf Coast states can be found in Appendix D.

4.4 Upwind/Downwind Linkages

The linkages between upwind states and downwind nonattainment receptors and maintenance-only receptors in the eastern U.S. are provided by receptor site in Table 4-3 and by upwind state in Table 4-4 and Table 4-5.

Table 4-3. Upwind states that are “linked” to each downwind nonattainment and maintenance-only receptor in the eastern U.S.

Site	State	County	Linked Upwind States										
			MD	NJ	NY	OH	PA	VA	WV				
90010017	CT	Fairfield	MD	NJ	NY	OH	PA	VA	WV				
90013007	CT	Fairfield	IN	MD	MI	NJ	NY	OH	PA	VA	WV		
90019003	CT	Fairfield	IN	MD	MI	NJ	NY	OH	PA	VA	WV		
90099002	CT	New Haven	MD	NJ	NY	OH	PA	VA					
211110067	KY	Jefferson	IL	IN	MI	OH							
240251001	MD	Harford	DC	IL	IN	KY	MI	OH	PA	TX	VA	WV	
260050003	MI	Allegan	AR	IL	IN	IA	KS	MO	OK	TX	WI		
360850067	NY	Richmond	IN	KY	MD	NJ	OH	PA	VA	WV			
361030002	NY	Suffolk	IL	IN	MD	MI	NJ	OH	PA	VA	WV		
390610006	OH	Hamilton	IL	IN	KY	MI	MO	TN	TX	WV			
421010024	PA	Philadelphia	DE	IL	IN	KY	MD	NJ	OH	TN	TX	VA	WV
480391004	TX	Brazoria	AR	IL	LA	MS	MO						
481210034	TX	Denton	LA	OK									
482010024	TX	Harris	LA										
482011034	TX	Harris	LA	MO	OK								
482011039	TX	Harris	AR	IL	LA	MS	MO	OK					
484392003	TX	Tarrant	AL	KS	LA	OK							
484393009	TX	Tarrant	AL	LA	OK								
551170006	WI	Sheboygan	IL	IN	KS	LA	MI	MO	OK	TX			

Table 4-4. Linkages between each upwind state and downwind nonattainment receptors in the eastern U.S.

Upwind State	Downwind Nonattainment Receptors		
AL	Tarrant Co, TX (484392003)	Tarrant Co, TX (484393009)	
AR	Brazoria Co, TX (480391004)		
IL	Brazoria Co, TX (480391004)	Sheboygan Co, WI (551170006)	

Upwind State	Downwind Nonattainment Receptors		
IN	Fairfield Co, CT (090019003)	Sheboygan Co, WI (551170006)	
KS	Tarrant Co, TX (484392003)	Sheboygan Co, WI (551170006)	
LA	Brazoria Co, TX (480391004)	Tarrant Co, TX (484392003)	Tarrant Co, TX (484393009)
	Sheboygan Co, WI (551170006)		
MD	Fairfield Co, CT (090019003)	New Haven Co, CT (090099002)	
MI	Fairfield Co, CT (090019003)	Sheboygan Co, WI (551170006)	
MS	Brazoria Co, TX (480391004)		
MO	Brazoria Co, TX (480391004)	Sheboygan Co, WI (551170006)	
NJ	Fairfield Co, CT (090019003)	New Haven Co, CT (090099002)	
NY	Fairfield Co, CT (090019003)	New Haven Co, CT (090099002)	
OH	Fairfield Co, CT (090019003)	New Haven Co, CT (090099002)	
OK	Tarrant Co, TX (484392003)	Tarrant Co, TX (484393009)	Sheboygan Co, WI (551170006)
PA	Fairfield Co, CT (090019003)	New Haven Co, CT (090099002)	
TX	Sheboygan Co, WI (551170006)		
VA	Fairfield Co, CT (090019003)	New Haven Co, CT (090099002)	
WV	Fairfield Co, CT (090019003)		

Table 4-5. Linkages between each upwind states and downwind maintenance-only receptors in the eastern U.S.

Upwind State	Downwind Maintenance Receptors		
AR	Allegan Co, MI (260050003)	Harris Co, TX (482011039)	
DE	Philadelphia Co, PA (421010024)		
DC	Harford Co, MD (240251001)		
IL	Jefferson Co, KY (211110067)	Harford Co, MD (240251001)	Allegan Co, MI (260050003)
	Suffolk Co, NY (361030002)	Hamilton Co, OH (390610006)	Philadelphia Co, PA (421010024)
	Harris Co, TX (482011039)		
IN	Fairfield Co, CT (090013007)	Jefferson Co, KY (211110067)	Harford Co, MD (240251001)
	Allegan Co, MI (260050003)	Richmond Co, NY (360850067)	Suffolk Co, NY (361030002)
	Hamilton Co, OH (390610006)	Philadelphia Co, PA (421010024)	
IA	Allegan Co, MI (260050003)		
KS	Allegan Co, MI (260050003)		
KY	Harford Co, MD (240251001)	Richmond Co, NY (360850067)	Hamilton Co, OH (390610006)
	Philadelphia Co, PA (421010024)		
LA	Denton Co, TX (481210034)	Harris Co, TX (482010024)	Harris Co, TX (482011034)
	Harris Co, TX (482011039)		
MD	Fairfield Co, CT (090010017)	Fairfield Co, CT (090013007)	Richmond Co, NY (360850067)
	Suffolk Co, NY (361030002)	Philadelphia Co, PA (421010024)	
MI	Fairfield Co, CT (090013007)	Jefferson Co, KY (211110067)	Harford Co, MD (240251001)

Upwind State	Downwind Maintenance Receptors		
	Suffolk Co, NY (361030002)	Hamilton Co, OH (390610006)	
MS	Harris Co, TX (482011039)		
MO	Allegan Co, MI (260050003)	Hamilton Co, OH (390610006)	Harris Co, TX (482011034)
	Harris Co, TX (482011039)		
NJ	Fairfield Co, CT (090010017)	Fairfield Co, CT (090013007)	Richmond Co, NY (360850067)
	Suffolk Co, NY (361030002)	Philadelphia Co, PA (421010024)	
NY	Fairfield Co, CT (090010017)	Fairfield Co, CT (090013007)	
OH	Fairfield Co, CT (090010017)	Fairfield Co, CT (090013007)	Jefferson Co, KY (211110067)
	Harford Co, MD (240251001)	Richmond Co, NY (360850067)	Suffolk Co, NY (361030002)
	Philadelphia Co, PA (421010024)		
OK	Allegan Co, MI (260050003)	Denton Co, TX (481210034)	Harris Co, TX (482011034)
	Harris Co, TX (482011039)		
PA	Fairfield Co, CT (090010017)	Fairfield Co, CT (090013007)	Harford Co, MD (240251001)
	Richmond Co, NY (360850067)	Suffolk Co, NY (361030002)	
TN	Hamilton Co, OH (390610006)	Philadelphia Co, PA (421010024)	
TX	Harford Co, MD (240251001)	Allegan Co, MI (260050003)	Hamilton Co, OH (390610006)
	Philadelphia Co, PA (421010024)		
VA	Fairfield Co, CT (090010017)	Fairfield Co, CT (090013007)	Harford Co, MD (240251001)
	Richmond Co, NY (360850067)	Suffolk Co, NY (361030002)	Philadelphia Co, PA (421010024)
WV	Fairfield Co, CT (090010017)	Fairfield Co, CT (090013007)	Harford Co, MD (240251001)

Upwind State	Downwind Maintenance Receptors		
	Richmond Co, NY (360850067)	Suffolk Co, NY (361030002)	Hamilton Co, OH (390610006)
	Philadelphia Co, PA (421010024)		
WI	Allegan Co, MI (260050003)		

4.5 Corroboration of Upwind/Downwind Linkages

As a corollary analysis to the source apportionment air quality modeling used in this rule to establish upwind state-to-downwind nonattainment “linkages”, EPA used a technique involving independent meteorological inputs to examine the general plausibility of these linkages. Using the HYSPLIT (HYbrid Single-Particle Lagrangian Integrated Trajectory) model along with observation-based meteorological wind fields, EPA created air flow back trajectories for each of the 19 nonattainment or maintenance-only receptors on days with a measured exceedance in 2011 and in several other recent high ozone years (i.e., 2005, 2007, 2010, and 2012) at each of these sites. One focus of this analysis was on trajectories for exceedance days occurring in 2011, since this was the year of meteorology that was used for air quality modeling to support this rule. The results of this analysis indicate that for each receptor, back trajectories on certain exceedance days in 2011 passed over a portion of each upwind state linked to that receptor. This finding generally corroborates the linkages modeled for the final CSAPR Update.

A second focus of this analysis was to examine year-to-year differences in transport patterns over the multi-year time period. For this purpose we examined trajectories for exceedance days occurring in 2005, 2007, 2010, and 2012 which are other recent years with high ozone concentrations in the eastern U.S. Looking at these years collectively, EPA finds that for each receptor, the back trajectories crossed over a portion of each upwind state linked to the receptor upstream of days with measured exceedances at the receptor site. This finding suggests that the linkages established for this rule using the source-apportionment modeling with 2011 meteorology are robust with respect to the use of different meteorological years. Thus, the results of the trajectory analysis corroborate and add confidence to the upwind/downwind linkages in the final CSAPR Update. In addition, comparing the back trajectories on exceedance day in 2011 to those in the other four years analyzed indicates that high ozone day transport patterns that

occurred in 2011 are generally representative of the most prevalent transport patterns on exceedance days during these other high ozone years. Details of the back trajectory analysis are provided in Appendix E.

5. Analysis of Contributions Captured by Various Thresholds

In this section we present a summary of the amount of upwind contribution to each receptor in the eastern U.S. based on the 1 percent of the NAAQS threshold in comparison to the amount of contribution based on two other thresholds: 0.5 percent of the NAAQS and 5 percent of the NAAQS. This analysis is similar to the analysis of alternative thresholds performed for the original CSAPR rulemaking. The concentration associated with each of these thresholds, as used in this analysis, is given in Table 5-1.

Table 5-1. Concentrations associated with thresholds of 0.5 percent, 1 percent, and 5 percent.

0.5 Percent Threshold	1 Percent Threshold	5 Percent Threshold
0.375 ppb	0.75 ppb	3.75 ppb

For the analysis of thresholds we used the 2017 modeled contributions described above in section 4 to calculate several “metrics” (i.e., measures of contribution) for each receptor as listed in Table 5-2. In this table “x” refers to one of the thresholds included in this analysis, namely, 0.5 percent, 1 percent, and 5 percent.

Table 5-2. Contribution metrics used for the analysis of thresholds.

Threshold Analysis Metrics
In-State Contribution
Total Contribution from All Upwind States
Upwind Contribution as a Percent of Receptor 2017 Design Value
Upwind Contribution as a Percent of Total U.S. Anthropogenic Ozone at the Receptor
Number of Upwind States that Contribute at or Above “x” Percent Threshold
Total Contribution from Upwind States using a “x” Percent Threshold
Percent of Total Upwind Contribution Captured with “x” Percent Threshold

The method for calculating each of the metrics in Table 5-2 is as follows:

1. In-State Contribution

- Amount of contribution from emissions from the state in which the receptor is located.

2. Total Contribution from All Upwind States

- Sum of contributions from all upwind states, without consideration of any contribution threshold²³.

3. Upwind Contribution as a Percent of Receptor 2017 Design Value

- Ratio of total contribution from all upwind states (metric 2) divided by the design value (As noted above in section 4, the sum of all upwind state contributions, the in-state contribution, and the total contribution from background sources is equivalent to the 2017 average design value.)

4. Upwind Contribution as a Percent of Total U.S. Anthropogenic Ozone at the Receptor

- Ratio of total contribution from all upwind states (metric 2) divided by the sum of the in-state contribution (metric 1) and the total upwind state contributions (metric 2), expressed as a percent.

5. Number of Upwind States that Contribute At or Above “x” Percent Threshold

- Count of the number of upwind states that contribute amounts at or above the given threshold.

6. Total Contribution from Upwind States using a “x” Percent Threshold

- Sum of contributions from all upwind states the individually contribute at or above the given threshold.

7. Percent of Upwind Contribution Captured with “x” Percent Threshold

- Total contribution using an “x” percent threshold (metric 5) divided by the total contribution from all upwind states (metric 2), expressed as a percent.

Tables containing the data for each of the metrics for each nonattainment and maintenance receptor identified by this rulemaking at each of the analyzed thresholds are provided in Appendix F.

²³ Note that metrics 1 and 2 do not include contributions from fires, biogenics, offshore sources, or boundary conditions. Therefore, metrics 1 and 2 do not sum to the total average 2017 design value.

The data for metric 2 and metric 4 in Table F-1 indicate that the total amount of transport from all upwind states comprises a very large portion of the 8-hour ozone concentrations at the nonattainment and maintenance receptor sites in the eastern U.S. For example, the modeling results indicate that approximately 90 percent of the U.S. anthropogenic ozone concentration at some of the receptors in the New York City area and at the receptor in Allegan Co., MI is due to transport from upwind states. For the receptor in Sheboygan Co., WI, more than 75 percent of the U.S. anthropogenic ozone concentration is due to transport from upwind states. For receptors in Harford Co., MD, Hamilton Co., OH, Jefferson Co., KY, and Philadelphia Co., PA the portion of ozone that is due to upwind transport is in the range of 50 to 65 percent of anthropogenic ozone concentrations. In Dallas and Houston, transport is 20 to 30 percent of the total anthropogenic ozone at most receptors in these two areas. Thus, the total collective contribution from upwind state's sources represent a significant portion of the ozone concentrations at downwind nonattainment and maintenance receptor locations in the eastern U.S.

The data for metric 6 and metric 7 in Tables F-3 and F-4, respectively, further indicate that 0.5 percent and 5 percent are reasonable lower and upper alternatives for evaluating the 1 percent threshold for several reasons: (1) a 0.5 percent threshold would capture nearly all of the total amount of transport from upwind states at 12 of the 19 receptors (e.g., over 90 percent at seven receptors and between 85 and 90 percent at an additional five receptors), whereas (2) a 5 percent threshold would not capture any upwind transport at the seven receptors in Texas.

The data in Appendix F confirm that a 1 percent threshold is appropriate to identify those upwind states subject to further analysis for this final rule in that this threshold captures a significantly greater percentage of the total amount of upwind transport at most of the receptors compared to a 5 percent threshold (see metric 7 in Table F-4) while also capturing nearly all of the upwind transport that would be captured with a 0.5 percent threshold at most of receptors (see Table F-5). Specifically, the data for metric 7 in Table F-4 show that the 1 percent threshold captures between 34 percent and 64 percent of total upwind transport at the receptors in Texas that would be completely ignored with the higher 5 percent threshold. Because the percent of total upwind transport captured at a particular threshold declines as the threshold increases, thresholds between 1 and 5 percent (e.g., 2 and 3 percent) would also be expected to capture less of the total upwind transport at each receptor, particularly at the Texas receptors. In addition, the data in Table F-5 shows that the 1 percent threshold captures over 90 percent of the total upwind

transport that would be captured by a lower 0.5 percent threshold at nine receptors and between 85 and 90 percent of total transport that would captured by a 0.5 percent threshold at an additional five receptors. Although a lower 0.5 percent threshold would provide relatively modest increases in the overall percentage of ozone transport captured, the data for metric 5 in Table F-2 show that the lower threshold would result in significantly more linkages and would potentially add more states than the 1 percent threshold. The EPA does not believe that the additional upwind transport captured at this lower threshold is sufficient to merit linking additional upwind states because the air quality benefits would be limited. Thus, a 1 percent threshold provides an appropriate balance between alternative higher and lower thresholds.

In view of results of this analysis it is unlikely that examining other alternative thresholds beyond or between 0.5 percent and 5 percent would lead to a different conclusion that 1 percent is the appropriate threshold for this final rule. Further interpretation of the contribution summaries presented in Tables F-1 through F-5 with respect to decisions on the selection of thresholds for the final rule can be found in section IV.B.3 of the final rule preamble.

6. References

- Abt Associates, 2014. User's Guide: Modeled Attainment Test Software.
http://www.epa.gov/scram001/modelingapps_mats.htm
- Camalier, L., W. Cox, and P. Dolwick, 2007. The Effects of Meteorology on Ozone in Urban Areas and Their Use in Assessing Ozone Trends. *Atmospheric Environment*, **41**, 7127-7137.
- Gilliam, R.C. and J.E. Pleim, 2010. Performance Assessment of New Land Surface and Planetary Boundary Layer Physics in the WRF-ARW. *J. Appl. Meteor. Climatol.*, **49**, 760–774.
- Henderson, B.H., F. Akhtar, H.O.T. Pye, S.L. Napelenok, W.T. Hutzell, 2014. A Database and Tool for Boundary Conditions for Regional Air Quality Modeling: Description and Evaluations, *Geoscientific Model Development*, **7**, 339-360.
- Hong, S-Y, Y. Noh, and J. Dudhia, 2006. A New Vertical Diffusion Package with an Explicit Treatment of Entrainment Processes. *Mon. Wea. Rev.*, **134**, 2318–2341.
- Houyoux, M.R., Vukovich, J.M., Coats, C.J., Wheeler, N.J.M., Kasibhatla, P.S., 2000. Emissions Inventory Development and Processing for the Seasonal Model for Regional Air Quality (SMRAQ) project, *Journal of Geophysical Research – Atmospheres*, **105(D7)**, 9079-9090.
- Iacono, M.J., J.S. Delamere, E.J. Mlawer, M.W. Shephard, S.A Clough, and W.D. Collins, 2008. Radiative Forcing by Long-Lived Greenhouse Gases: Calculations with the AER Radiative Transfer Models, *J. Geophys. Res.*, **113**, D13103.
- Kain, J.S., 2004. The Kain-Fritsch Convective Parameterization: An Update, *J. Appl. Meteor.*, **43**, 170-181.
- Ma, L-M. and Tan Z-M, 2009. Improving the Behavior of Cumulus Parameterization for Tropical Cyclone Prediction: Convective Trigger, *Atmospheric Research*, **92**, 190-211.
- Morrison, H.J., A. Curry, and V.I. Khvorostyanov, 2005. A New Double-Moment Microphysics Parameterization for Application in Cloud and Climate Models. Part I: Description, *J. Atmos. Sci.*, **62**, 1665–1677.
- Morrison, H. and A. Gettelman, 2008. A New Two-Moment Bulk Stratiform Cloud Microphysics Scheme in the Community Atmosphere Model, version 3 (CAM3). Part I: Description and Numerical Tests, *J. Climate*, **21**, 3642-3659.
- Pleim, J.E. and A. Xiu, 2003. Development of a Land-Surface Model. Part II: Data Assimilation, *J. Appl. Meteor.*, **42**, 1811–1822
- Pleim, J.E., 2007a. A Combined Local and Nonlocal Closure Model for the Atmospheric Boundary Layer. Part I: Model Description and Testing, *J. Appl. Meteor. Climatol.*, **46**, 1383–1395.

- Pleim, J.E., 2007b. A Combined Local and Nonlocal Closure Model for the Atmospheric Boundary Layer. Part II: Application and Evaluation in a Mesoscale Meteorological Model, *J. Appl. Meteor. Climatol.*, **46**, 1396–1409.
- Ramboll Environ, 2015. User's Guide Comprehensive Air Quality Model with Extensions version 6.20, www.camx.com. Ramboll Environ International Corporation, Novato, CA.
- Ramboll Environ, 2014. wrfcamx version 4.0 Release Notes. May 06, 2013. www.camx.com. Ramboll Environ International Corporation, Novato, CA.
- Ruiz, L.H. and Yarwood, G., 2013. Interactions between Organic Aerosol and NO_y: Influence on Oxidant Production. Prepared for the Texas AQRP (Project 12-012), by the University of Texas at Austin, and Ramboll Environ International Corporation, Novato, CA. http://aqrp.ceer.utexas.edu/viewprojectsFY12-13.cfm?Prop_Num=12-012
- Skamarock, W.C., J.B. Klemp, J. Dudhia, et al., 2008. A Description of the Advanced Research WRF Version 3. NCAR Tech. Note NCAR/TN-475+STR. http://www.mmm.ucar.edu/wrf/users/docs/arw_v3.pdf
- Simon, H., K.R. Baker, and S.B. Phillips, 2012. Compilation and Interpretation of Photochemical Model Performance Statistics Published between 2006 and 2012, *Atmospheric Environment*, **61**, 124-139.
- Stammer, D., F.J. Wentz, and C.L. Gentemann, 2003. Validation of Microwave Sea Surface Temperature Measurements for Climate Purposes, *J. of Climate*, **16(1)**, 73-87.
- U.S. Environmental Protection Agency, 2014a. Modeling Guidance for Demonstrating Attainment of Air Quality Goals for Ozone, PM_{2.5}, and Regional Haze, Research Triangle Park, NC. (http://www.epa.gov/ttn/scram/guidance/guide/Draft_O3-PM-RH_Modeling_Guidance-2014.pdf)
- U.S. Environmental Protection Agency, 2014b. Meteorological Model Performance for Annual 2011 Simulation WRF v3.4, Research Triangle Park, NC. (<http://www.epa.gov/scram001/>)
- U.S. Environmental Protection Agency, 2015. 2011 National Emissions Inventory, version 2, Research Triangle Park, NC. (<https://www.epa.gov/air-emissions-inventories/2011-national-emissions-inventory-nei-documentation>)
- U.S. Environmental Protection Agency, 2016. Preparation of Emissions Inventories for the Version 6.3, 2011 Emissions Modeling Platform, Research Triangle Park, NC. (<https://www.epa.gov/air-emissions-modeling/2011-version-6-air-emissions-modeling-platforms>)
- Xiu, A., and J.E. Pleim, 2001, Development of a Land Surface Model. Part I: Application in a Meso scale Meteorological Model, *J. Appl. Meteor.*, **40**, 192-209.

Yantosca, B. 2004. GEOS-CHEMv7-01-02 User's Guide, Atmospheric Chemistry Modeling Group, Harvard University, Cambridge, MA.

Yarwood, G., J. Jung, O. Nopmongcol, and C. Emery, 2012. Improving CAMx Performance in Simulating Ozone Transport from the Gulf of Mexico. Prepared for the Texas Commission on Environmental Quality. September 2012. Ramboll Environ International Corporation, Novato, CA.

Yarwood, G., T. Sakulyanontvittaya, O. Nopmongcol, and B. Koo, 2014. Ozone Depletion by Bromine and Iodine over the Gulf of Mexico Final Report. Prepared for the Texas Commission on Environmental Quality. November 2014. Ramboll Environ International Corporation, Novato, CA.

Zhang, L., J. R. Brook, and R. Vet. 2003. A Revised Parameterization for Gaseous Dry Deposition in Air-Quality Models, *Atmos. Chem. Phys.*, **3**, 2067–2082.

This page intentionally left blank

Appendix A
Analysis of Meteorology in 2011

This page intentionally left blank

This appendix contains (1) tabular summaries of average temperature anomalies based on observed data for May through September by climate region for the 2005 through July 2016, (2) maps of the June through August statewide temperature and precipitation ranks and anomalies for the 2005 through July 2016, and (3) graphical summaries of the total number of cooling degree days for June, July, and August in each climate region of the eastern U.S. (i.e., Northeast, Ohio Valley, Upper Midwest, Southeast, and South) for the period 1990 through 2015.

Table A-1. Temperature anomalies by month for May through September for each climate region for the years 2005 through 2016.

2005	May	Jun	Jul	Aug	Sep
Northeast	CC	WW	W	WW	WW
Southeast	CC	N	W	WW	W
Ohio Valley	C	W	W	W	W
Upper Midwest	C	WW	W	N	WW
South	C	W	N	N	WW
Northern Rockies	C	N	W	N	W
Southwest	W	N	W	N	W
Northwest	W	C	WW	W	N
West	W	C	WW	W	N

Unshaded boxes with the “N” marker represent near-normal temperatures that fall within the interquartile range. Blue colors indicate cooler than normal conditions, with the number of “C”s indicating the degree of the anomaly. CCC = coolest on record, CC = coolest 10th percentile, C = coolest 25th percentile. Red colors indicate warmer than normal conditions, with the number of “W”s indicating the degree of the anomaly. WWW = warmest on record, WW = warmest 10th percentile, W = warmest 25th percentile. N/A = data not available.

2006	May	Jun	Jul	Aug	Sep
Northeast	N	W	WW	N	N
Southeast	N	N	W	WW	N
Ohio Valley	C	N	W	W	C
Upper Midwest	W	N	WW	W	C
South	W	W	W	N	C
Northern Rockies	W	W	WW	W	N
Southwest	WW	W	WW	N	CC
Northwest	W	WW	WW	N	N
West	W	WW	WWW	N	N

2007	May	Jun	Jul	Aug	Sep
Northeast	W	W	C	W	W
Southeast	N	N	C	WWW	W
Ohio Valley	W	W	C	WW	W
Upper Midwest	W	W	N	W	W
South	N	C	CC	W	W
Northern Rockies	W	W	WW	W	W
Southwest	W	W	WW	WWW	W
Northwest	W	W	WWW	N	N
West	W	W	WW	WW	N

2008	May	Jun	Jul	Aug	Sep
Northeast	C	W	W	C	N
Southeast	C	WW	N	C	N
Ohio Valley	C	W	C	C	N
Upper Midwest	C	N	N	N	W
South	N	W	N	C	CC
Northern Rockies	C	C	N	N	N
Southwest	N	W	W	W	N
Northwest	N	N	W	W	N
West	N	W	W	WW	W

2009	May	Jun	Jul	Aug	Sep
Northeast	N	C	CC	W	C
Southeast	N	W	CC	N	N
Ohio Valley	N	W	CC	C	N
Upper Midwest	N	C	CC	C	W
South	N	W	N	N	C
Northern Rockies	N	C	C	C	WW
Southwest	WW	C	W	W	W
Northwest	W	C	WW	W	WW
West	WW	C	W	N	WWW

2010	May	Jun	Jul	Aug	Sep
Northeast	WW	W	WW	W	W
Southeast	WW	WW	WW	WW	W
Ohio Valley	W	WW	W	WW	N
Upper Midwest	W	N	W	WW	C
South	W	WW	N	WW	W
Northern Rockies	C	N	N	W	N
Southwest	C	W	W	W	WWW
Northwest	CC	C	N	N	W
West	CC	W	W	N	W

2011	May	Jun	Jul	Aug	Sep
Northeast	W	W	WW	N	WW
Southeast	N	WW	WW	WW	N
Ohio Valley	N	W	WW	W	C
Upper Midwest	N	N	WW	W	N
South	N	WW	WWW	WWW	N
Northern Rockies	C	N	W	W	W
Southwest	C	W	WW	WWW	W
Northwest	CC	C	C	W	WW
West	C	C	N	W	WW

2012	May	Jun	Jul	Aug	Sep
Northeast	WW	N	WW	W	N
Southeast	WW	C	WW	N	N
Ohio Valley	WW	N	WW	N	C
Upper Midwest	W	W	WW	N	N
South	WW	W	WW	N	N
Northern Rockies	W	W	WW	W	W
Southwest	WW	WW	W	WW	W
Northwest	N	C	W	WW	W
West	W	W	N	WWW	WW

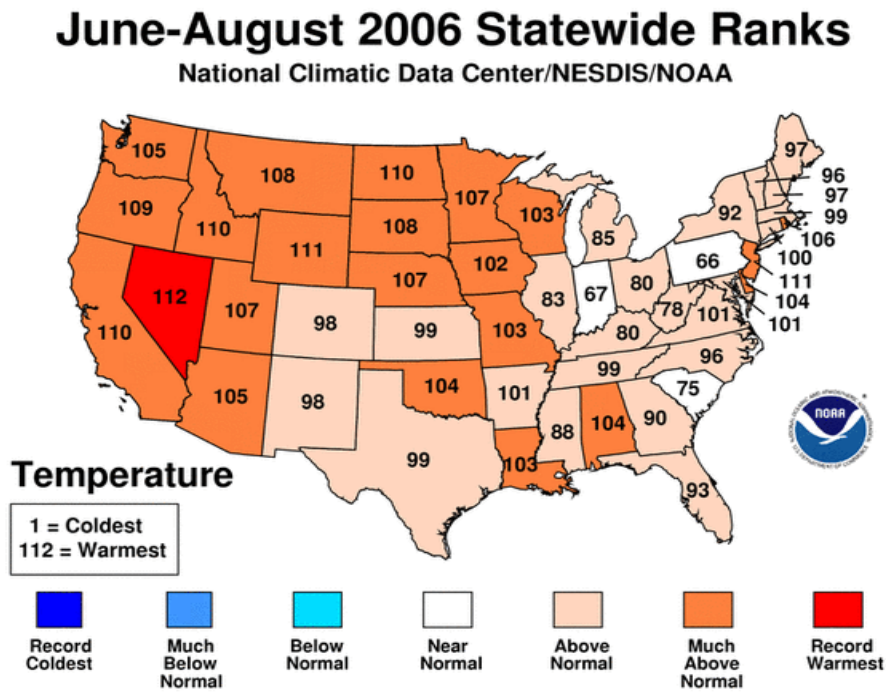
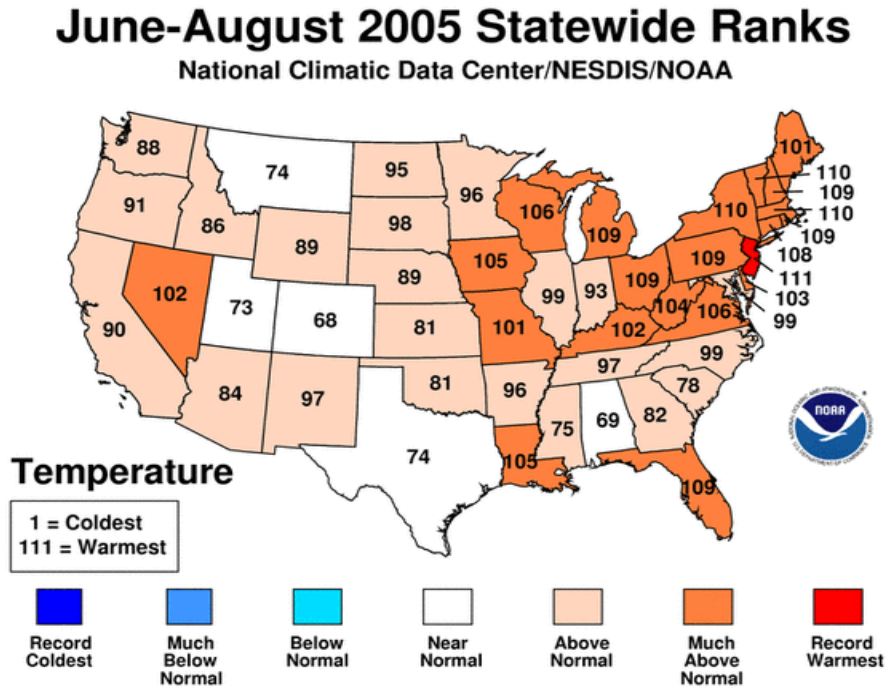
2013	May	Jun	Jul	Aug	Sep
Northeast	W	W	WW	N	N
Southeast	C	W	C	C	N
Ohio Valley	N	N	C	C	N
Upper Midwest	N	N	N	N	W
South	C	W	C	N	W
Northern Rockies	N	N	N	W	WW
Southwest	W	WW	W	W	W
Northwest	W	W	WW	WW	WW
West	W	WW	WW	N	W

2014	May	Jun	Jul	Aug	Sep
Northeast	W	W	N	N	W
Southeast	W	W	C	N	W
Ohio Valley	N	W	CC	N	N
Upper Midwest	N	W	CC	N	N
South	N	N	C	N	N
Northern Rockies	N	C	N	N	N
Southwest	N	W	W	C	WW
Northwest	W	N	WW	W	W
West	W	W	WW	N	WW

2015	May	Jun	Jul	Aug	Sep
Northeast	WWW	N	N	W	WW
Southeast	W	WW	W	N	N
Ohio Valley	W	W	N	C	W
Upper Midwest	N	N	N	N	WWW
South	C	N	W	N	WW
Northern Rockies	C	WW	N	N	WW
Southwest	C	WW	C	WW	WWW
Northwest	W	WWW	W	W	N
West	N	WWW	C	WW	WW

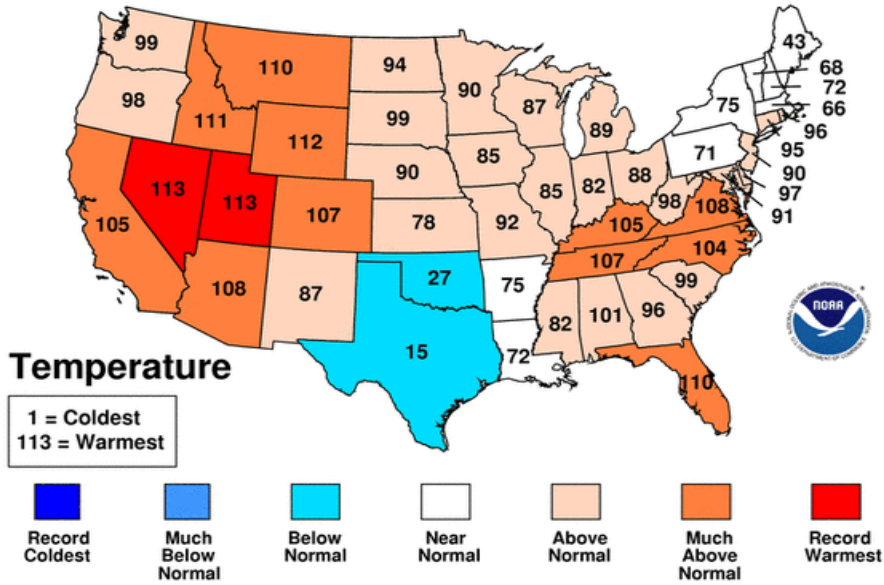
2016	May	Jun	Jul	Aug	Sep
Northeast	N	W	W	N/A	N/A
Southeast	N	W	WW	N/A	N/A
Ohio Valley	N	W	W	N/A	N/A
Upper Midwest	N	W	N	N/A	N/A
South	C	W	WW	N/A	N/A
Northern Rockies	N	WW	N	N/A	N/A
Southwest	C	WWW	WW	N/A	N/A
Northwest	W	WW	C	N/A	N/A
West	N	WW	W	N/A	N/A

Figure A-1. Statewide average temperature ranks for the period June through August for the years 2005 through 2016 (data for 2016 are only available for June and July).



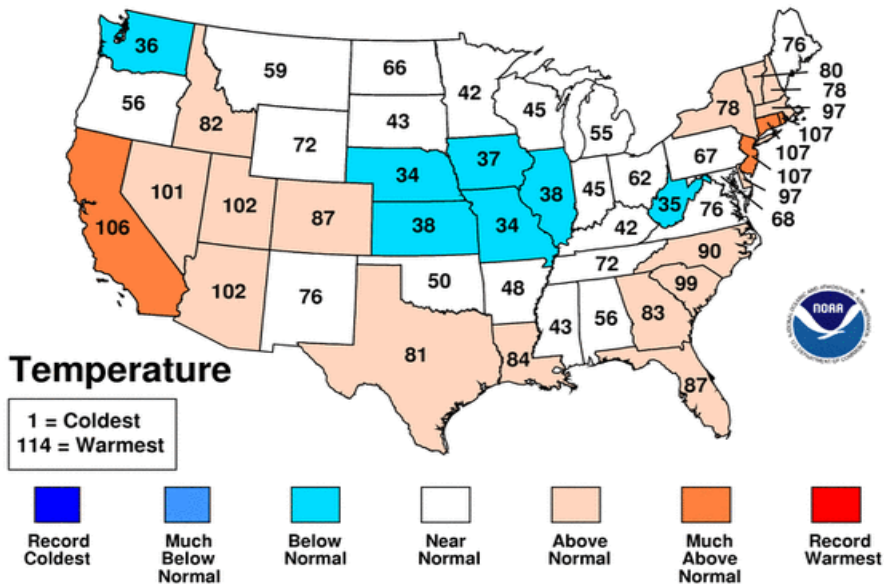
June-August 2007 Statewide Ranks

National Climatic Data Center/NESDIS/NOAA



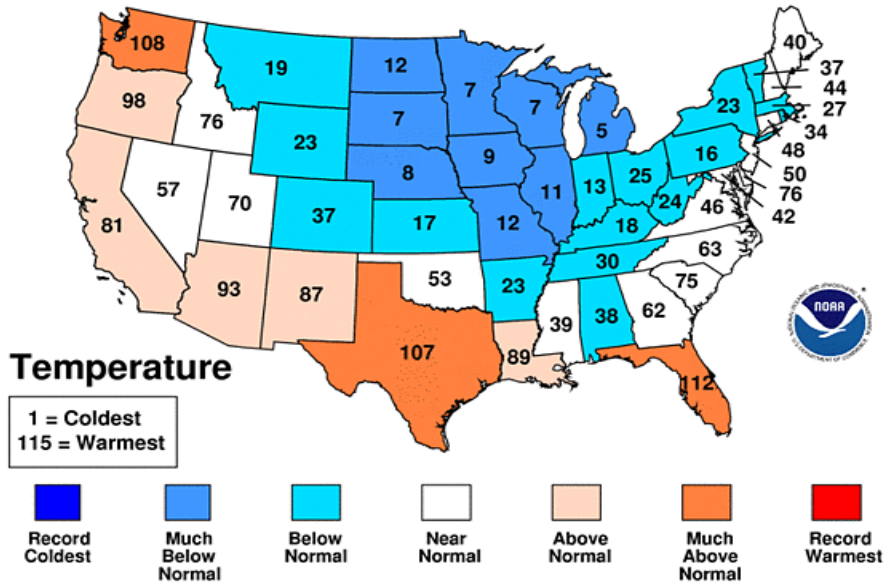
June-August 2008 Statewide Ranks

National Climatic Data Center/NESDIS/NOAA



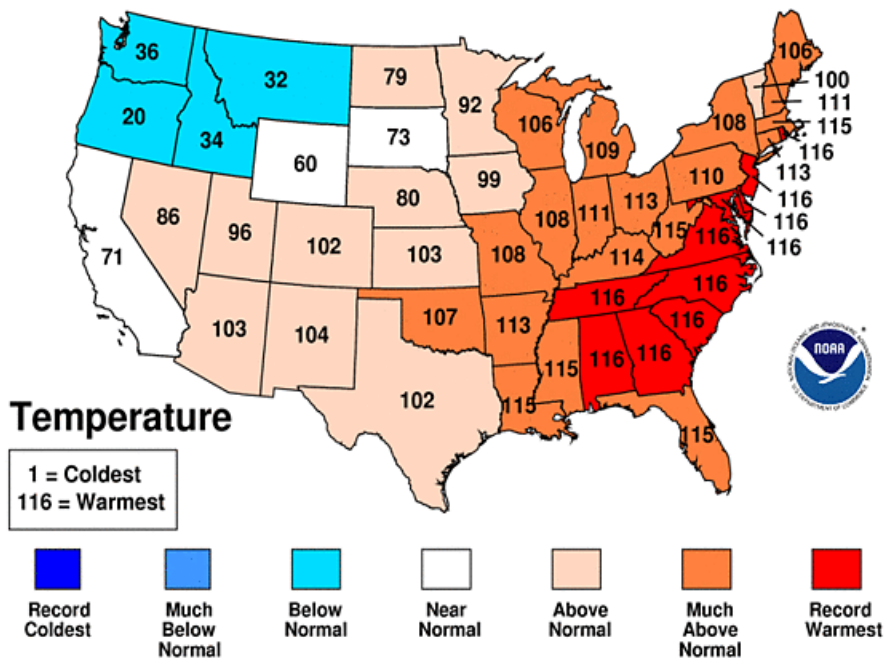
June-August 2009 Statewide Ranks

National Climatic Data Center/NESDIS/NOAA



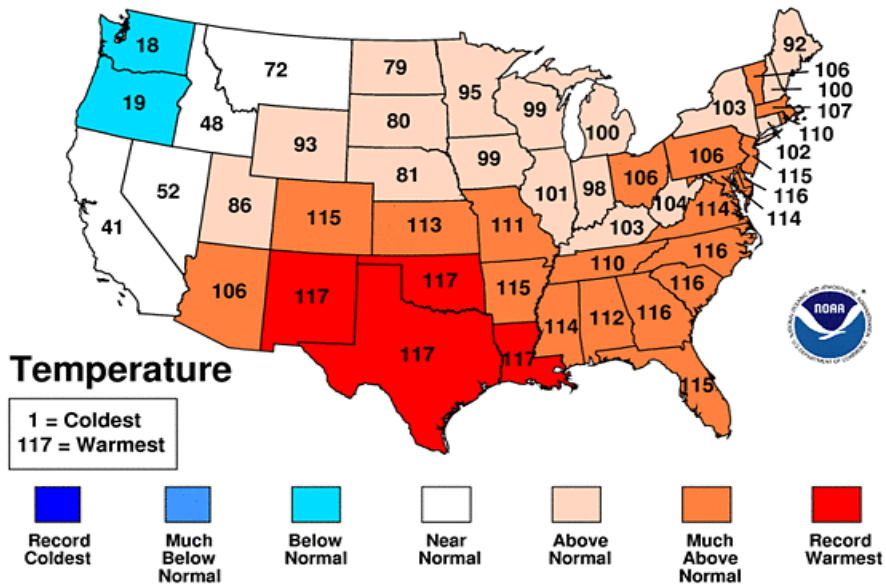
June-August 2010 Statewide Ranks

National Climatic Data Center/NESDIS/NOAA



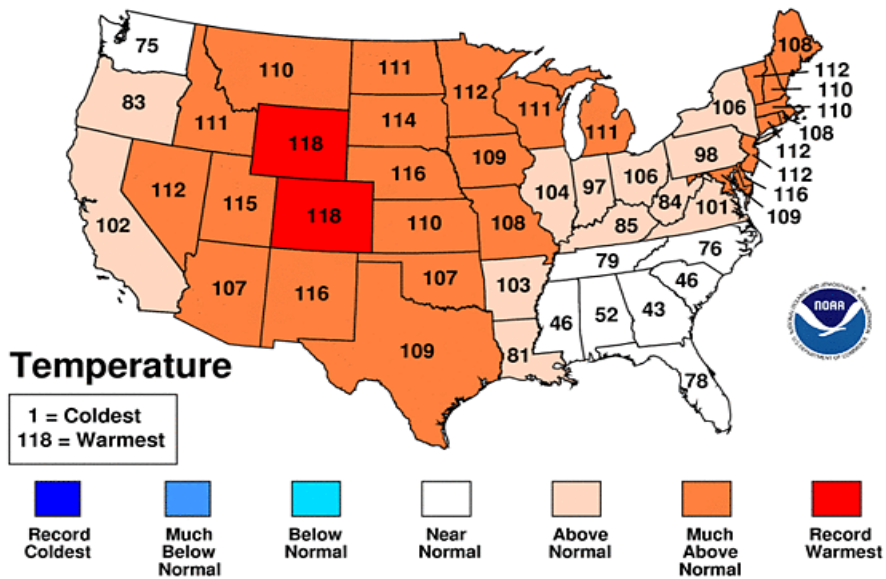
June-August 2011 Statewide Ranks

National Climatic Data Center/NESDIS/NOAA



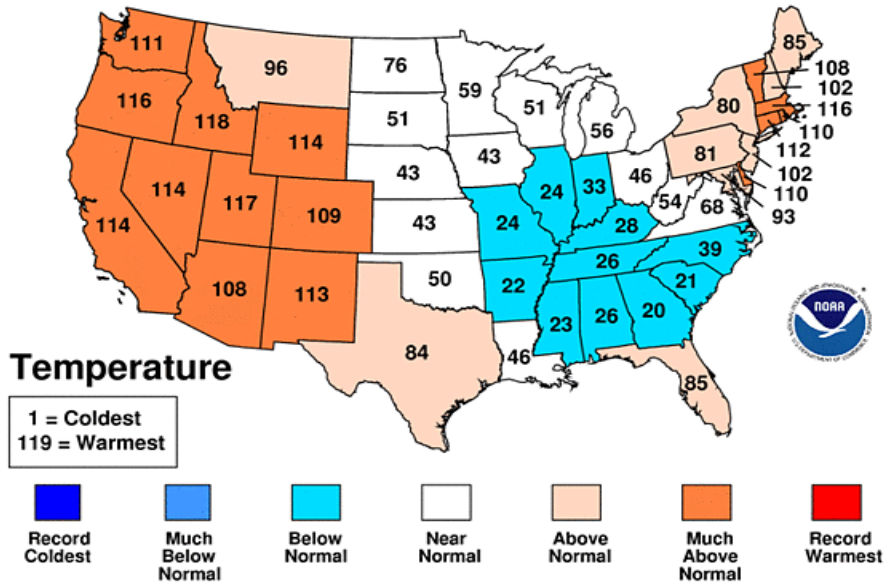
June-August 2012 Statewide Ranks

National Climatic Data Center/NESDIS/NOAA



June-August 2013 Statewide Ranks

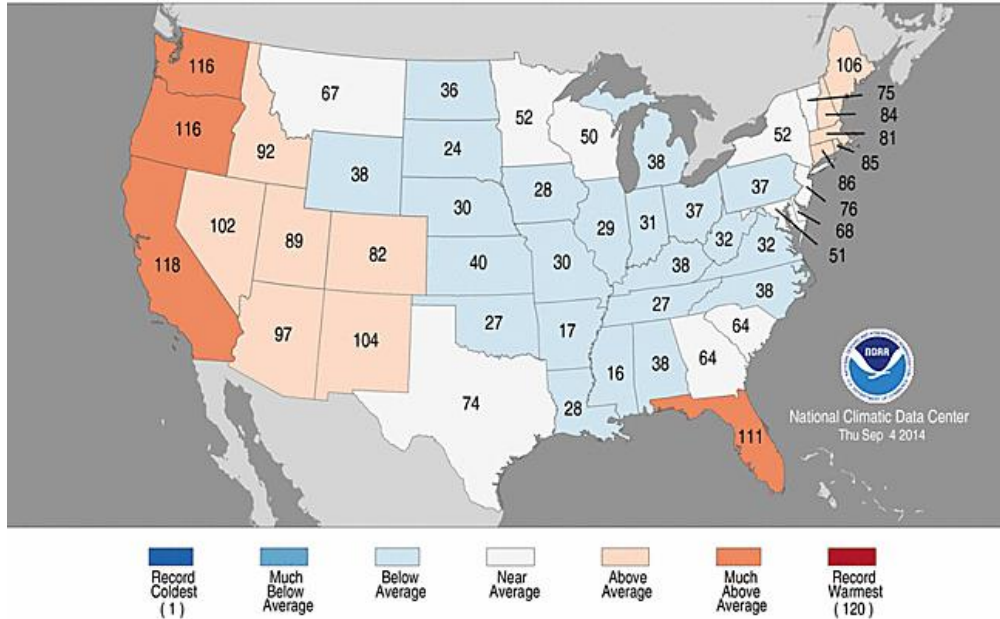
National Climatic Data Center/NESDIS/NOAA



Statewide Average Temperature Ranks

June-August 2014

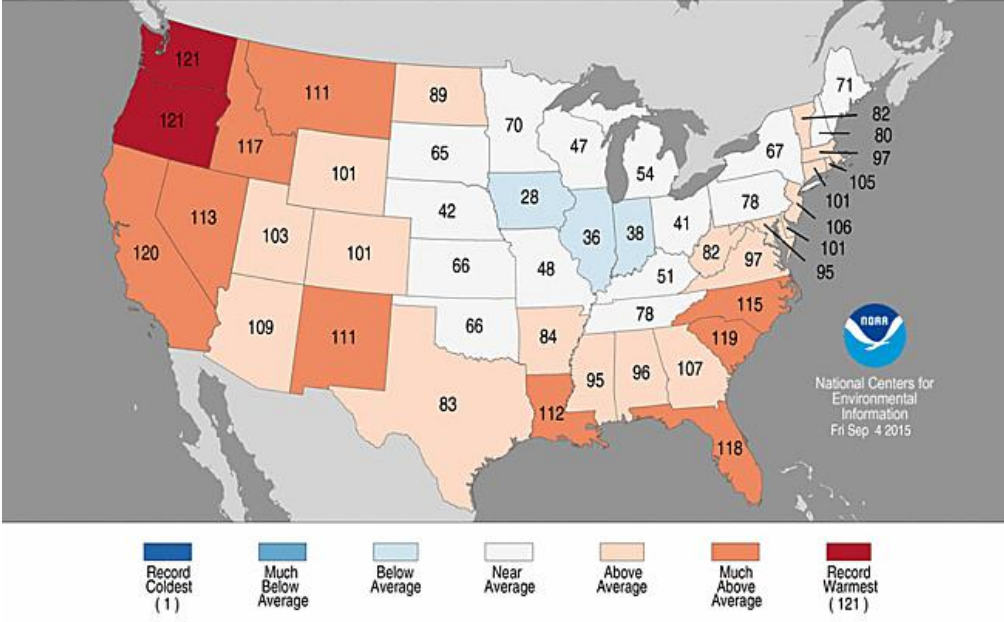
Period: 1895-2014



Statewide Average Temperature Ranks

June–August 2015

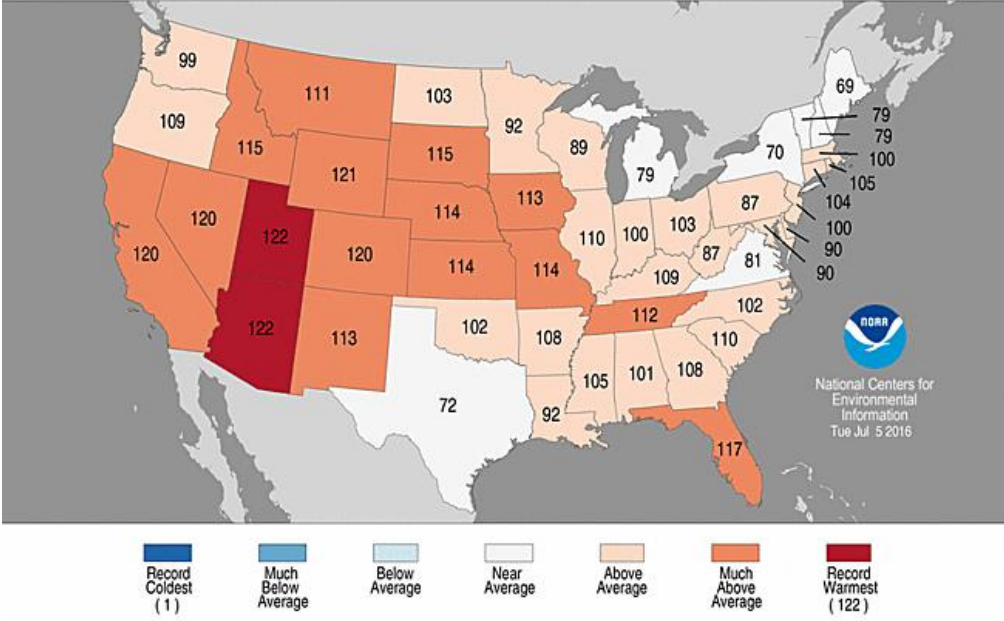
Period: 1895–2015



Statewide Average Temperature Ranks

June 2016

Period: 1895–2016



Statewide Average Temperature Ranks

July 2016

Period: 1895-2016

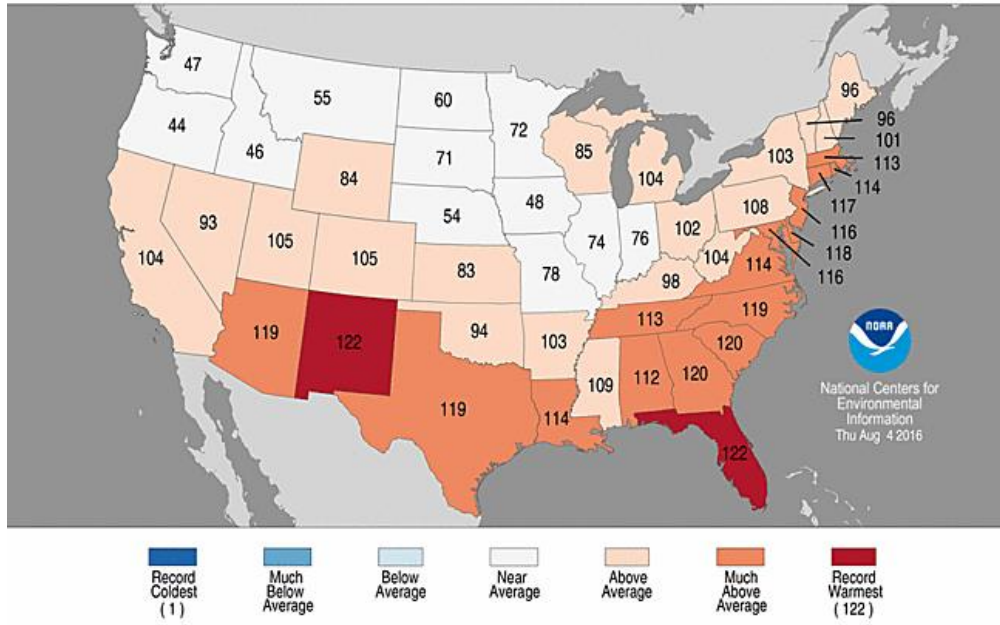
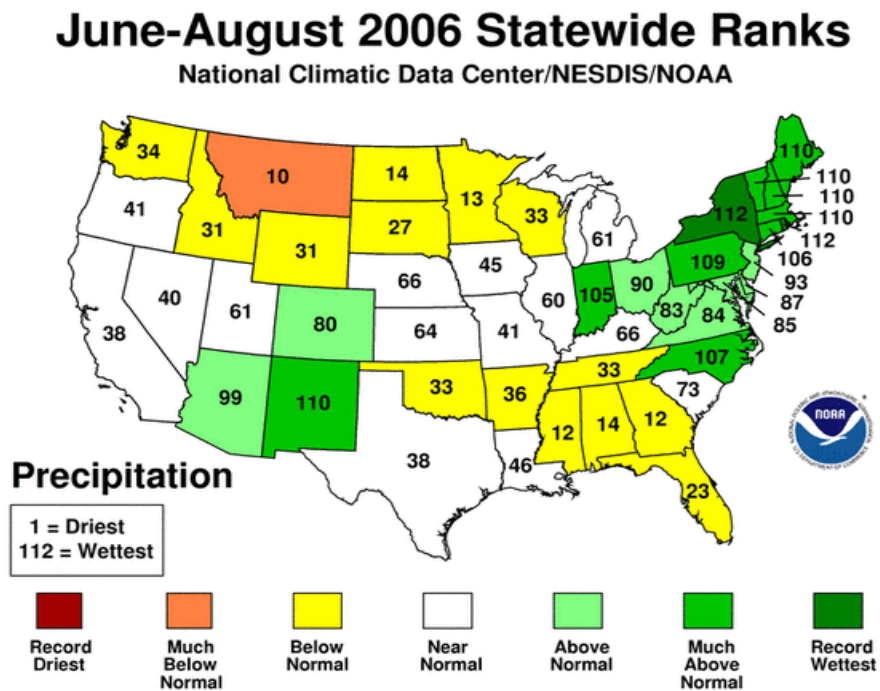
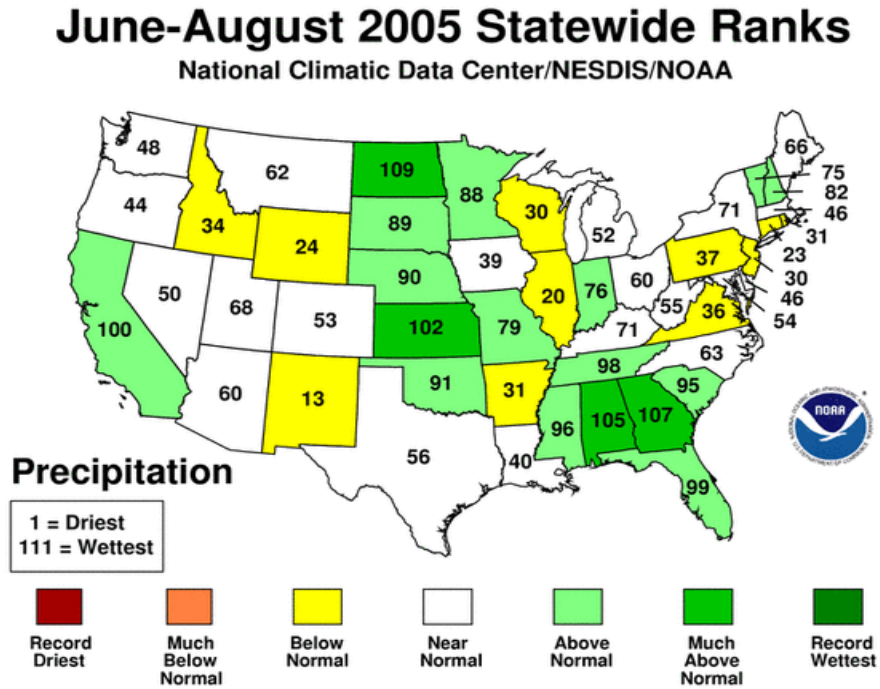
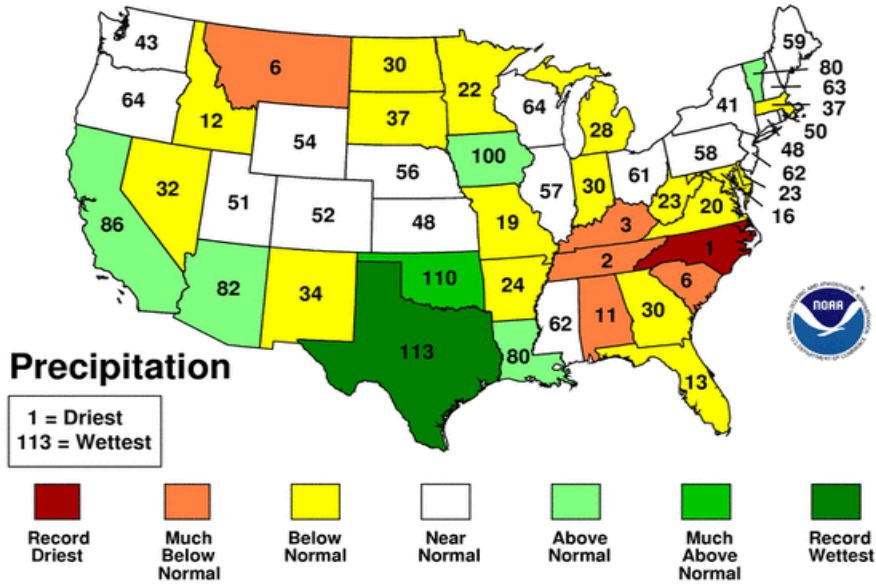


Figure A-2. Statewide average precipitation ranks for the period June through August for the years 2005 through 2016 (data for 2016 are only available for June and July).



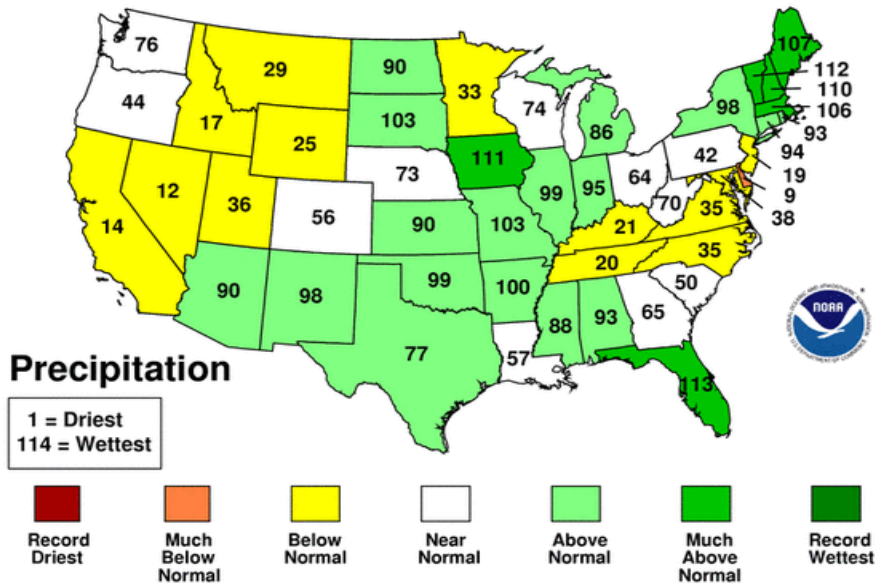
June-August 2007 Statewide Ranks

National Climatic Data Center/NESDIS/NOAA



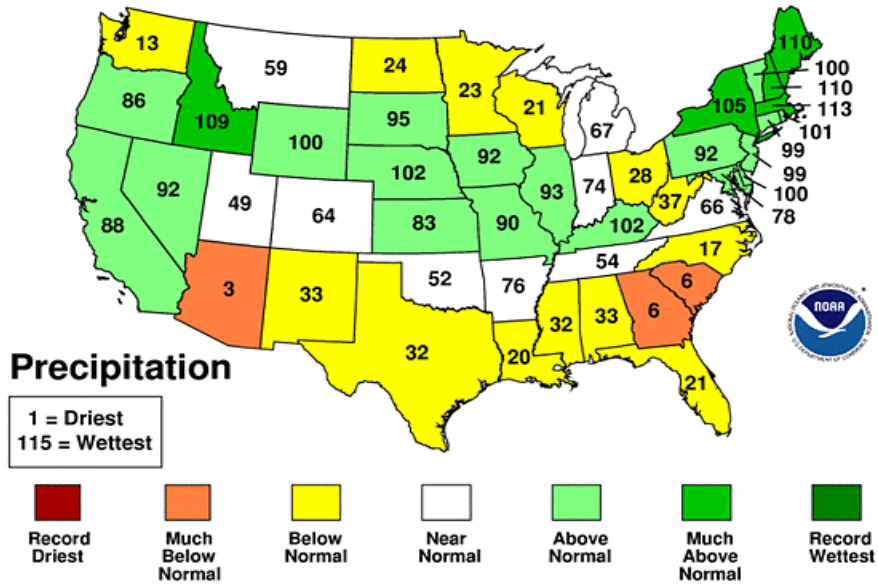
June-August 2008 Statewide Ranks

National Climatic Data Center/NESDIS/NOAA



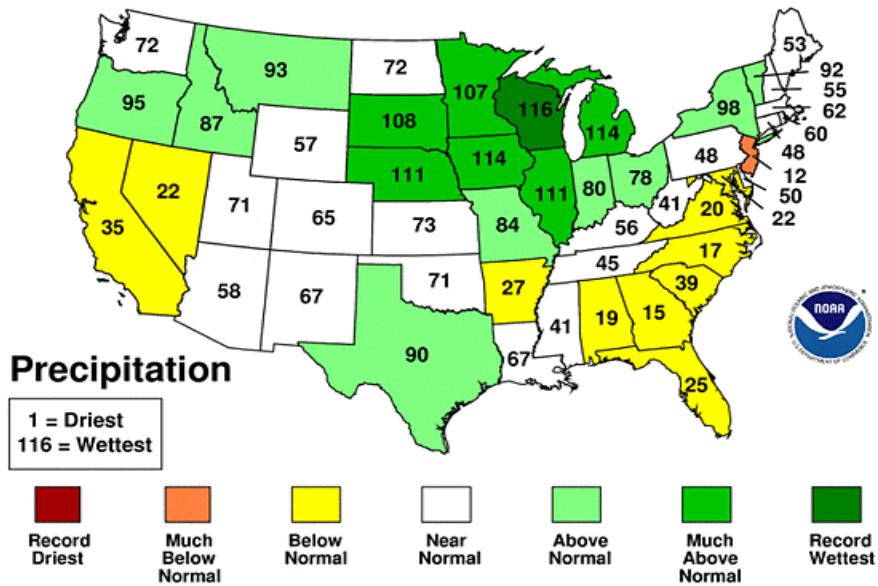
June-August 2009 Statewide Ranks

National Climatic Data Center/NESDIS/NOAA



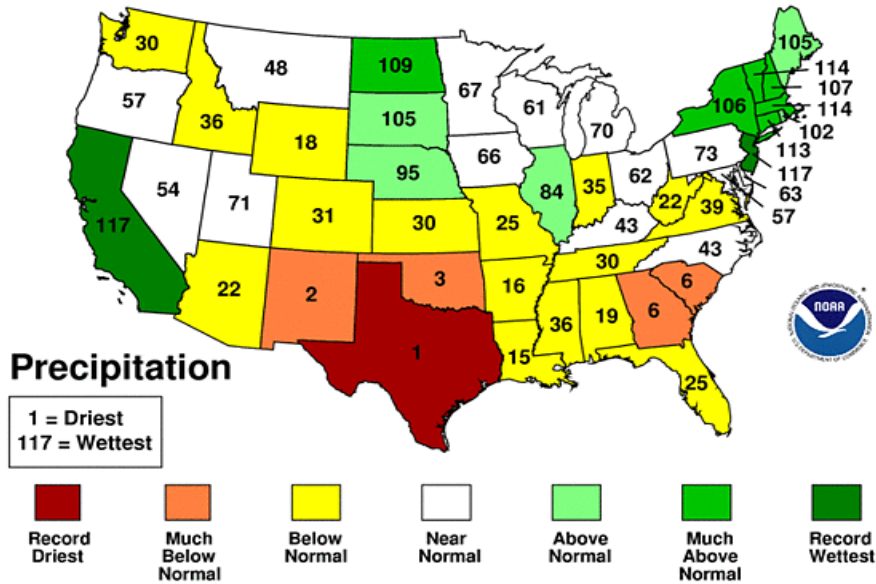
June-August 2010 Statewide Ranks

National Climatic Data Center/NESDIS/NOAA



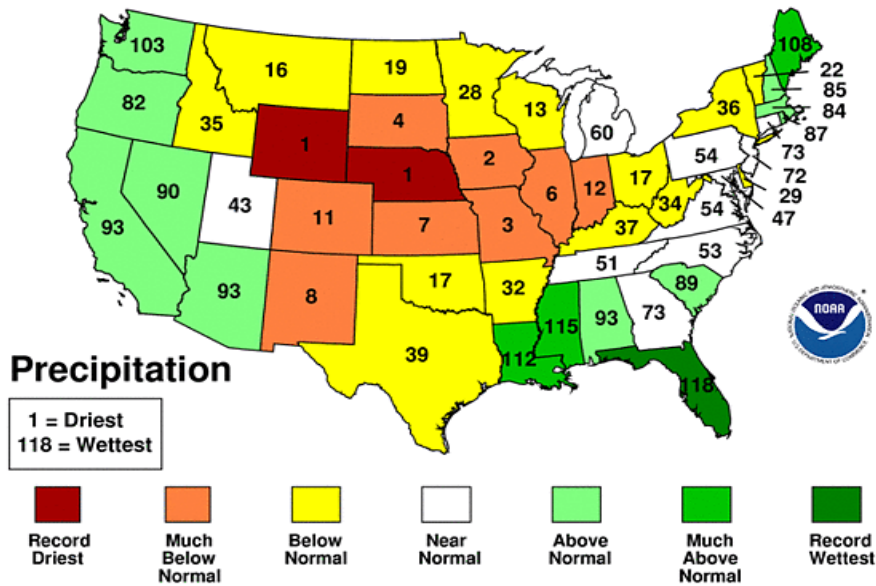
June-August 2011 Statewide Ranks

National Climatic Data Center/NESDIS/NOAA



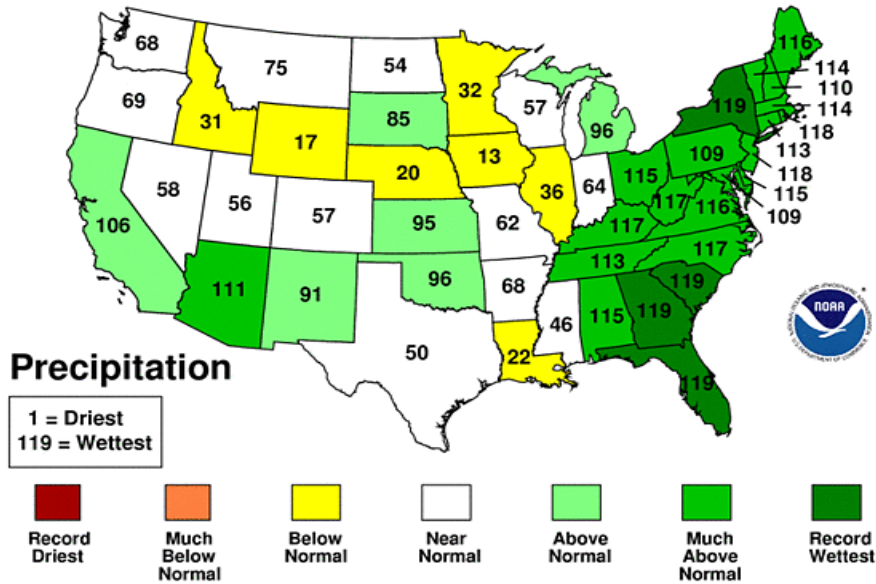
June-August 2012 Statewide Ranks

National Climatic Data Center/NESDIS/NOAA



June-August 2013 Statewide Ranks

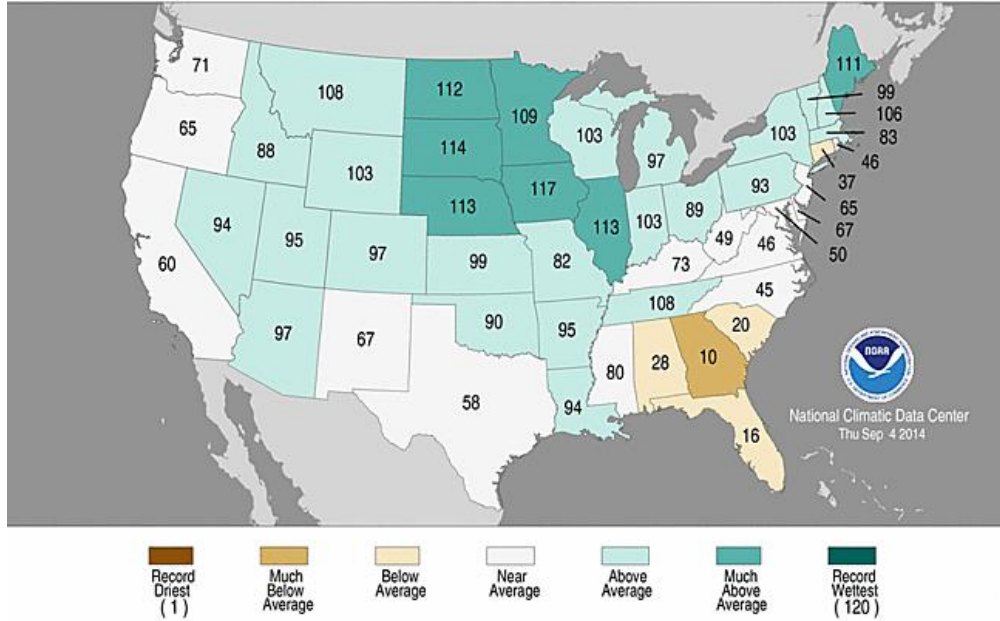
National Climatic Data Center/NESDIS/NOAA



Statewide Precipitation Ranks

June-August 2014

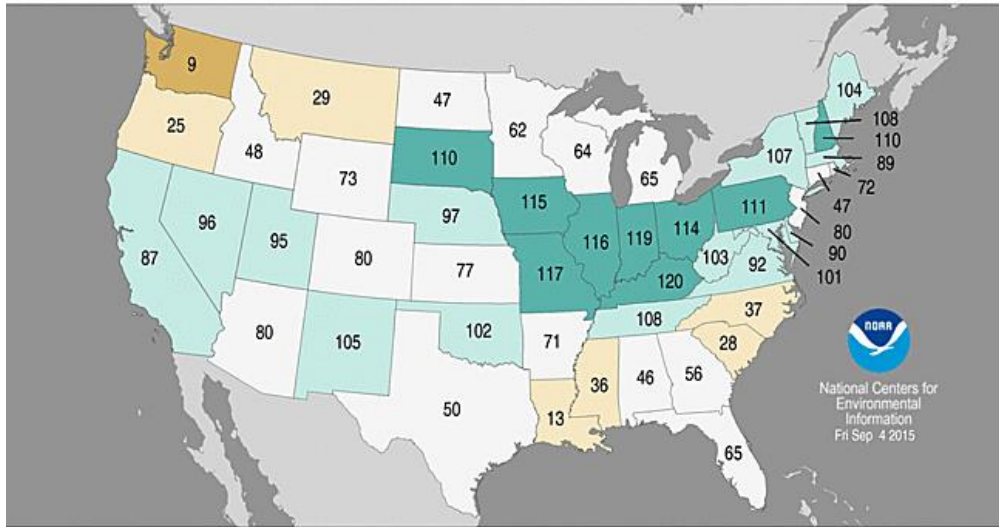
Period: 1895-2014



Statewide Precipitation Ranks

June–August 2015

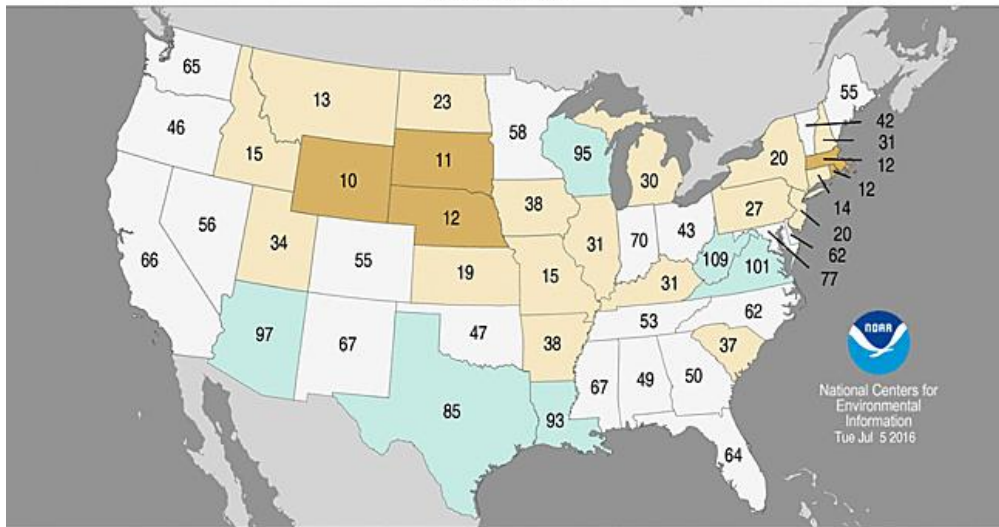
Period: 1895–2015



Statewide Precipitation Ranks

June 2016

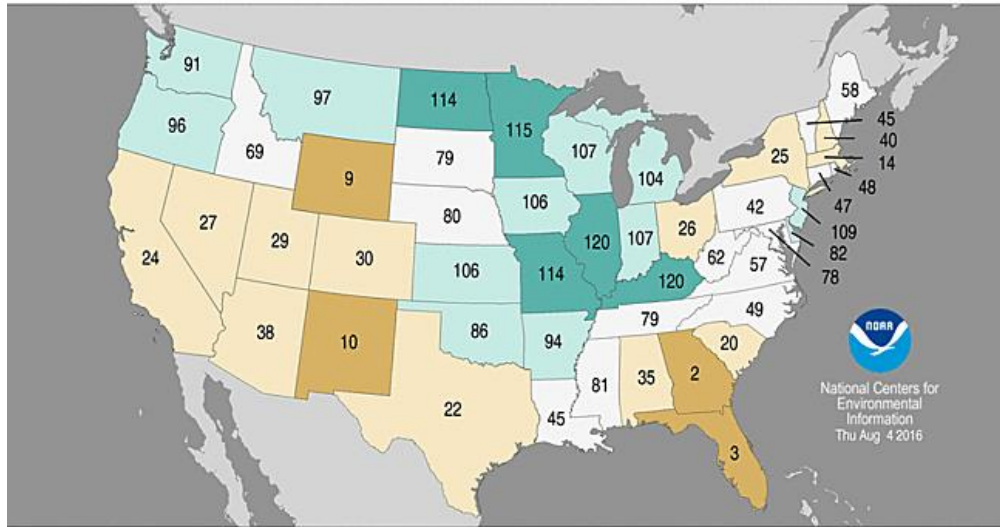
Period: 1895–2016



Statewide Precipitation Ranks

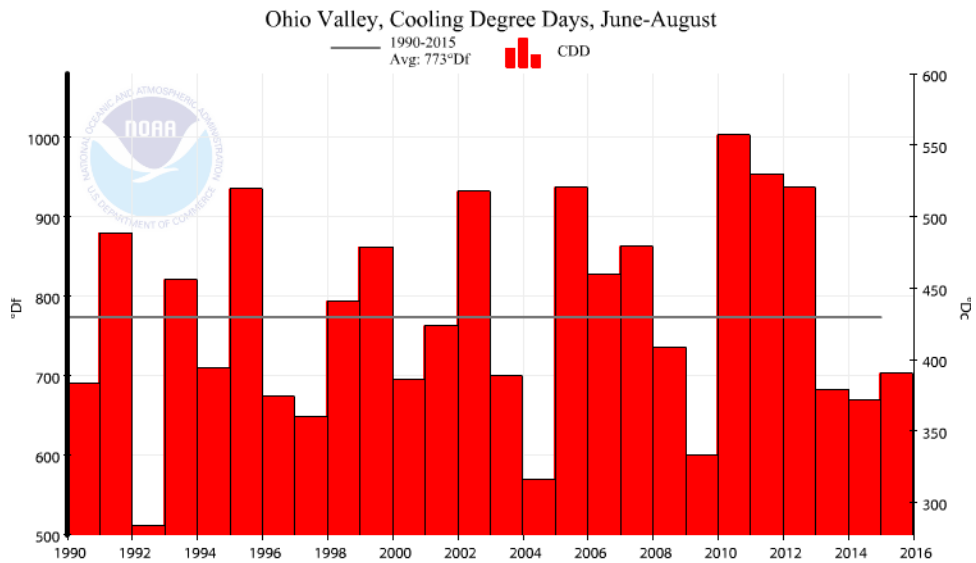
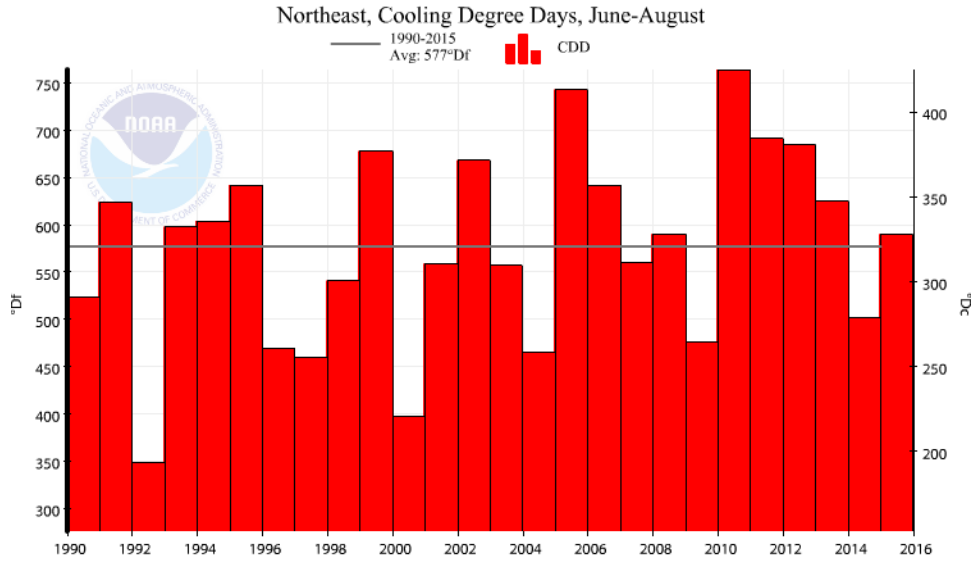
July 2016

Period: 1895-2016

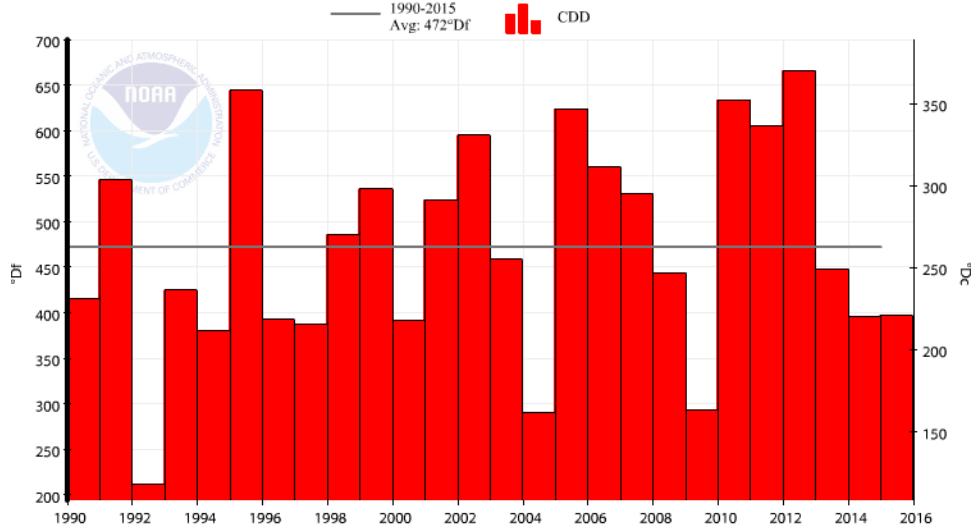


NCEP
National Centers for
Environmental
Information
Thu Aug 4 2016

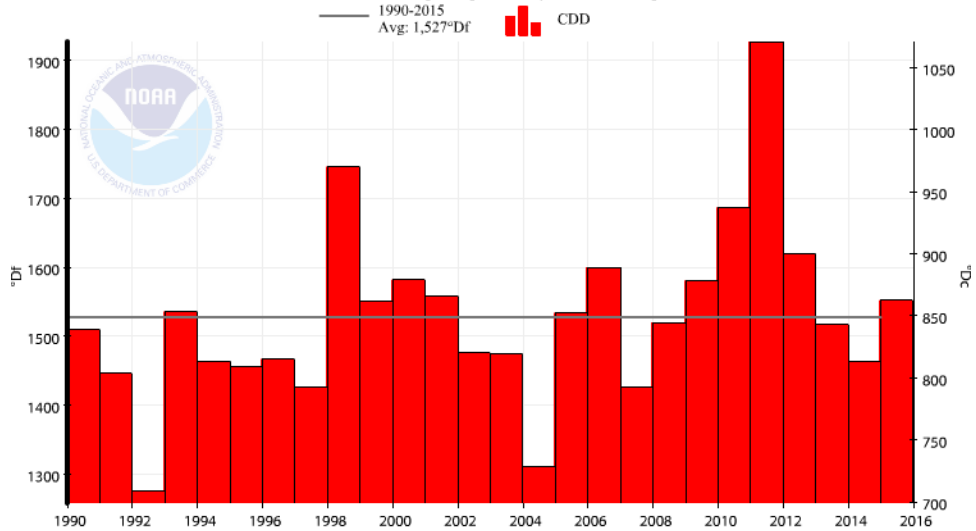
Figure A-3. Cooling degree days for June through August from 1990 through 2015 for each climate region in the eastern U.S. (i.e., the Northeast, Ohio Valley, Upper Midwest, Southeast, and South climate regions). Note that the range of the y-axis differs by climate region.




Upper Midwest, Cooling Degree Days, June-August

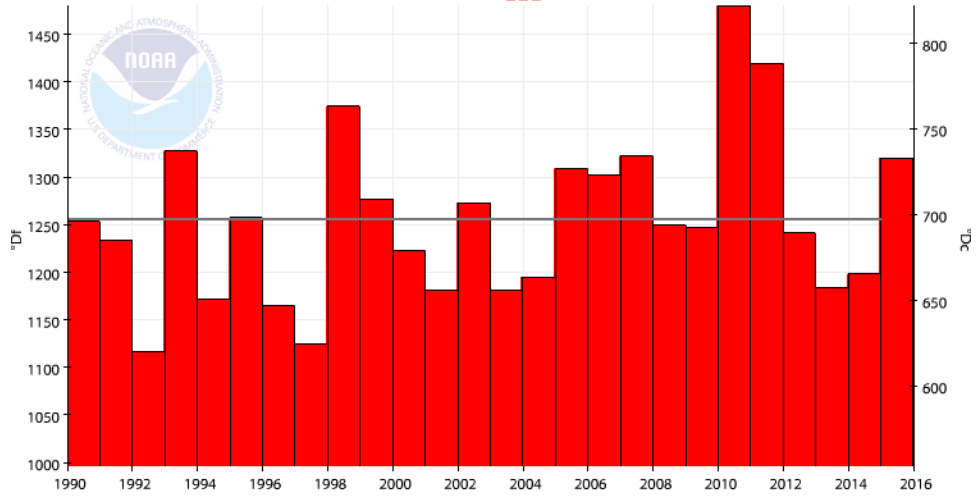


South, Cooling Degree Days, June-August



Southeast, Cooling Degree Days, June-August

— 1990-2015 Avg: 1,255°Df  CDD



This page intentionally left blank

Appendix B

2011 Model Performance Evaluation

An operational model evaluation was conducted for the 2011 base year CAMx v6.20 model simulation performed for the 12 km U.S. modeling domain. The purpose of this evaluation is to examine the ability of the 2011 air quality modeling platform to represent the magnitude and spatial and temporal variability of measured (i.e., observed) ozone concentrations within the modeling domain. The evaluation presented here is based on model simulations using the v6.3 version of the 2011 emissions platform (i.e., case name 2011ek_cb6v2_v6_11g). The model evaluation for ozone focuses on comparisons of model predicted 8-hour daily maximum concentrations to the corresponding observed data at monitoring sites in the EPA Air Quality System (AQS) and the Clean Air Status and Trends Network (CASTNet). The locations of the ozone monitoring sites in these two networks are shown in Figures A-1a and A-1b.

Included in the evaluation are statistical measures of model performance based upon model-predicted versus observed concentrations that were paired in space and time. Model performance statistics were calculated for several spatial scales and temporal periods. Statistics were calculated for individual monitoring sites, and in aggregate for monitoring sites within each state and within each of nine climate regions of the 12 km U.S. modeling domain. The regions include the Northeast, Ohio Valley, Upper Midwest, Southeast, South, Southwest, Northern Rockies, Northwest and West^{1,2}, which are defined based upon the states contained within the National Oceanic and Atmospheric Administration (NOAA) climate regions (Figure A-2)³ as defined in Karl and Koss (1984).

¹ The nine climate regions are defined by States where: Northeast includes CT, DE, ME, MA, MD, NH, NJ, NY, PA, RI, and VT; Ohio Valley includes IL, IN, KY, MO, OH, TN, and WV; Upper Midwest includes IA, MI, MN, and WI; Southeast includes AL, FL, GA, NC, SC, and VA; South includes AR, KS, LA, MS, OK, and TX; Southwest includes AZ, CO, NM, and UT; Northern Rockies includes MT, NE, ND, SD, WY; Northwest includes ID, OR, and WA; and West includes CA and NV.

² Note most monitoring sites in the West region are located in California (see Figures 2A-2a and 2A-2b), therefore statistics for the West will be mostly representative of California ozone air quality.

³ NOAA, National Centers for Environmental Information scientists have identified nine climatically consistent regions within the contiguous U.S., <http://www.ncdc.noaa.gov/monitoring-references/maps/us-climate-regions.php>.

For maximum daily average 8-hour (MDA8) ozone, model performance statistics were created for the period May through September.⁴ The aggregate statistics by state and by climate region are presented and in this appendix. Model performance statistics by monitoring site for MDA8 ozone based on days with observed values ≥ 60 ppb can be found in the docket in the file named “Final CSAPR Update 2011 Ozone Model Performance Statistics by Site”. Performance statistics by site calculated for days with observed values ≥ 75 ppb can be found in the docket in the file “Supplemental 2011 O3 Model Performance Statistics_Final CSAPR Update”.

In addition to the above performance statistics, we prepared several graphical presentations of model performance for MDA8 ozone. These graphical presentations include:

- (1) density scatter plots of observed AQS data and predicted MDA8 ozone concentrations for May through September;
- (2) regional maps that show the mean bias and error as well as normalized mean bias and error calculated for MDA8 ≥ 60 ppb for May through September at individual AQS and CASTNet monitoring sites;
- (3) bar and whisker plots that show the distribution of the predicted and observed MDA8 ozone concentrations by month (May through September) and by region and by network; and
- (4) time series plots (May through September) of observed and predicted MDA8 ozone concentrations for the 19 projected 2017 nonattainment and maintenance-only sites.

The Atmospheric Model Evaluation Tool (AMET) was used to calculate the model performance statistics used in this document (Gilliam et al., 2005). For this evaluation of the ozone predictions in the 2011 CAMx modeling platform, we have selected the mean bias, mean error, normalized mean bias, and normalized mean error to characterize model performance, statistics which are consistent with the recommendations in Simon et al. (2012) and the draft photochemical modeling guidance (U.S. EPA, 2014c). As noted above, we calculated the performance statistics by climate region for the period May through September.

Mean bias (MB) is the average of the difference (predicted – observed) divided by the total number of replicates (n). Mean bias is given in units of ppb and is defined as:

⁴ In calculating the ozone season statistics we limited the data to those observed and predicted pairs with observations that are greater than or equal 60 ppb in order to focus on concentrations at the upper portion of the distribution of values.

$$MB = \frac{1}{n} \sum_1^n (P - O) , \text{ where } P = \text{predicted and } O = \text{observed concentrations.}$$

Mean error (ME) calculates the absolute value of the difference (predicted - observed) divided by the total number of replicates (n). Mean error is given in units of ppb and is defined as:

$$ME = \frac{1}{n} \sum_1^n |P - O|$$

Normalized mean bias (NMB) is the average the difference (predicted - observed) over the sum of observed values. NMB is a useful model performance indicator because it avoids over inflating the observed range of values, especially at low concentrations. Normalized mean bias is given in percentage units and is defined as:

$$NMB = \frac{\sum_1^n (P-O)}{\sum_1^n (O)} * 100$$

Normalized mean error (NME) is the absolute value of the difference (predicted - observed) over the sum of observed values. Normalized mean error is given in percentage units and is defined as:

$$NME = \frac{\sum_1^n |P-O|}{\sum_1^n (O)} * 100$$

As described in more detail below, the model performance statistics indicate that the 8-hour daily maximum ozone concentrations predicted by the 2011 CAMx modeling platform closely reflect the corresponding 8-hour observed ozone concentrations in space and time in each region of the 12 km U.S. modeling domain. The acceptability of model performance was judged by considering the 2011 CAMx performance results in light of the range of performance found in recent regional ozone model applications (NRC, 2002; Phillips et al., 2007; Simon et al., 2012; U.S. EPA, 2005; U.S. EPA, 2009; U.S. EPA, 2011). These other modeling studies represent a wide range of modeling analyses that cover various models, model configurations, domains, years and/or episodes, chemical mechanisms, and aerosol modules. Overall, the ozone model performance results for the 2011 CAMx simulations are within the range found in other recent peer-reviewed and regulatory applications. The model performance results, as described in this

document, demonstrate that the predictions from the 2011 modeling platform correspond closely to observed concentrations in terms of the magnitude, temporal fluctuations, and geographic differences for 8-hour daily maximum ozone.

The density scatter plots of MDA8 ozone are provided Figure A-3. The 8-hour ozone model performance bias and error statistics by network for the ozone season (May-September average) for each region and each state are provided in Tables A-1 and A-2, respectively. The statistics shown were calculated using data pairs on days with observed 8-hour ozone of ≥ 60 ppb. The distributions of observed and predicted 8-hour ozone by month in the period May through September for each region are shown in Figures A-4 through A-12. Spatial plots of the mean bias and error as well as the normalized mean bias and error for individual monitors are shown in Figures A-13 through A-16. Time series plots of observed and predicted MDA 8-hour ozone during the period May through September at the 19 nonattainment and maintenance sites (see Table A-3) are provided in Figure A-17, (a) through (s).

The density scatter plots in Figure A-3 provide a qualitative comparison of model-predicted and observed MDA8 ozone concentrations. In these plots the intensity of the colors indicates the density of individual observed/predicted paired values. The greatest number of individual paired values is denoted by the core area in white. The plots indicate that the predictions correspond to the observations in that a large number of observed/predicted paired values lie along or close to the 1:1 line shown on each plot. Overall, the model tends to over-predict the observed values to some extent, particularly at low and mid-range concentrations generally < 60 ppb in each of the regions. This feature is most evident in the South and Southeast regions. In the West region, high concentrations are under-predicted and low and mid-range concentrations are over-predicted. Observed and predicted values are in close agreement in the Southwest and Northwest regions.

As indicated by the statistics in Table A-1, bias and error for 8-hour daily maximum ozone are relatively low in each region. Generally, mean bias for 8-hour ozone ≥ 60 ppb during the period May through September is within ± 5 ppb⁵ at AQS sites in the eastern climate regions (i.e., Northeast, Ohio Valley, Upper Midwest, Southeast, and South) and at rural CASTNet sites

⁵ Note that “within ± 5 ppb” includes values that are greater than or equal to -5 ppb and less than or equal to 5 ppb.

in the Northeast, Ohio Valley, Upper Midwest, and Southeast. The mean error is less than 10 ppb in all regions, except the West. Normalized mean bias is within ± 5 percent for AQS sites in all regions of the East, except for the South where the normalized mean bias of -6.6 percent is also relatively small. The mean bias and normalized mean bias statistics indicate a tendency for the model to under predicted MDA8 ozone concentrations in the western regions for AQS and CASTNet sites. The normalized mean error is less than 15 percent for both networks in all regions, except for the CASTNet sites in the West. Looking at model performance for individual states (Table A-2) indicates that mean bias is within ± 5 ppb for a majority of the states and within ± 10 ppb for all but two states. The mean error is less than 10 ppb for nearly all states and greater than 15 ppb for only one state. The normalized mean bias is within ± 10 percent for all states in the East, except for North Dakota and South Dakota. The normalized mean error is within ± 15 percent for nearly all states nationwide.

The monthly distributions of 8-hour daily maximum model predicted ozone generally corresponds well with that of the observed concentrations, as indicated by the graphics in Figures A-4 through A-12. The distribution of predicted concentrations tends to be close to that of the observed data at the 25th percentile, median and 75th percentile values for each region, although there is a small persistent overestimation bias in the Northeast, Southeast, and Ohio Valley regions, and a tendency for under-prediction in the western regions (i.e., Southwest, Northern Rockies, Northwest,⁶ and West), particularly at CASTNet sites in the West region.

Figures A-13 through A-16 show the spatial variability in bias and error at monitor locations. Mean bias, as seen from Figure A-13, is within ± 5 ppb at many sites across the East with over-prediction of 5 to 10 ppb or more at some of the sites from the Southeast into the Northeast. Elsewhere in the U.S., mean bias is generally in the range of -5 to -10 ppb. The most notable exception is in portions of California where the mean bias is in the range of -10 to -15 ppb at a number of interior sites. Figure A-14 indicates that the normalized mean bias for days with observed 8-hour daily maximum ozone greater than or equal to 60 ppb is within ± 10 percent at the vast majority of monitoring sites across the modeling domain. There are regional differences in model performance, where the model tends to over-predict at some sites from the

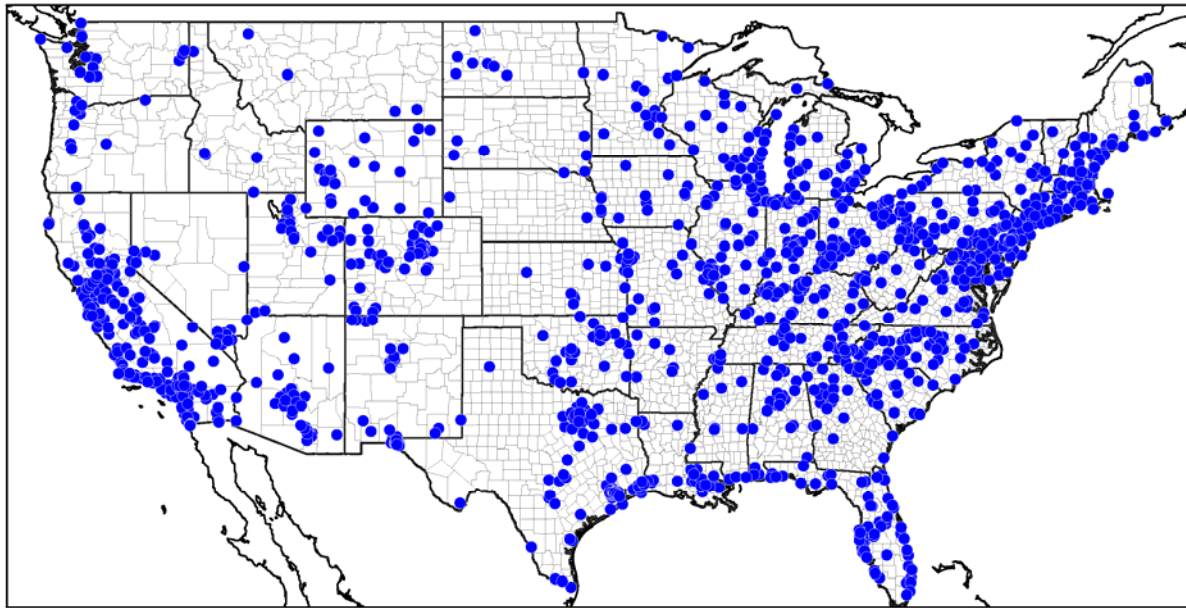
⁶ Note that the over-prediction at CASTNet sites in the Northwest seen in Figure A-11 may not be representative of performance in rural areas of this region because there are so few observed and predicted data values in this region.

Southeast into the Northeast and generally under predict in the Southwest, Northern Rockies, Northwest and West. Model performance in the Ohio Valley and Upper Midwest states shows that most sites are within ± 10 percent with only a few sites outside of this range.

Model error, as seen from Figure A-15, is 10 ppb or less at most of the sites across the modeling domain. Figure A-16 indicates that the normalized mean error for days with observed 8-hour daily maximum ozone greater than or equal to 60 ppb is within 15 percent at the vast majority of monitoring sites across the modeling domain. Somewhat greater error (i.e., greater than 15 percent) is evident at sites in several areas most notably within portions of the Northeast and in portions of Florida, and the western most part of the modeling domain.

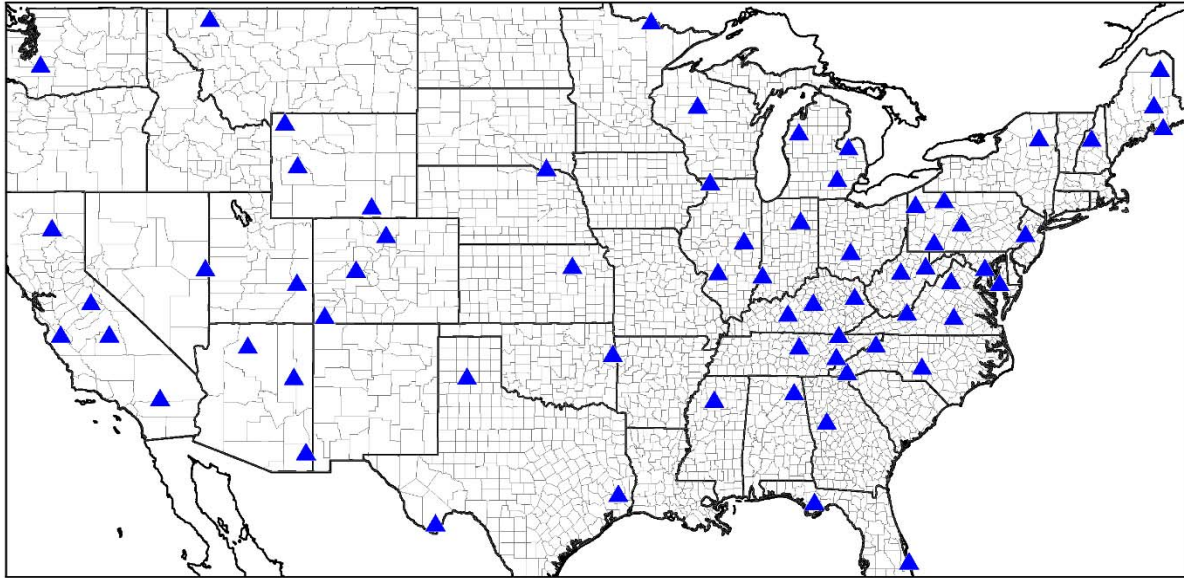
In addition to the above analysis of overall model performance, we also examine how well the modeling platform replicates day to day fluctuations in observed 8-hour daily maximum concentrations using data for the 19 nonattainment and maintenance-only sites. For this site-specific analysis we present the time series of observed and predicted 8-hour daily maximum concentrations by site over the period May through September. The results, as shown in Figures A-17 (a) through (s), indicate that the modeling platform generally replicates the day-to-day variability in ozone during this time period at these sites. That is, days with high modeled concentrations are generally also days with high measured concentrations and, conversely, days with low modeled concentrations are also days with low measured concentrations in most cases. For example, model predictions at several sites not only accurately capture the day-to-day variability in the observations, but also appear to have relatively low bias on individual days: Jefferson County, KY; Hamilton County, OH; Philadelphia County, PA; Richmond County, NY; and Suffolk County, NY. The sites in Fairfield County, CT, New Haven County, CT, Harford County, MD, and Allegan County, MI each track closely with the observations, but there is a tendency to over predict on several days. Other sites generally track well and capture day-to-day variability but underestimate ozone on some of the days with measured high ozone concentrations: Brazoria County, TX; Denton County, TX; Harris County, TX; Tarrant County, TX; and Sheboygan County, WI. Note that at the site in Brazoria County, TX and at that Harris County, TX site 482011039, there is an extended period from mid-July to mid-August with very low observed ozone concentrations, mostly in the range of 30 to 40 ppb. The model also predicted generally low ozone concentrations at these sites during this period, but the modeled

values were in the range of 40 to 60 ppb which is not quite as low as the observed values. Looking across all 19 sites indicates that the modeling platform is able to capture the both the site-to-site differences in the short-term variability and the general magnitude of the observed ozone concentrations.



CIRCLE=AQS_Daily;

Figure A-1a. AQS ozone monitoring sites.



TRIANGLE=CASTNET;

Figure A-1b. CASTNet ozone monitoring sites.

U.S. Climate Regions

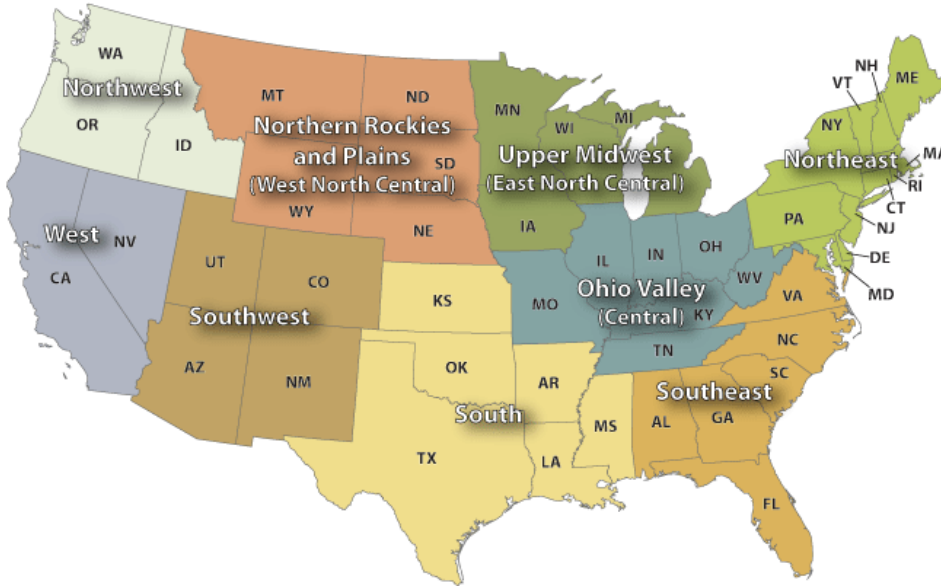


Figure A-2. NOAA climate regions (source: <http://www.ncdc.noaa.gov/monitoring-references/maps/us-climate-regions.php#references>)

Table A-1. Performance statistics for MDA8 ozone \geq 60 ppb for May through September by climate region, for AQS and CASTNet networks.

Network	Climate Region	No. of Obs	MB (ppb)	ME (ppb)	NMB (%)	NME (%)
AQS	Northeast	4,085	2.2	7.6	3.2	11.1
	Ohio Valley	6,325	0.1	7.6	0.1	11.2
	Upper Midwest	1,162	-3.1	7.5	-4.6	11.0
	Southeast	4,840	3.3	7.1	4.9	10.7
	South	5,694	-4.5	8.4	-6.6	12.1
	Southwest	6,033	-6.2	8.4	-9.5	12.7
	Northern Rockies	380	-6.6	7.8	-10.5	12.4
	Northwest	79	-5.8	8.8	-9.1	13.8
	West	8,655	-8.6	10.3	-12.2	14.6
CASTNet	Northeast	264	2.3	6.1	3.4	9.0
	Ohio Valley	433	-2.3	6.3	-3.4	9.4
	Upper Midwest	38	-4.1	5.9	-6.0	8.8
	Southeast	201	1.2	5.4	1.8	8.3
	South	215	-7.9	8.6	-11.9	12.9
	Southwest	382	-8.4	9.2	-12.8	14.0
	Northern Rockies	110	-8.4	8.7	-13.3	13.7
	Northwest	-	-	-	-	-
	West	425	-13.6	13.8	-18.6	19.0

Table A-2. Performance statistics for MDA8 ozone \geq 60 ppb for May through September by state based on data at AQS network sites.

State	No. of Obs	MB (ppb)	ME (ppb)	NMB (%)	NME (%)
AL	739	4.0	7.2	5.9	10.9
AZ	2334	-6.2	9.2	-9.4	13.8
AR	252	-3.4	8.5	-5.1	12.6
CA	7533	-8.9	10.6	-12.4	14.9
CO	2067	-6.1	8.0	-9.3	12.0
CT	245	3.0	10.1	4.2	14.3
DE	232	2.3	6.9	3.4	10.0
DC	87	2.5	11.7	3.6	16.8
FL	581	3.1	7.7	4.7	11.7
GA	829	3.8	7.7	5.7	11.4
ID	51	-10.0	10.4	-15.8	16.3

State	No. of Obs	MB (ppb)	ME (ppb)	NMB (%)	NME (%)
IL	782	-2.6	8.5	-3.8	12.7
IN	1142	0.0	6.8	0.0	10.1
IA	126	-3.1	6.7	-4.9	10.5
KS	352	-4.8	7.6	-7.1	11.4
KY	845	1.2	7.7	1.8	11.5
LA	711	1.8	7.7	2.7	11.3
ME	101	-1.4	6.5	-2.1	9.8
MD	766	3.4	8.2	4.8	11.8
MA	197	3.4	7.9	5.0	11.7
MI	638	-3.4	7.8	-5.0	11.4
MN	35	0.6	7.0	0.8	10.5
MS	260	2.3	8.5	3.4	12.9
MO	719	-1.2	7.7	-1.8	11.3
MT*	-	-	-	-	-
NE	41	-2.4	5.6	-3.9	8.8
NV	1122	-6.9	8.1	-10.4	12.2
NH	98	-4.8	8.3	-7.4	12.8
NJ	439	2.2	7.5	3.1	10.7
NM	961	-6.5	8.0	-9.9	12.3
NY	504	0.2	7.3	0.3	10.7
NC	1496	3.2	6.4	4.8	9.7
ND	10	-15.3	15.3	-24.5	24.5
OH	1624	0.3	7.8	0.4	11.5
OK	1475	-6.2	8.2	-9.0	11.9
OR	21	1.8	5.9	2.8	9.0
PA	1336	2.8	6.7	4.1	10.0
RI	75	1.8	8.1	2.7	12.0
SC	545	2.7	6.4	4.0	9.7
SD	21	-11.8	12.0	-18.7	19.0
TN	993	1.4	7.3	2.2	10.9
TX	2644	-6.0	8.7	-8.6	12.5
UT	671	-6.2	7.5	-9.7	11.7
VT	5	-5.7	8.3	-8.5	12.4
VA	650	2.8	7.7	4.1	11.5
WA	7	1.8	6.7	2.8	10.6
WV	220	2.9	6.4	4.4	9.8
WI	363	-3.0	7.2	-4.3	10.5
WY	308	-6.5	7.6	-10.3	12.0

*No statistics were calculated for Montana because there were no days with observed MDA8 ozone \geq 60 ppb in the ambient data set used for these calculations.

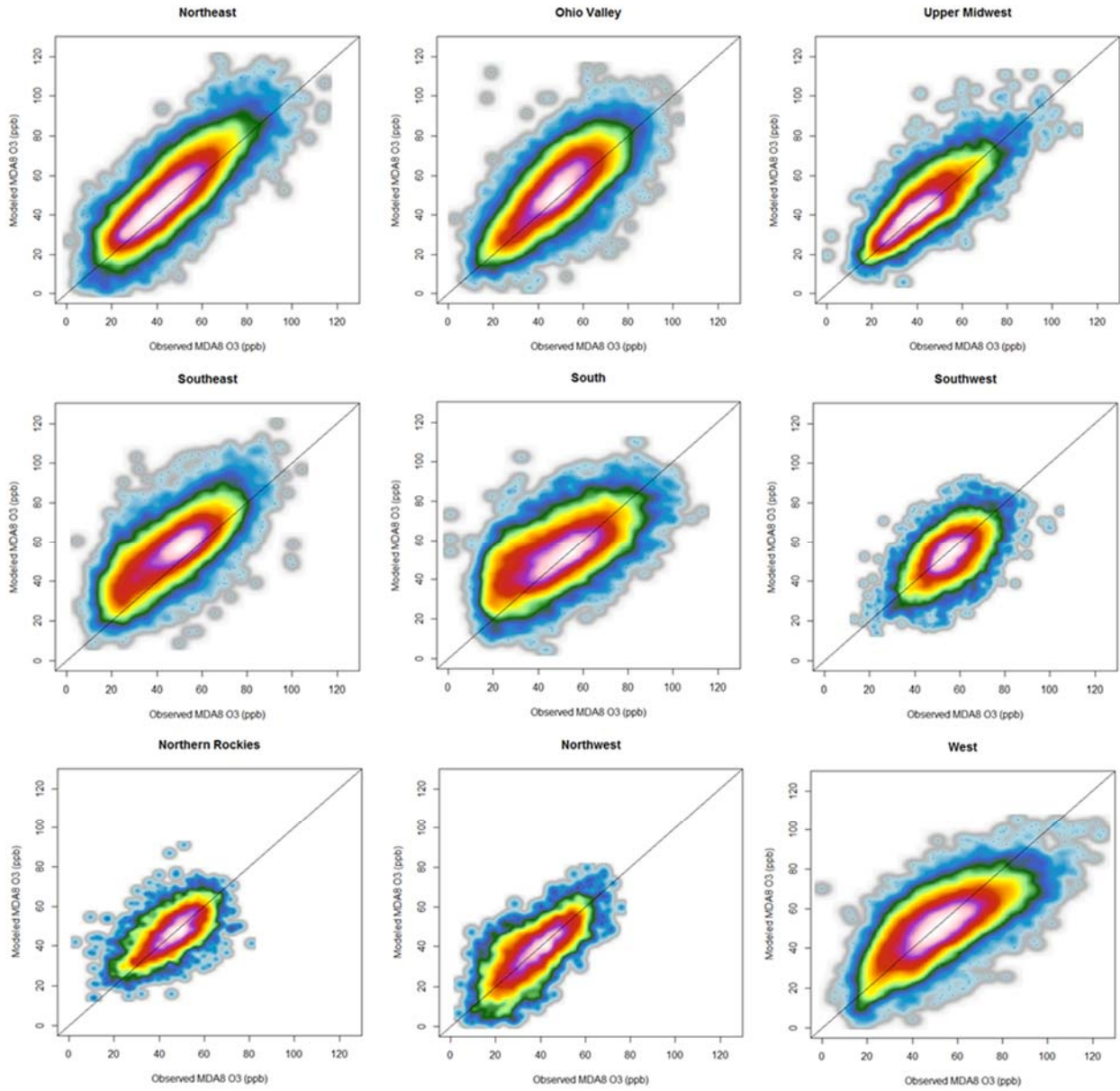


Figure A-3. Density scatter plots of observed vs predicted MDA8 ozone for the Northeast, Ohio River Valley, Upper Midwest, Southeast, South, Southwest, Northern Rockies, Northwest, and West regions.

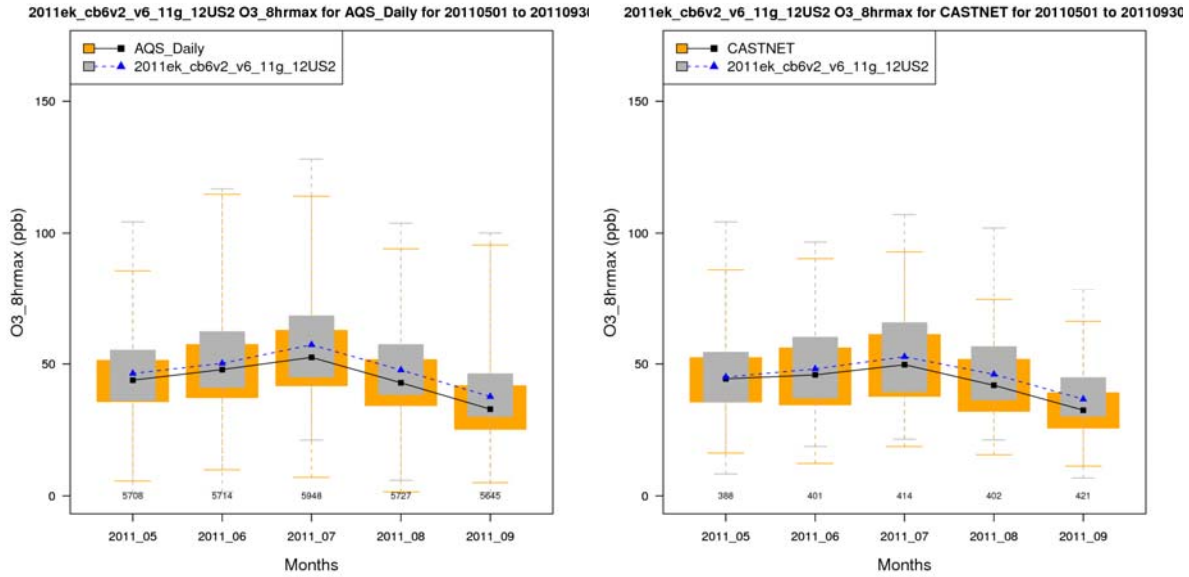


Figure A-4. Distribution of observed and predicted MDA8 ozone by month for the period May through September for the Northeast region, AQS Network (left) and CASTNet (right). [symbol = median; top/bottom of box = 75th/25th percentiles; top/bottom line = max/min values]

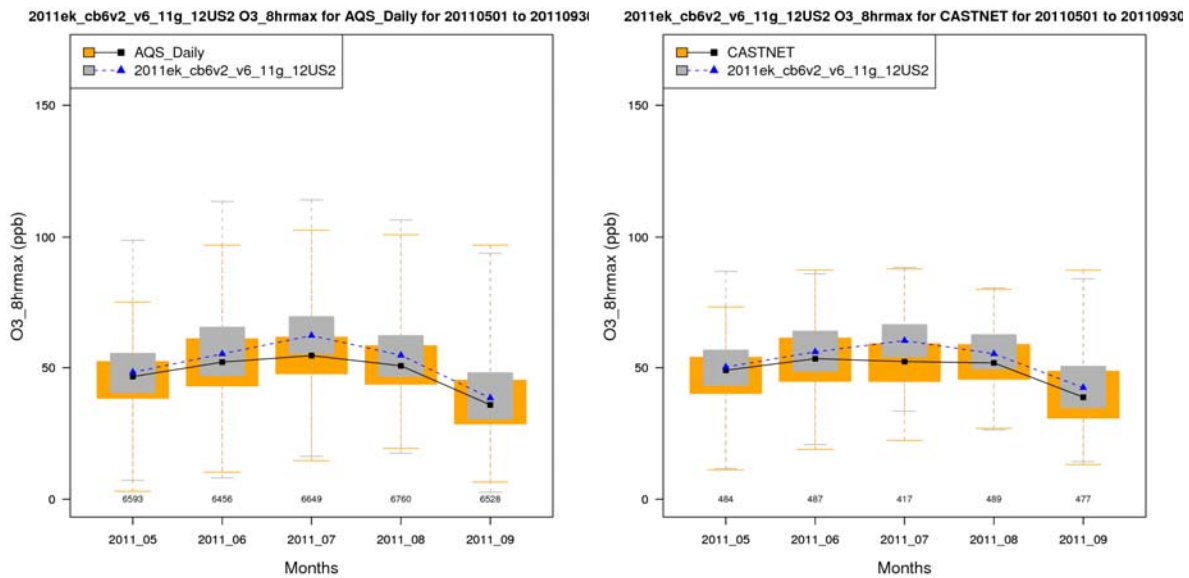


Figure A-5. Distribution of observed and predicted MDA8 ozone by month for the period May through September for the Ohio Valley region, AQS Network (left) and CASTNet (right).

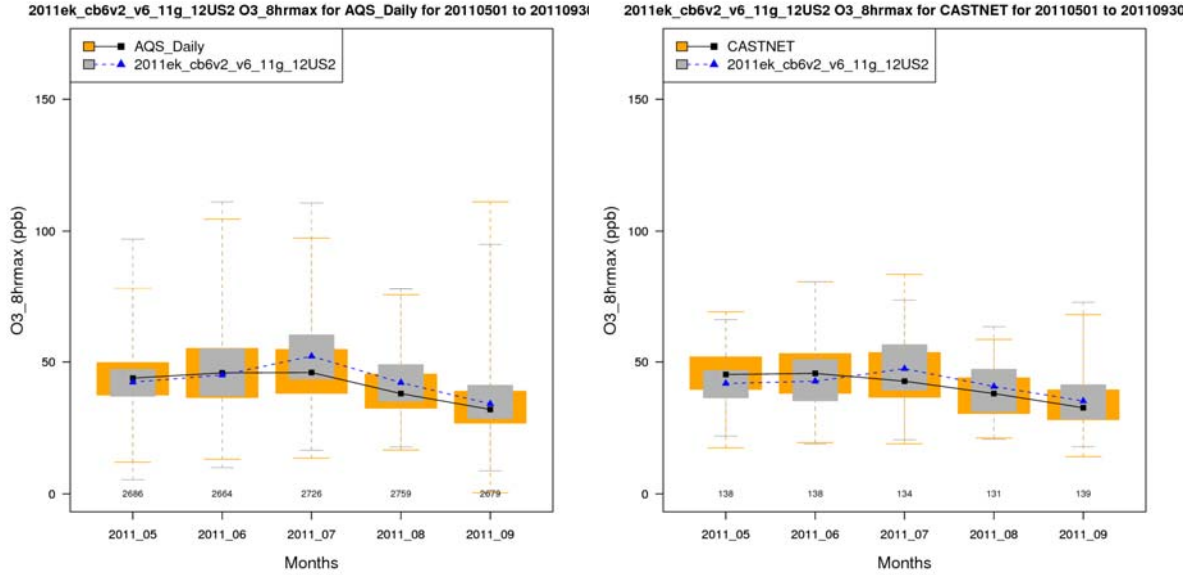


Figure A-6. Distribution of observed and predicted MDA8 ozone by month for the period May through September for the Upper Midwest region, AQS Network (left) and CASTNet (right).

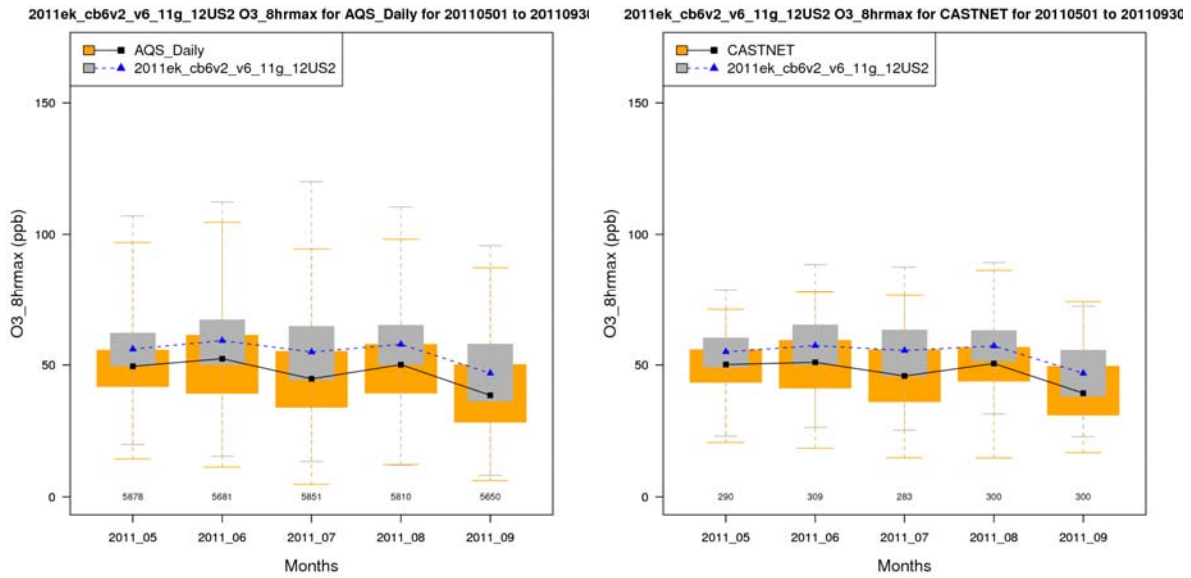


Figure A-7. Distribution of observed and predicted MDA8 ozone by month for the period May through September for the Southeast region, AQS Network (left) and CASTNet (right).

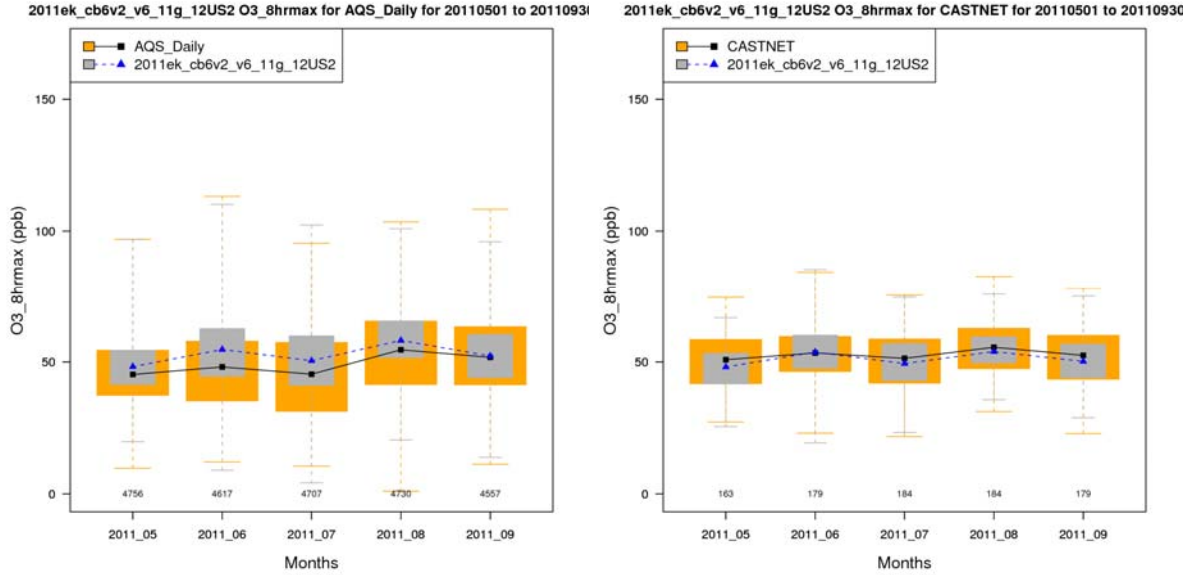


Figure A-8. Distribution of observed and predicted MDA8 ozone by month for the period May through September for the South region, AQS Network (left) and CASTNet (right).

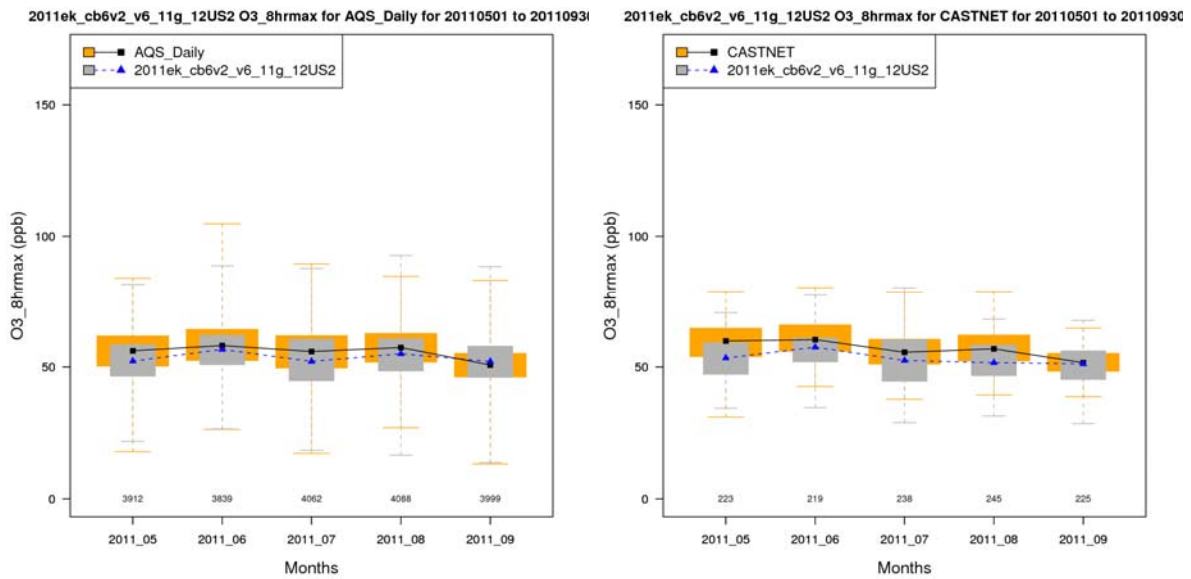


Figure A-9. Distribution of observed and predicted MDA8 ozone by month for the period May through September for the Southwest region, AQS Network (left) and CASTNet (right).

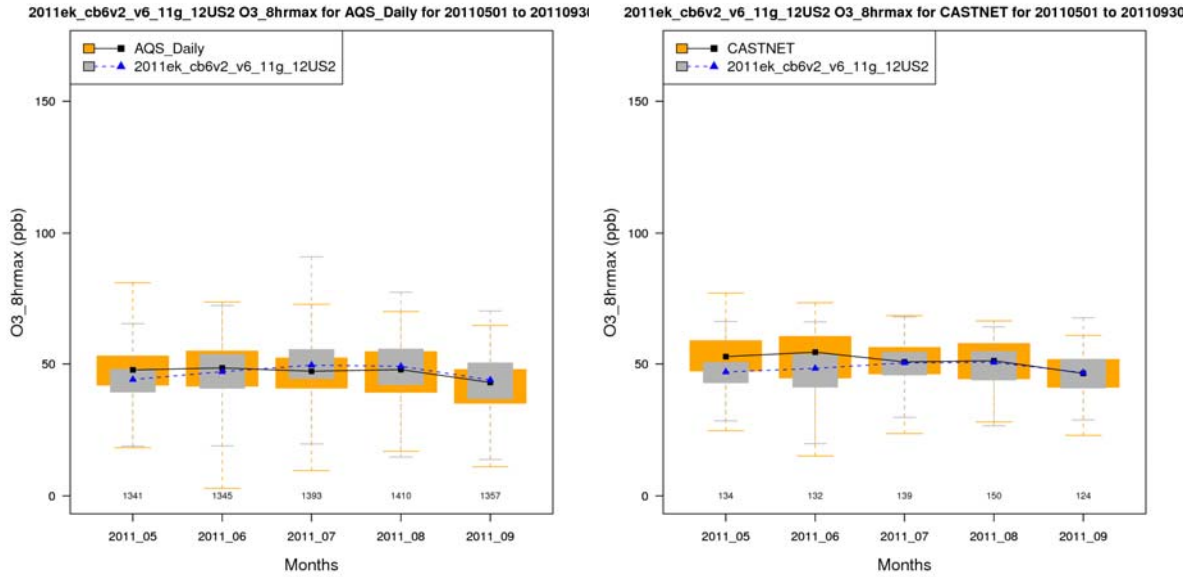


Figure A-10. Distribution of observed and predicted MDA8 ozone by month for the period May through September for the Northern Rockies region, AQS Network (left) and CASTNet (right).

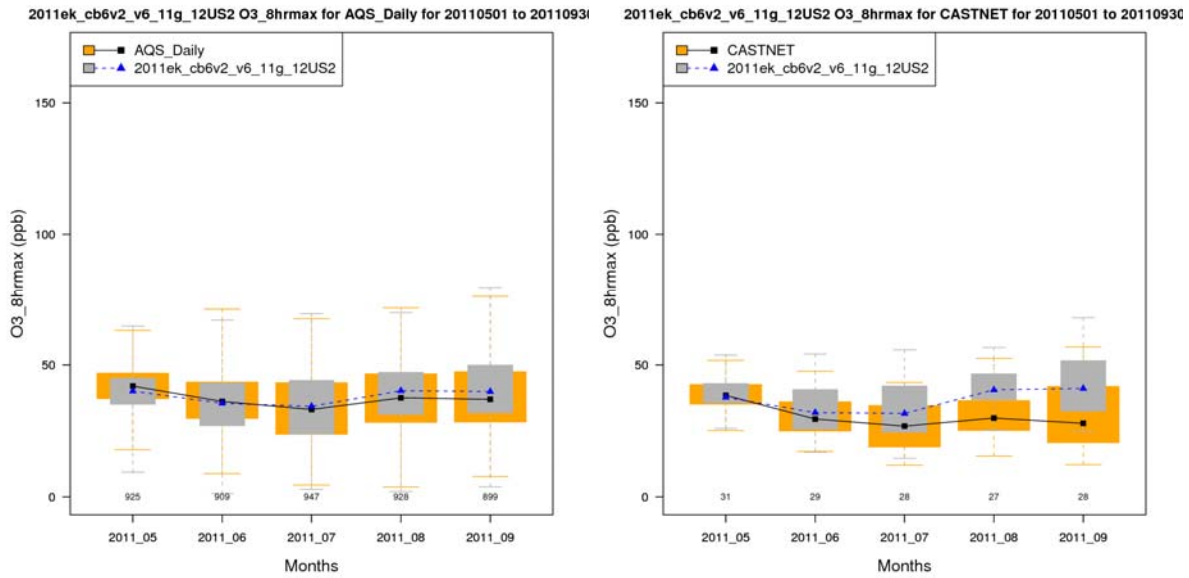


Figure A-11. Distribution of observed and predicted MDA8 ozone by month for the period May through September for the Northwest region, AQS Network (left) and CASTNet (right).

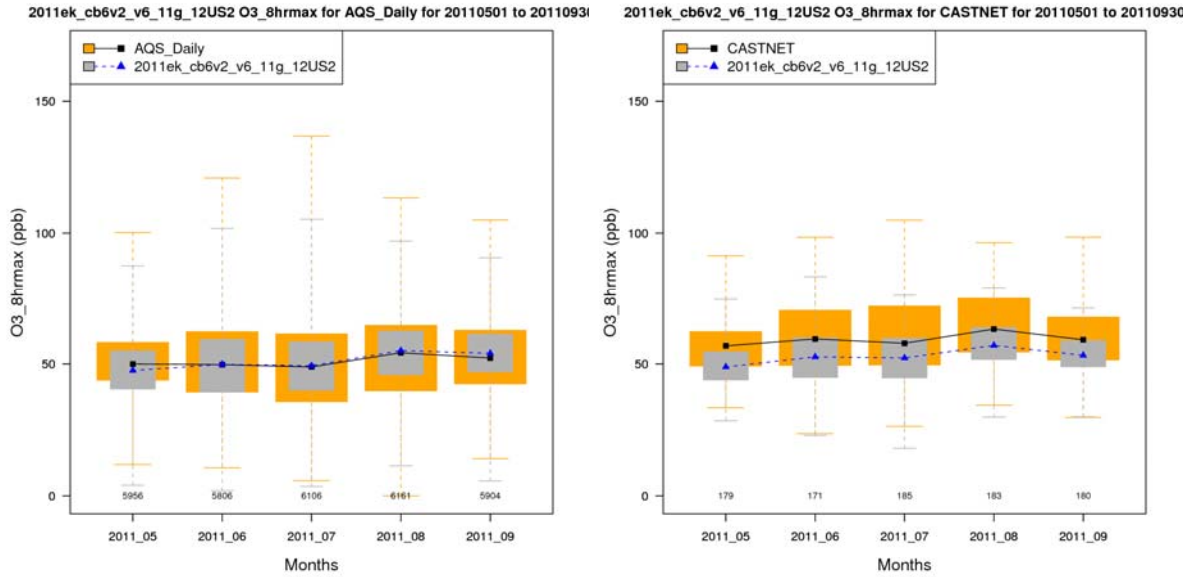


Figure A-12. Distribution of observed and predicted MDA8 ozone by month for the period May through September for the West region, AQS Network (left) and CASTNet (right).

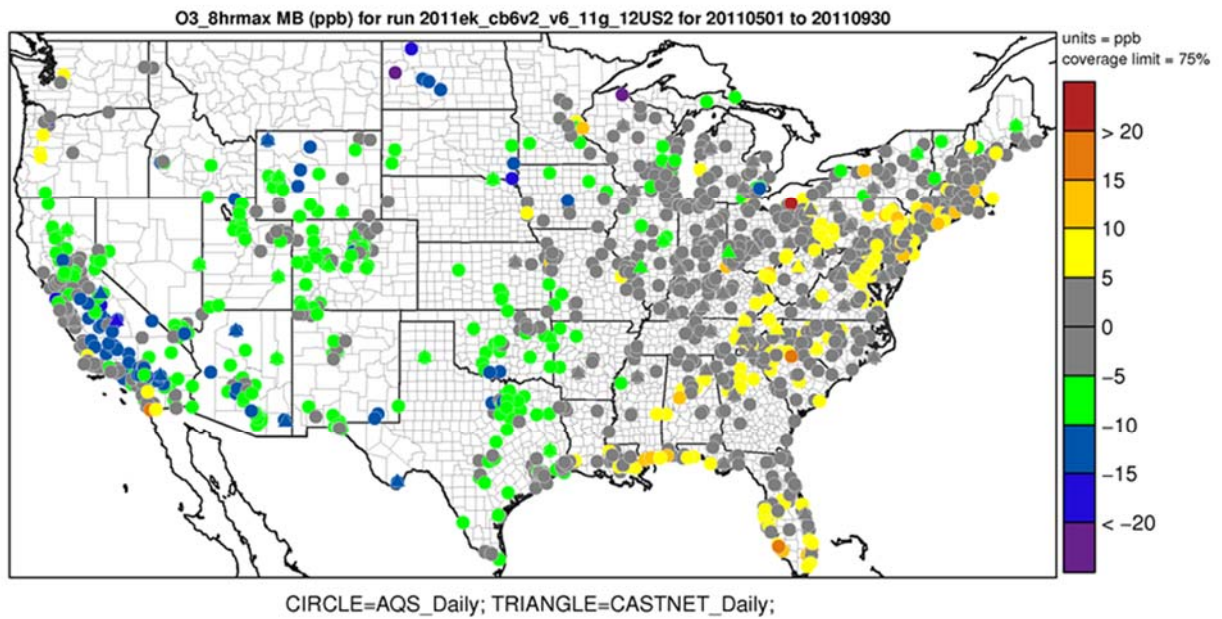


Figure A-13. Mean Bias (ppb) of MDA8 ozone ≥ 60 ppb over the period May-September 2011 at AQS and CASTNet monitoring sites.

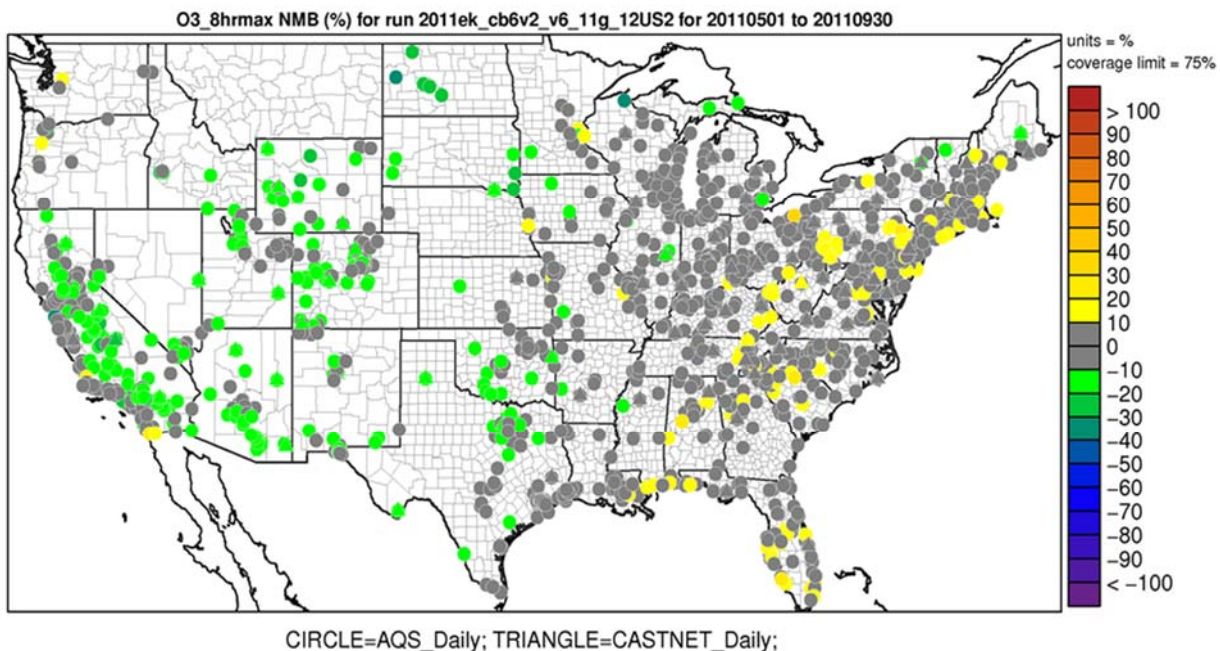


Figure A-14. Normalized Mean Bias (%) of MDA8 ozone ≥ 60 ppb over the period May-September 2011 at AQS and CASTNet monitoring sites.

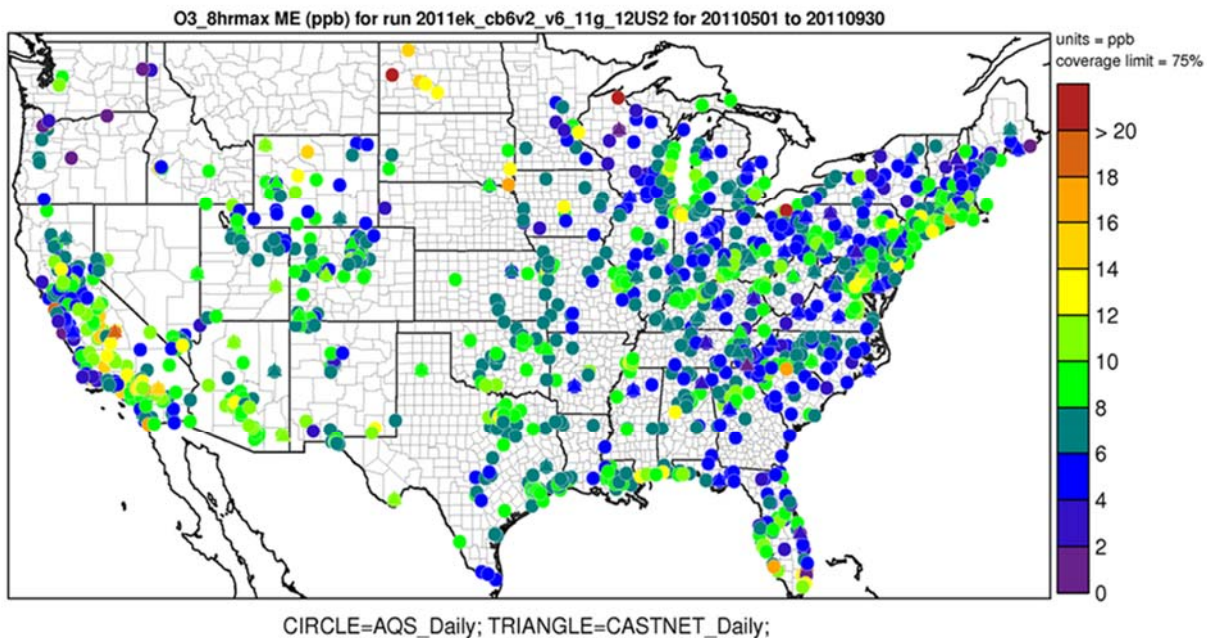


Figure A-15. Mean Error (ppb) of MDA8 ozone ≥ 60 ppb over the period May-September 2011 at AQS and CASTNet monitoring sites.

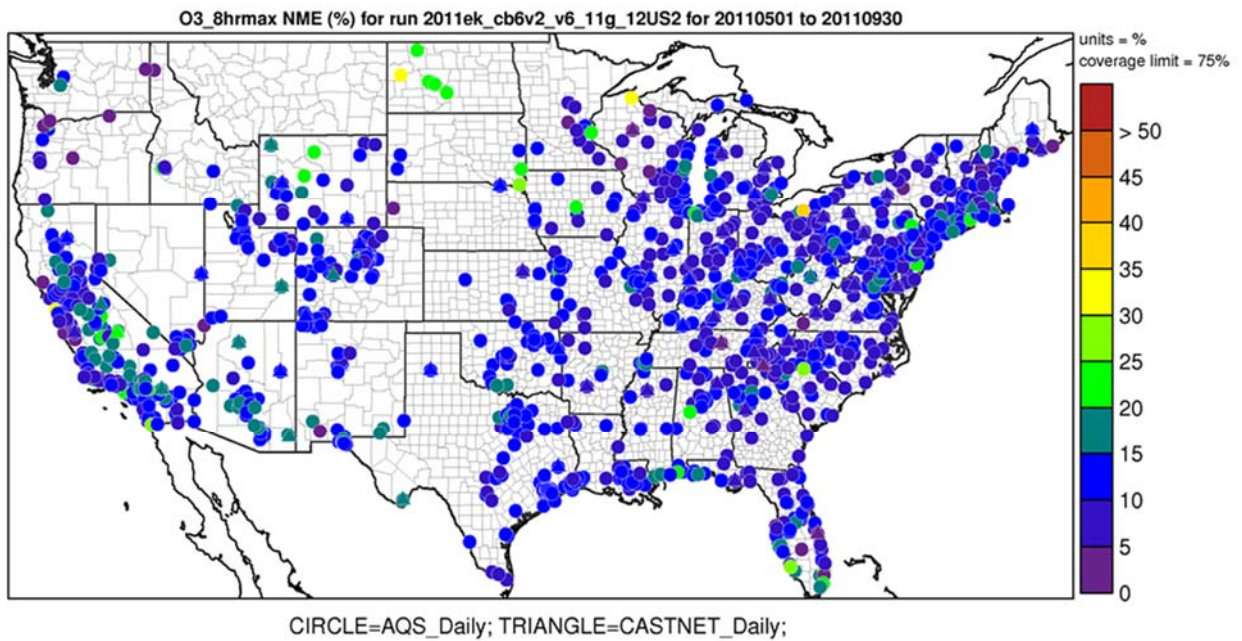


Figure A-16. Normalized Mean Error (%) of MDA8 ozone \geq 60 ppb over the period May-September 2011 at AQS and CASTNet monitoring sites.

Table A-3. Monitoring sites used for the ozone time series analysis.

Site	County	State
90010017	Fairfield	CT
90013007	Fairfield	CT
90019003	Fairfield	CT
90099002	New Haven	CT
211110067	Jefferson	KY
240251001	Harford	MD
260050003	Allegan	MI
360850067	Richmond	NY
361030002	Suffolk	NY
390610006	Hamilton	OH

Site	County	State
421010024	Philadelphia	PA
480391004	Brazoria	TX
481210034	Denton	TX
482010024	Harris	TX
482011034	Harris	TX
482011039	Harris	TX
484392003	Tarrant	TX
484393009	Tarrant	TX
551170006	Sheboygan	WI

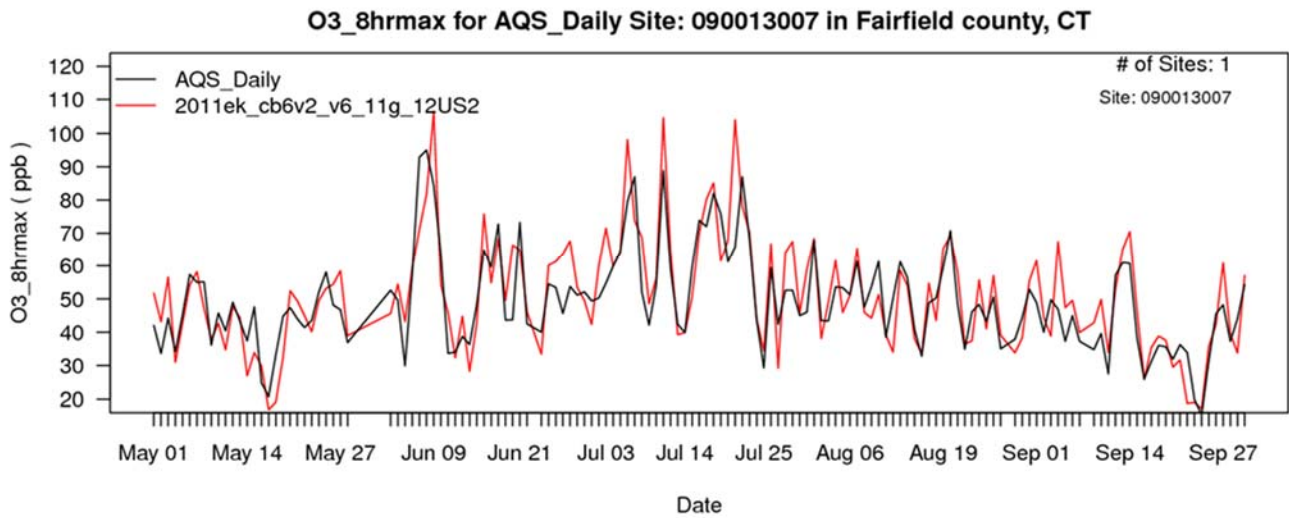


Figure A-17a. Time series of observed (black) and predicted (red) MDA8 ozone for May through September 2011 at site 090013007 in Fairfield Co., Connecticut.

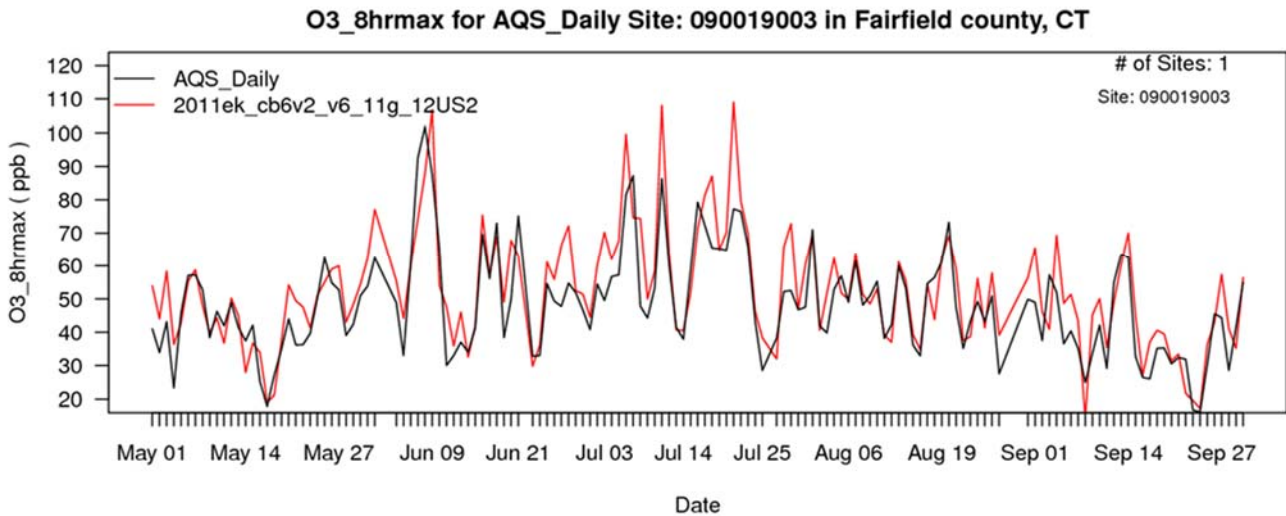


Figure A-17b. Time series of observed (black) and predicted (red) MDA8 ozone for May through September 2011 at site 090019003 in Fairfield Co., Connecticut.

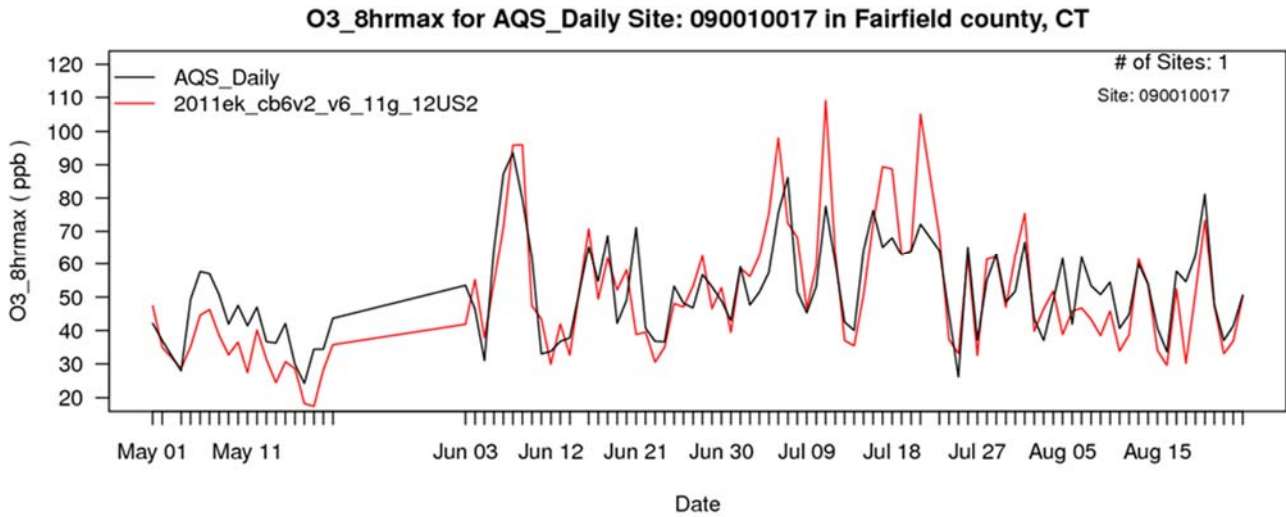


Figure A-17c. Time series of observed (black) and predicted (red) MDA8 ozone for May through September 2011 at site 090010017 in Fairfield Co., Connecticut.

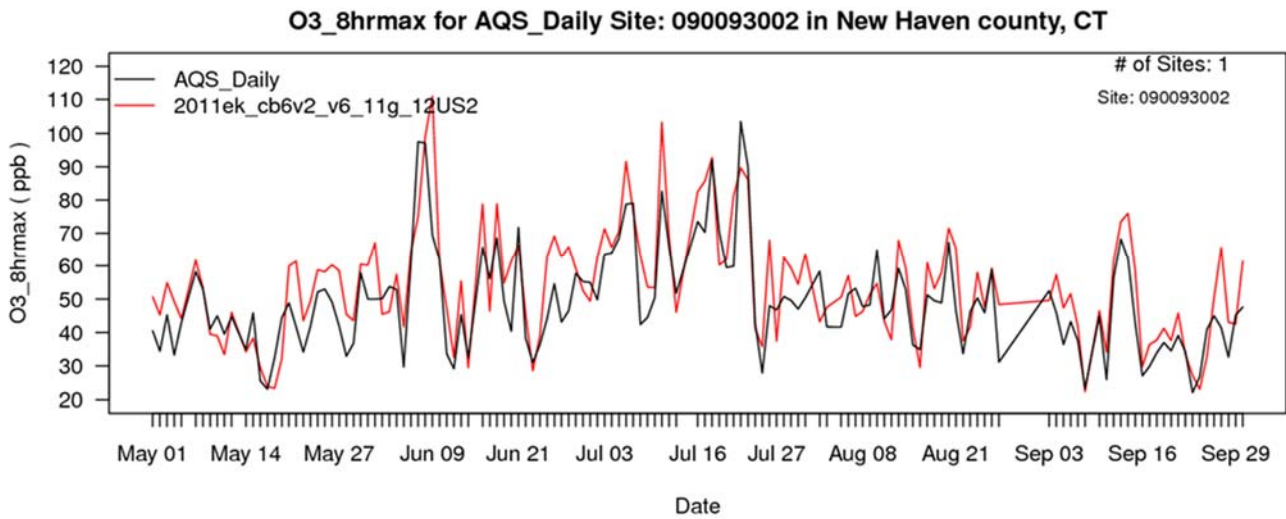


Figure A-17d. Time series of observed (black) and predicted (red) MDA8 ozone for May through September 2011 at site 090093002 in New Haven Co., Connecticut.

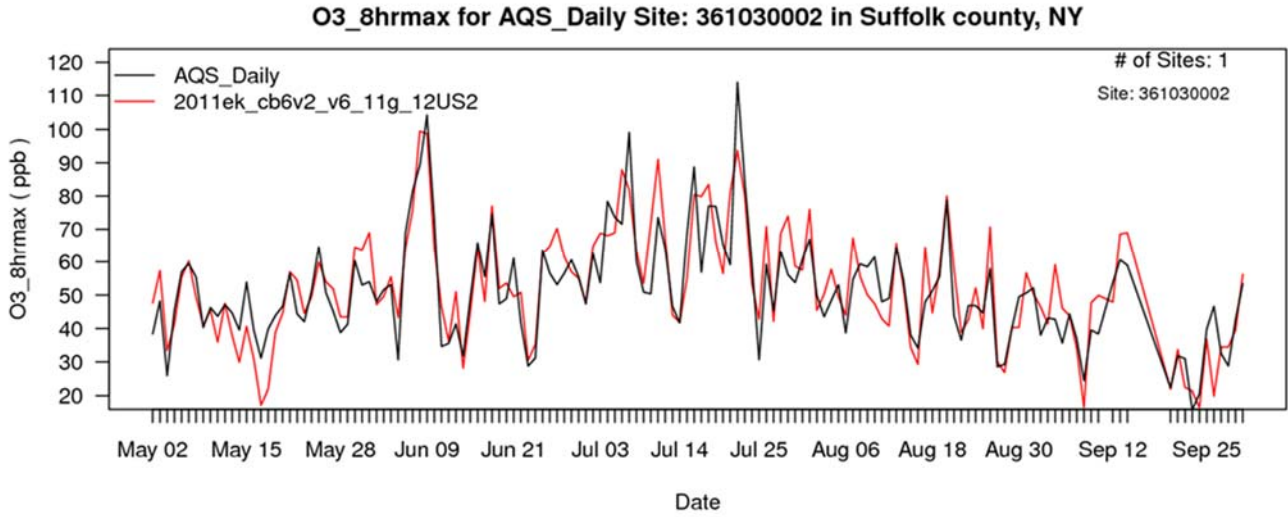


Figure A-17e. Time series of observed (black) and predicted (red) MDA8 ozone for May through September 2011 at site 361030002 in Suffolk Co., New York.

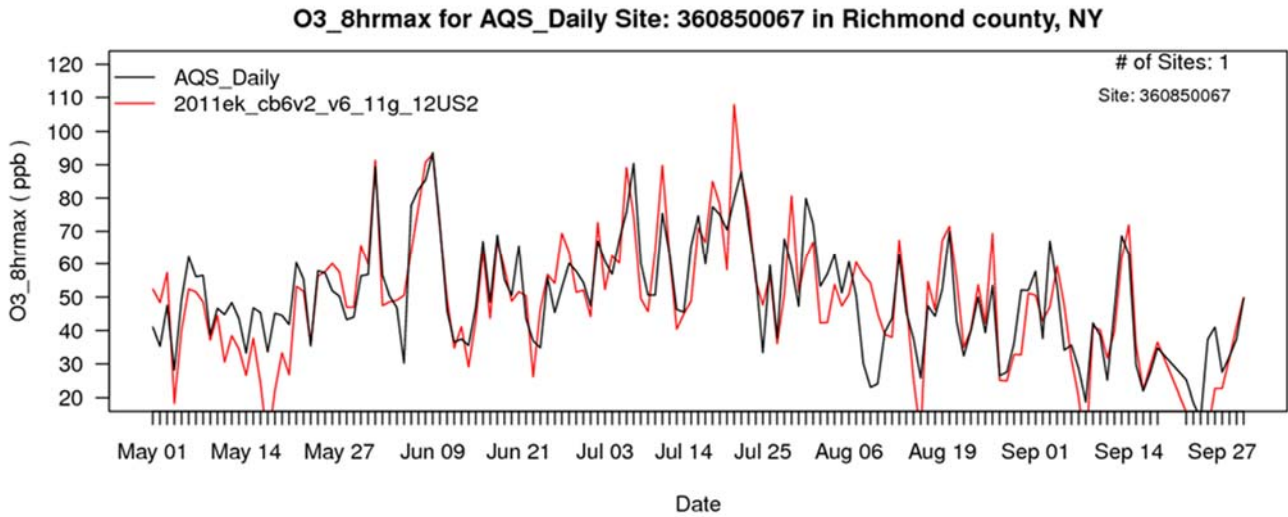


Figure A-17f. Time series of observed (black) and predicted (red) MDA8 ozone for May through September 2011 at site 360850067 in Richmond Co., New York.

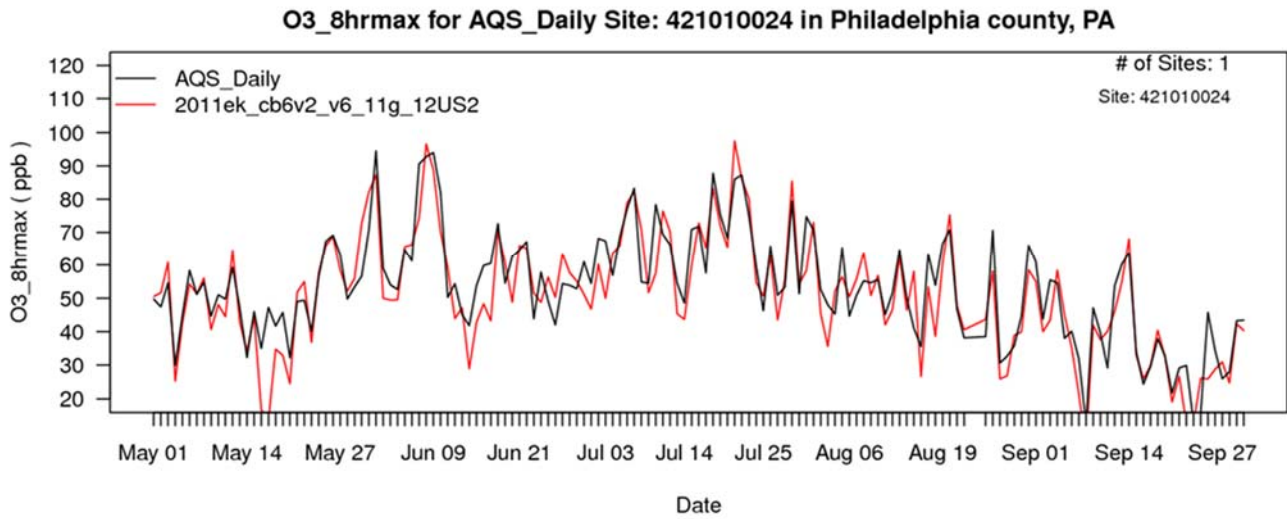


Figure A-17g. Time series of observed (black) and predicted (red) MDA8 ozone for May through September 2011 at site 421010024 in Philadelphia Co., Pennsylvania.

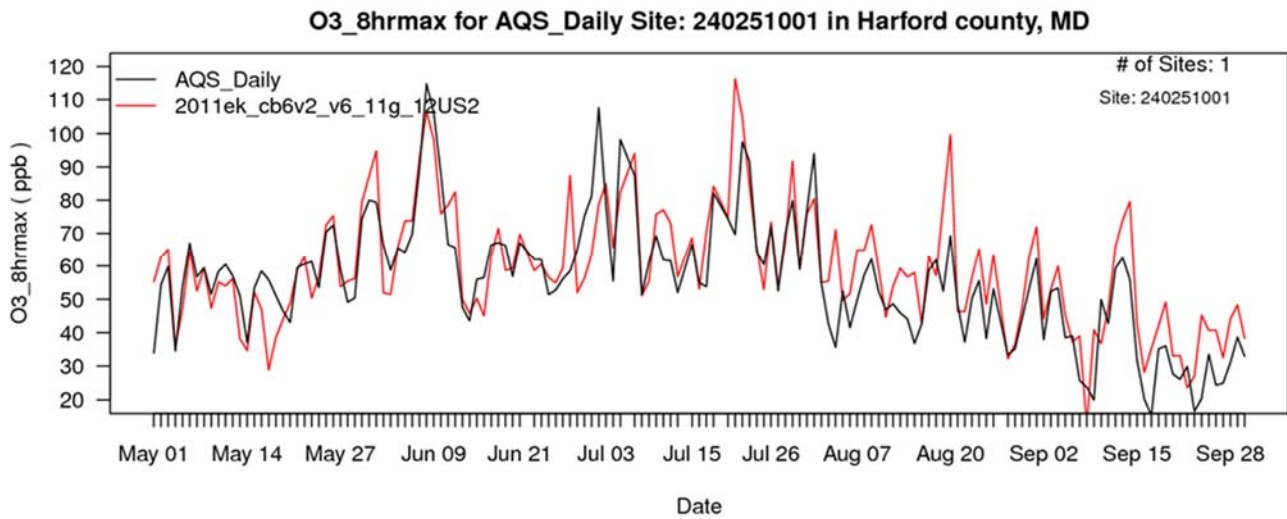


Figure A-17h. Time series of observed (black) and predicted (red) MDA8 ozone for May through September 2011 at site 240251001 in Harford Co., Maryland.

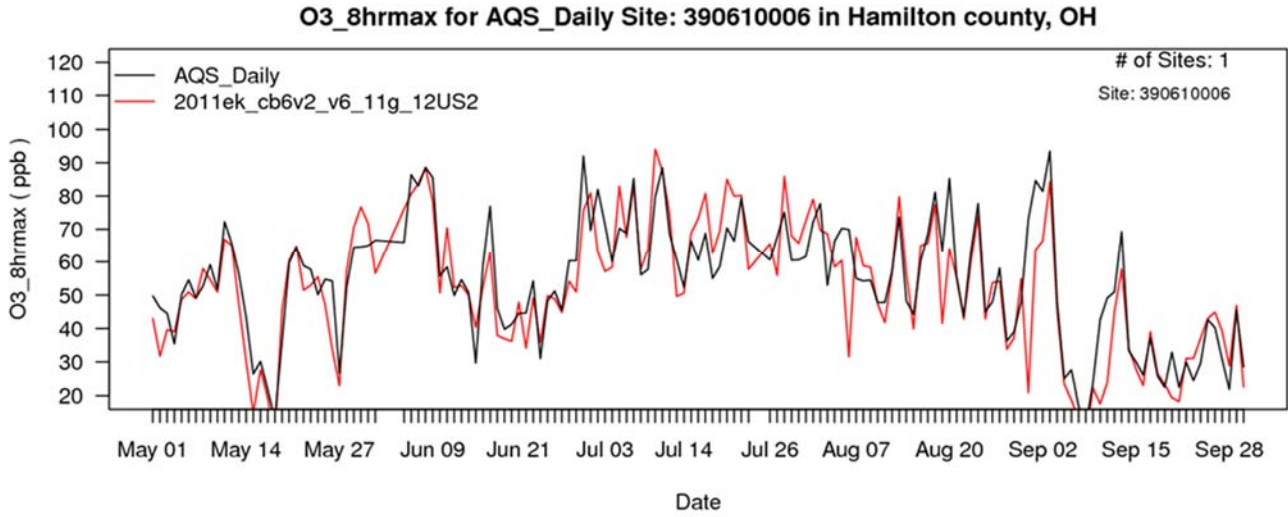


Figure A-17i. Time series of observed (black) and predicted (red) MDA8 ozone for May through September 2011 at site 390610006 in Hamilton Co., Ohio.

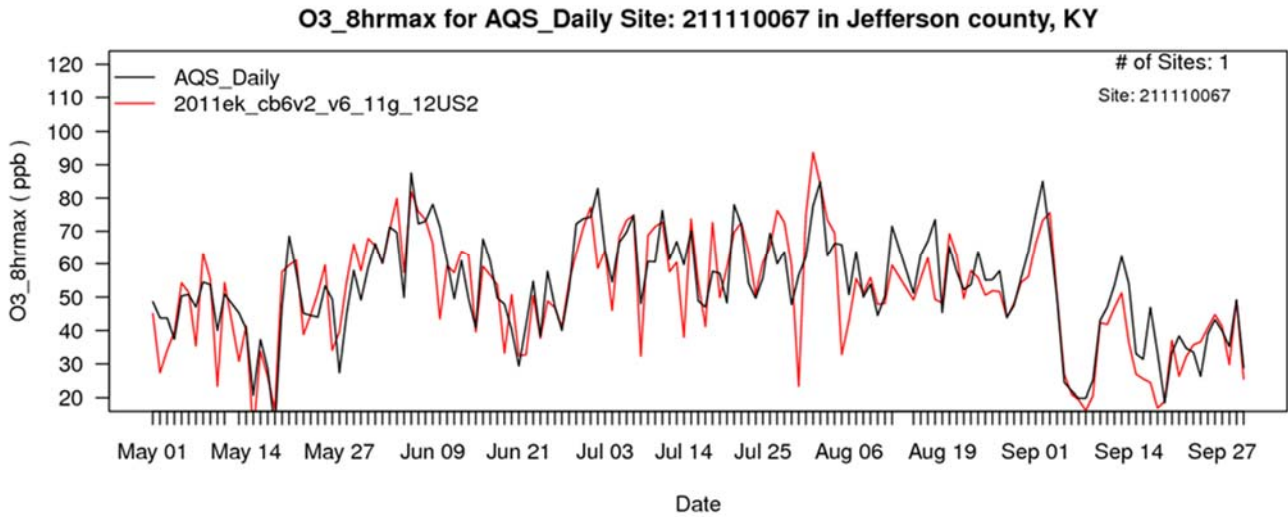


Figure A-17j. Time series of observed (black) and predicted (red) MDA8 ozone for May through September 2011 at site 211110067 in Jefferson Co., Kentucky.

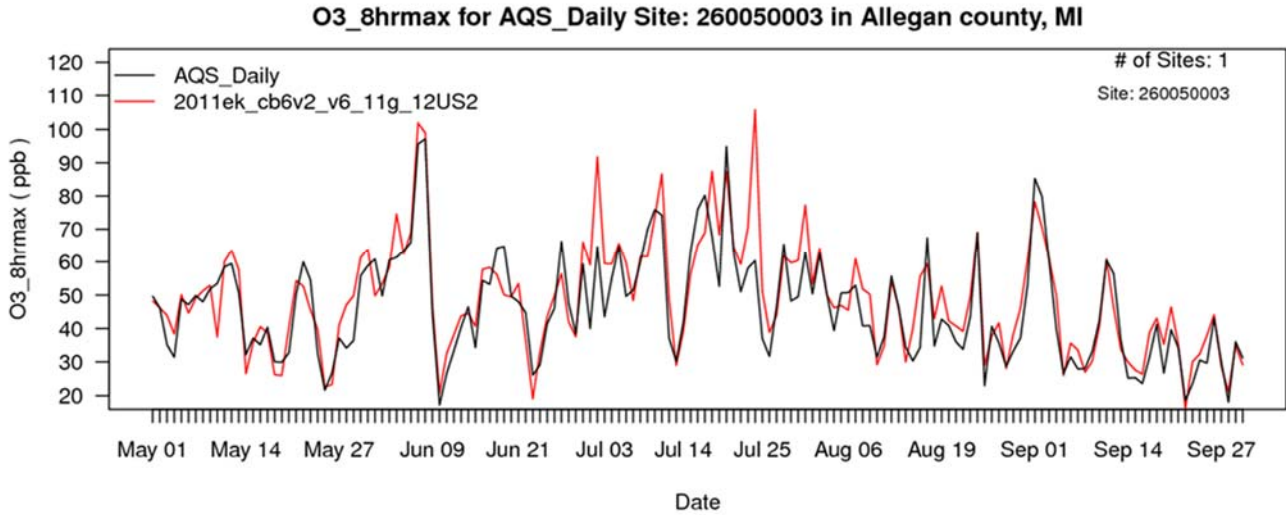


Figure A-17k. Time series of observed (black) and predicted (red) MDA8 ozone for May through September 2011 at site 26005003 in Allegan Co., Michigan.

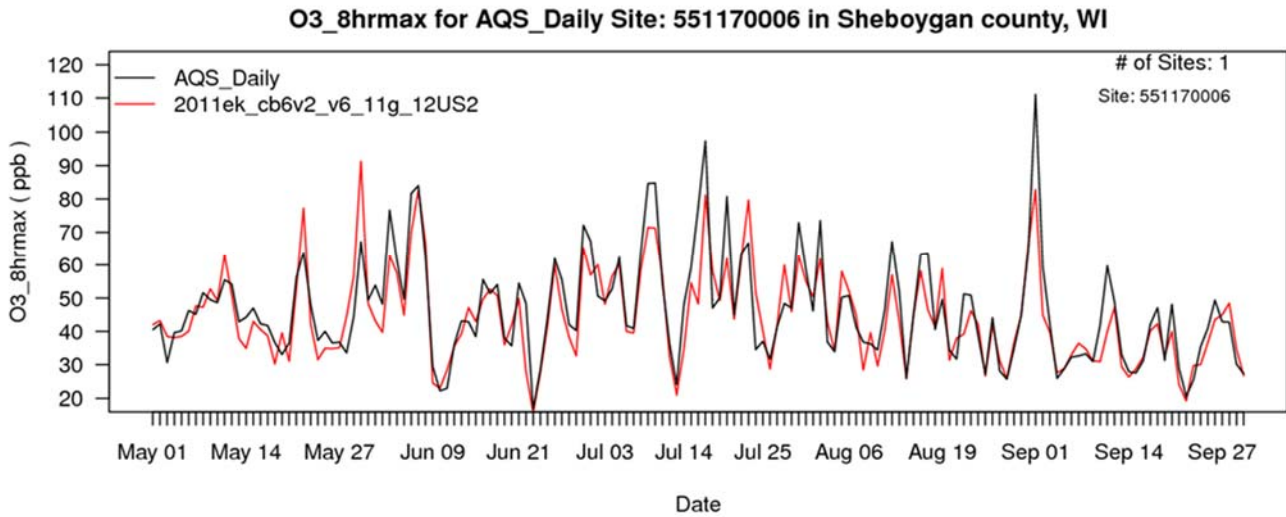


Figure A-17l. Time series of observed (black) and predicted (red) MDA8 ozone for May through September 2011 at site 551170006 in Sheboygan Co., Wisconsin.

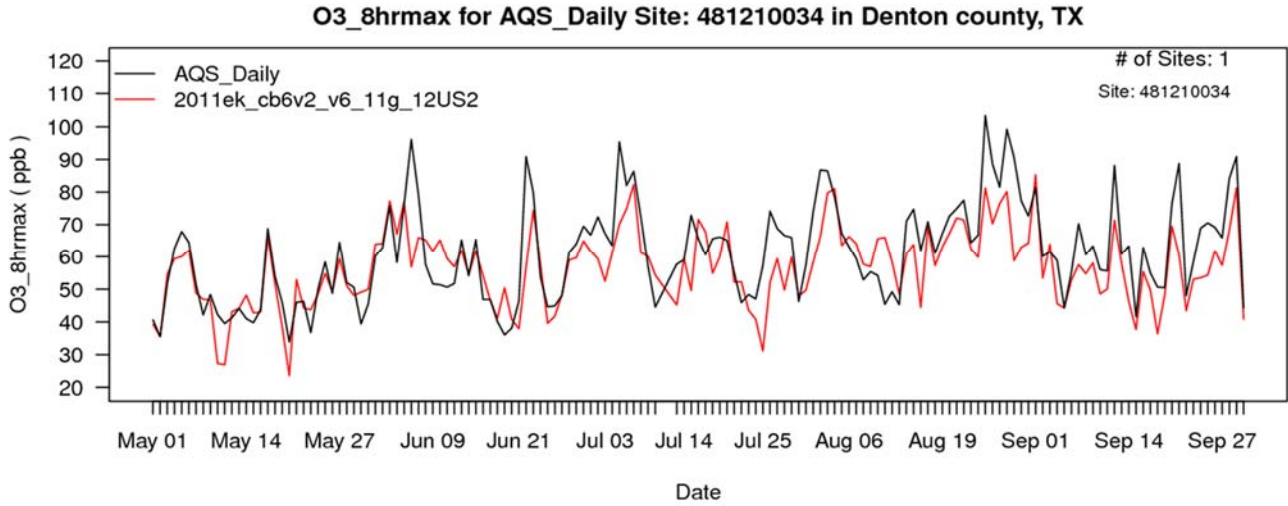


Figure A-17m. Time series of observed (black) and predicted (red) MDA8 ozone for May through September 2011 at site 481210034 in Denton Co., Texas.

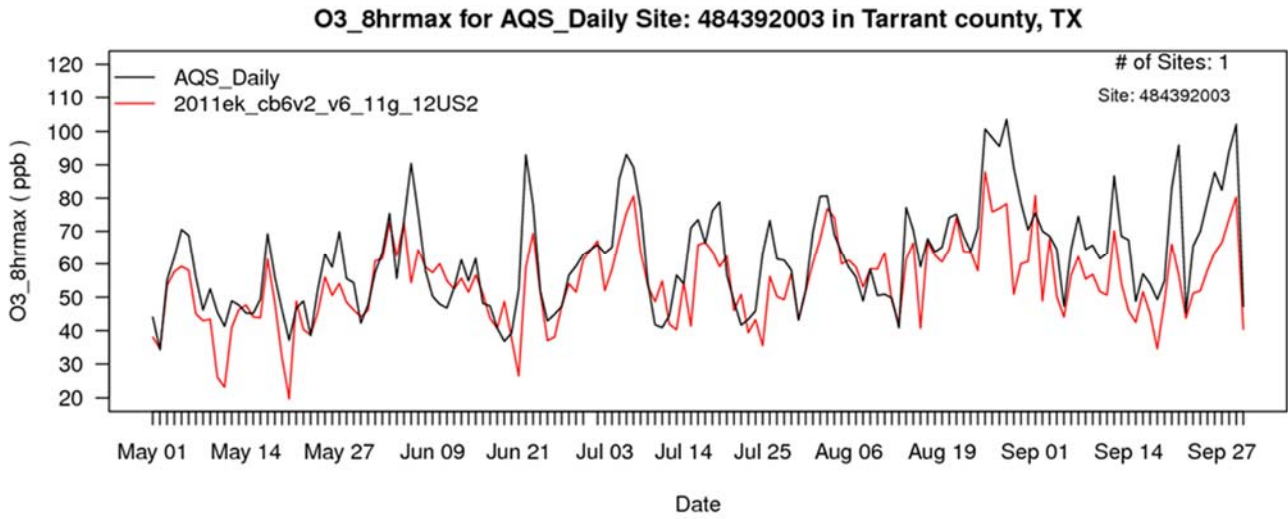


Figure A-17n. Time series of observed (black) and predicted (red) MDA8 ozone for May through September 2011 at site 484392003 in Tarrant Co., Texas.

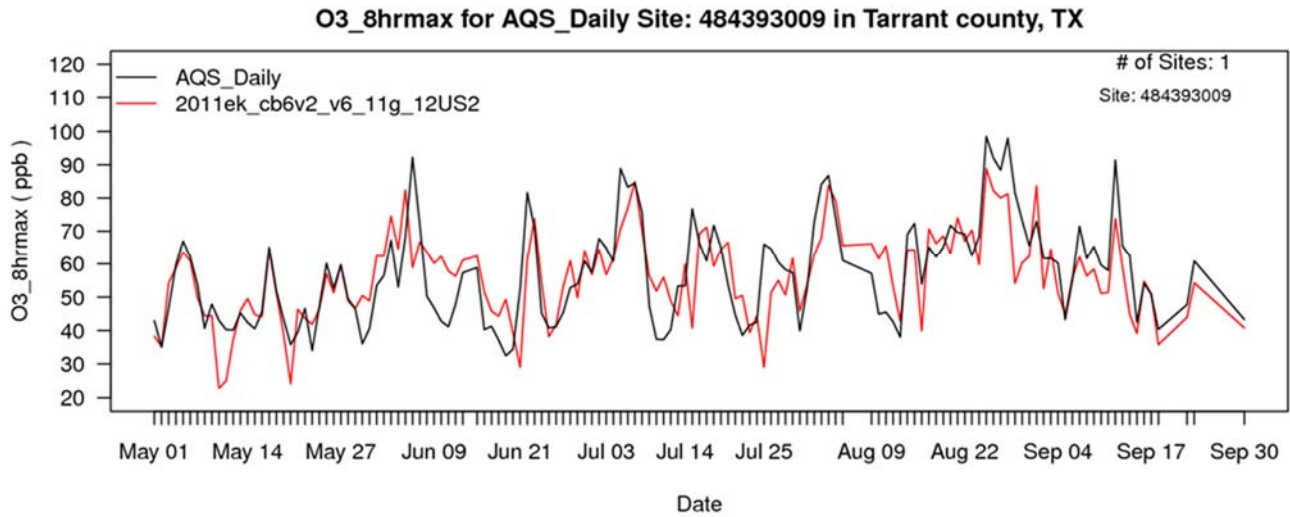


Figure A-17o. Time series of observed (black) and predicted (red) MDA8 ozone for May through September 2011 at site 484393009 in Tarrant Co., Texas.

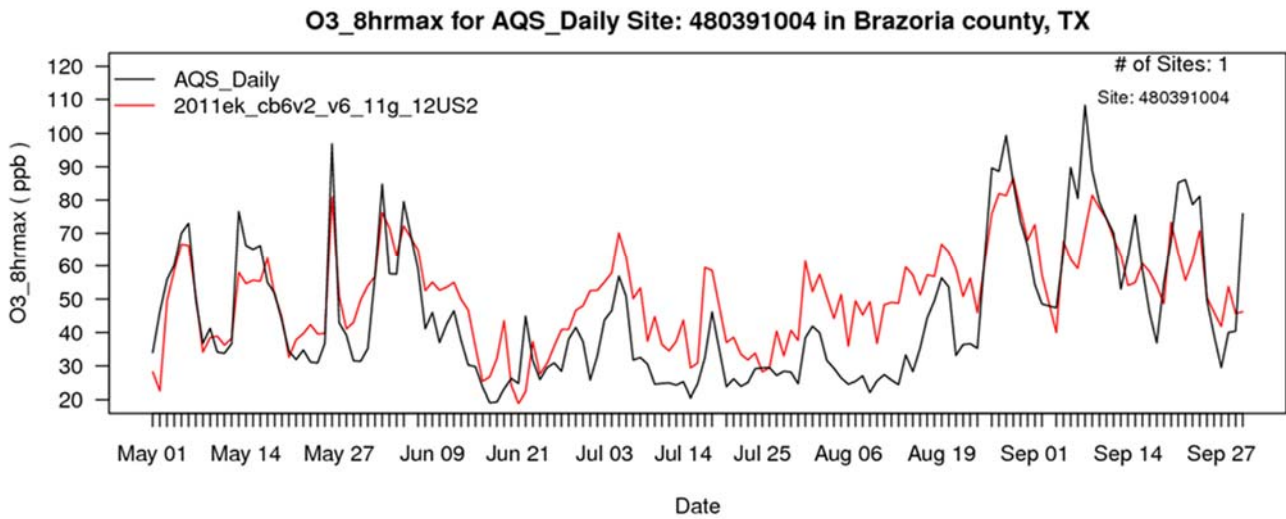


Figure A-17p. Time series of observed (black) and predicted (red) MDA8 ozone for May through September 2011 at site 480391004 in Brazoria Co., Texas.

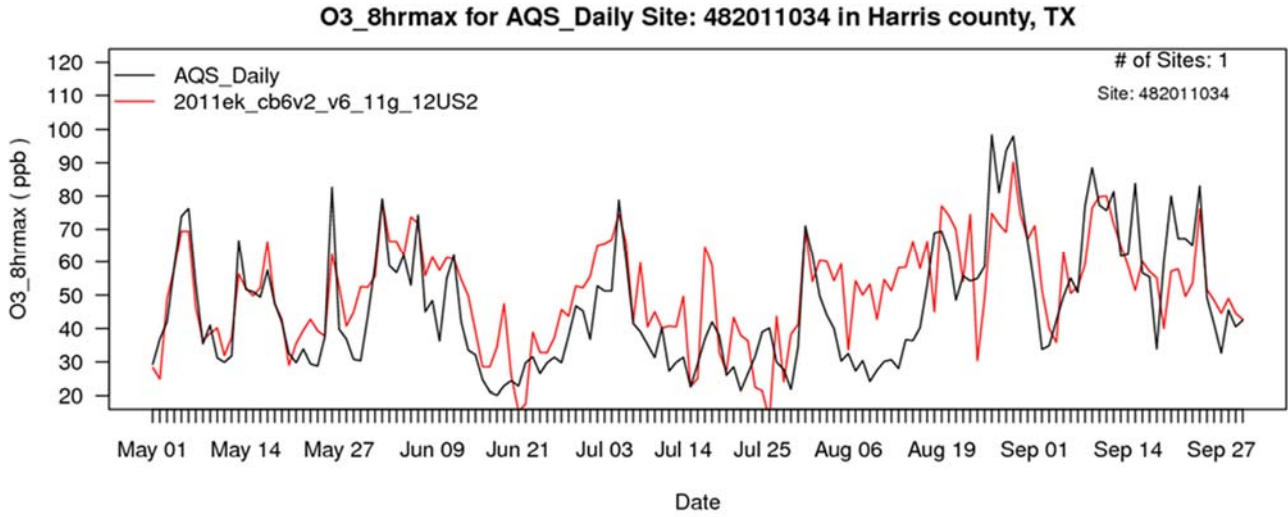


Figure A-17q. Time series of observed (black) and predicted (red) MDA8 ozone for May through September 2011 at site 482011034 in Harris Co., Texas.

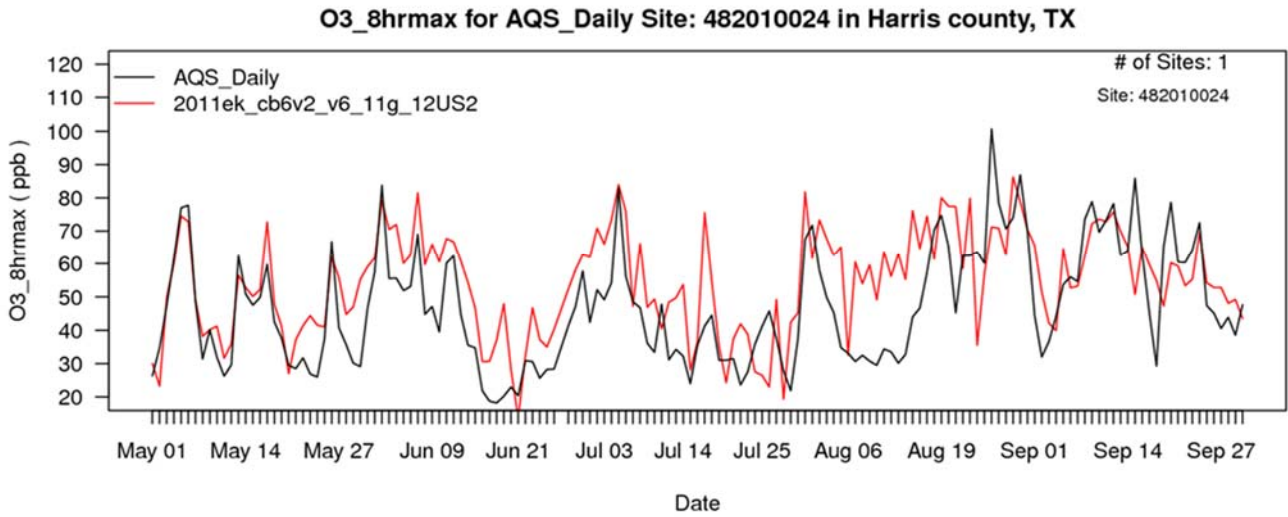


Figure A-17r. Time series of observed (black) and predicted (red) MDA8 ozone for May through September 2011 at site 482010024 in Harris Co., Texas.

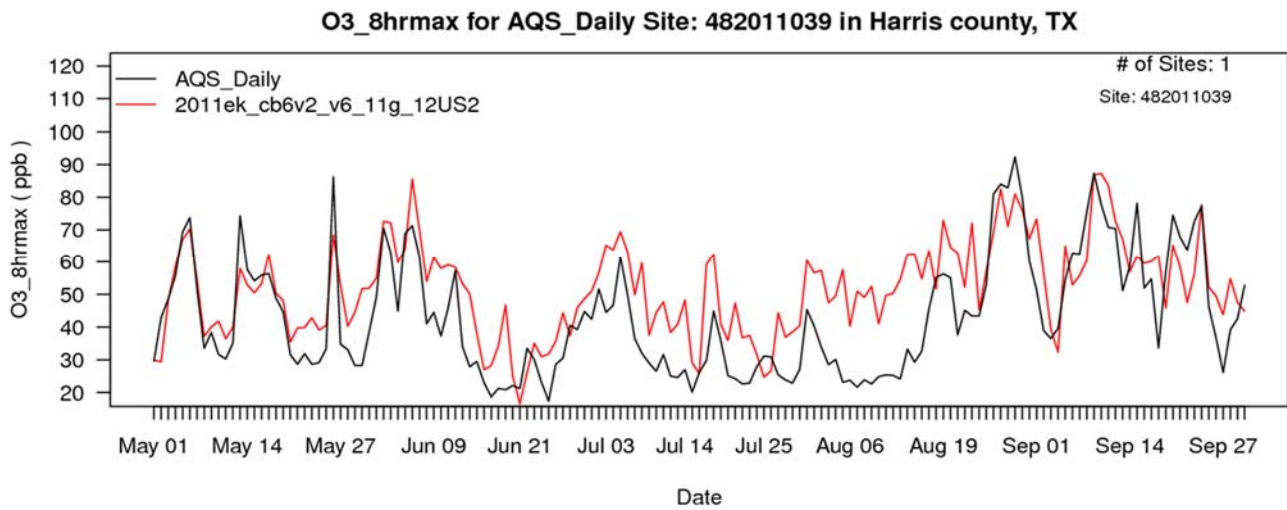


Figure A-17s. Time series of observed (black) and predicted (red) MDA8 ozone for May through September 2011 at site 482011039 in Harris Co., Texas.

This page intentionally left blank

Appendix C

Contributions to 2017 8-Hour Ozone Design Values at Projected 2017 Nonattainment and Maintenance-Only Sites

This page intentionally left blank

This appendix contains tables with the projected ozone contributions from 2017 anthropogenic NO_x and VOC emissions in each state to each projected 2017 nonattainment receptor and each maintenance-only receptor in the eastern U.S. Nonattainment and maintenance-only receptors are defined in section 3 of this TSD. In addition to the state contributions, we have included the contributions from each of the other categories tracked in the contribution modeling including point source emissions on Tribal lands, anthropogenic emissions in Canada and Mexico, emissions from Offshore sources, Fires, Biogenics, as well as contributions from Initial and Boundary concentrations.

For each monitoring site we provide the site ID, state name, and county name in the first three columns of the table. This information is followed by columns containing the projected 2017 average and maximum design values. Next we provide the contributions from each state and the District of Columbia, individually. Lastly, we provide the contributions from the Tribal, Canada and Mexico, Offshore, Fires, Initial and Boundary concentrations, and Biogenics categories. The units of the 2017 design values and contributions are “ppb”. Note that the contributions presented in these tables may not sum exactly to the 2017 average design value due to truncation of the contributions to two places to the right of the decimal.

Contributions to 2017 Nonattainment and Maintenance-Only Sites in the East (Part 1)

Monitor ID	State	County	2017 Average DV	2017 Maximum DV	AZ	AR	CA	CO	CT	DE	DC	FL	GA	ID	IL	IN	IA	KS	KY	LA	ME	MD	MA	MI	MN	MS	MO	MT	
90010017	Connecticut	Fairfield	74.1	76.6	0.11	0.04	0.10	0.03	0.09	6.04	0.07	0.03	0.13	0.01	0.47	0.64	0.11	0.17	0.40	0.05	0.01	1.61	0.06	0.49	0.08	0.07	0.26	0.02	
90013007	Connecticut	Fairfield	75.5	79.7	0.14	0.04	0.15	0.03	0.11	5.18	0.07	0.02	0.19	0.01	0.48	0.75	0.10	0.22	0.44	0.06	0.00	2.11	0.04	0.86	0.11	0.09	0.28	0.03	
90019003	Connecticut	Fairfield	76.5	79.5	0.15	0.04	0.15	0.03	0.11	3.89	0.07	0.02	0.20	0.01	0.47	0.76	0.10	0.22	0.45	0.05	0.00	2.12	0.03	0.84	0.11	0.09	0.28	0.03	
90099002	Connecticut	New Haven	76.2	79.2	0.08	0.04	0.09	0.04	0.09	7.55	0.05	0.03	0.09	0.02	0.54	0.69	0.11	0.17	0.44	0.06	0.00	1.60	0.12	0.47	0.10	0.05	0.29	0.03	
211110067	Kentucky	Jefferson	76.9	76.9	0.04	0.03	0.06	0.06	0.13	0.00	0.03	0.04	0.03	0.04	0.05	1.14	12.32	0.28	23.56	0.09	0.00	0.00	1.16	0.36	0.03	0.29	0.18		
240251001	Maryland	Harford	78.8	81.4	0.29	0.07	0.22	0.07	0.16	0.00	0.03	0.08	0.09	0.30	0.78	2.13	0.24	0.36	2.18	0.14	0.00	26.35	0.00	0.78	0.13	0.10	0.63	0.07	
260050003	Michigan	Allegan	74.7	77.7	0.32	0.08	2.07	0.05	0.22	0.00	0.00	0.13	0.20	0.01	23.61	8.33	0.81	1.22	0.47	0.53	0.00	0.01	0.00	2.86	0.07	0.42	3.78	0.01	
360850067	New York	Richmond	75.8	77.4	0.29	0.08	0.11	0.08	0.15	0.38	0.08	0.10	0.36	0.03	0.68	0.94	0.20	0.27	1.03	0.12	0.00	2.49	0.05	0.66	0.13	0.10	0.41	0.04	
361030002	New York	Suffolk	76.8	78.4	0.18	0.07	0.16	0.07	0.15	0.46	0.32	0.04	0.05	0.19	0.05	0.76	1.01	0.30	0.37	0.65	0.12	0.00	1.42	0.01	1.27	0.18	0.10	0.59	0.07
390610006	Ohio	Hamilton	74.6	77.4	0.73	0.06	0.61	0.08	0.18	0.00	0.00	0.11	0.58	0.04	1.25	7.24	0.30	0.43	10.88	0.24	0.00	0.00	0.00	0.93	0.23	0.29	0.80	0.10	
421010024	Pennsylvania	Philadelphia	73.6	76.9	0.60	0.10	0.27	0.09	0.18	0.03	1.32	0.18	0.16	0.62	0.02	2.75	2.06	0.32	2.36	0.20	0.00	5.22	0.02	0.34	0.08	0.19	0.62	0.04	
480391004	Texas	Brazoria	79.9	80.8	0.58	0.08	1.00	0.22	0.25	0.00	0.00	0.20	0.31	0.10	0.87	0.24	0.43	0.63	0.13	3.01	0.00	0.01	0.00	0.05	0.40	0.81	1.01	0.16	
482100034	Texas	Denton	75.0	77.4	0.68	0.09	0.51	0.13	0.25	0.00	0.00	0.31	0.40	0.06	0.11	0.12	0.08	0.56	0.13	1.89	0.00	0.00	0.11	0.04	0.50	0.27	0.43	0.09	
482100024	Texas	Harris	75.4	77.9	0.22	0.03	0.31	0.12	0.14	0.00	0.00	0.75	0.29	0.00	0.26	0.05	0.13	0.19	0.05	2.21	0.00	0.00	0.00	0.02	0.05	0.20	0.47	0.09	
482011034	Texas	Harris	75.7	76.6	0.53	0.04	0.60	0.11	0.14	0.00	0.00	0.75	0.33	0.06	0.54	0.09	0.41	0.61	0.05	3.03	0.00	0.01	0.00	0.12	0.36	0.66	0.94	0.13	
482011039	Texas	Harris	76.9	78.8	0.41	0.03	1.23	0.10	0.16	0.00	0.00	0.16	0.22	0.05	0.87	0.15	0.33	0.46	0.07	3.20	0.00	0.01	0.00	0.27	0.23	0.79	1.16	0.11	
484392003	Texas	Tarrant	77.3	79.7	0.79	0.09	0.54	0.11	0.31	0.00	0.00	0.34	0.48	0.07	0.17	0.16	0.20	1.13	0.16	1.75	0.00	0.01	0.00	0.22	0.11	0.54	0.31	0.11	
484393009	Texas	Tarrant	76.4	76.4	0.99	0.09	0.34	0.13	0.24	0.00	0.00	0.71	0.60	0.06	0.10	0.12	0.07	0.44	0.14	1.93	0.00	0.02	0.00	0.11	0.04	0.59	0.16	0.09	
551170006	Wisconsin	Sheboygan	76.2	78.7	0.24	0.08	0.55	0.08	0.17	0.00	0.00	0.11	0.12	0.02	17.90	6.49	0.58	0.95	0.68	1.05	0.00	0.02	0.00	2.62	0.07	0.54	1.67	0.03	

Contributions to 2017 Nonattainment and Maintenance-Only Sites in the East (Part 2)

Monitor ID	State	County	2017 Average DV	2017 Maximum DV	NE	NV	NH	NJ	NM	NY	NC	ND	OH	OK	OR	PA	RI	SC	SD	TN	TX	UT	VT	VA	WA	WV	WI	WY
90010017	Connecticut	Fairfield	74.1	76.6	0.07	0.01	0.02	9.38	0.05	18.81	0.38	0.03	1.42	0.21	0.00	7.78	0.01	0.08	0.02	0.20	0.37	0.04	0.01	1.72	0.00	0.82	0.14	0.12
90013007	Connecticut	Fairfield	75.5	79.7	0.08	0.01	0.00	8.14	0.08	16.82	0.49	0.04	1.83	0.23	0.00	8.77	0.01	0.14	0.02	0.31	0.42	0.04	0.00	1.77	0.01	0.94	0.16	0.11
90019003	Connecticut	Fairfield	76.5	79.5	0.08	0.01	0.00	9.52	0.08	17.22	0.51	0.04	1.83	0.23	0.00	9.28	0.00	0.15	0.02	0.32	0.42	0.04	0.00	1.92	0.01	1.04	0.16	0.12
90099002	Connecticut	New Haven	76.2	79.2	0.08	0.01	0.02	7.27	0.05	18.50	0.35	0.04	1.52	0.24	0.00	7.37	0.03	0.06	0.02	0.19	0.41	0.05	0.01	1.11	0.01	0.71	0.17	0.14
211110067	Kentucky	Jefferson	76.9	76.9	0.16	0.02	0.00	0.00	0.08	0.00	0.01	0.22	3.78	0.33	0.02	4.44	0.00	0.01	0.12	0.12	0.61	0.05	0.00	0.00	0.07	0.64	0.54	0.28
240251001	Maryland	Harford	78.8	81.4	0.16	0.02	0.00	0.06	0.12	0.13	0.45	0.08	3.59	0.41	0.02	4.66	0.00	0.10	0.06	0.65	0.80	0.07	0.00	5.21	0.03	3.31	0.24	0.19
260050003	Michigan	Allegan	74.7	77.7	0.16	0.01	0.00	0.00	0.21	0.00	0.05	0.01	0.09	1.62	0.00	0.02	0.00	0.05	0.02	0.69	2.64	0.06	0.00	0.02	0.00	0.03	2.52	0.11
360850067	New York	Richmond	75.8	77.4	0.12	0.02	0.00	11.90	0.13	5.32	0.50	0.05	2.41	0.33	0.01	14.61	0.00	0.13	0.04	0.48	0.69	0.08	0.01	2.31	0.01	1.92	0.31	0.19
361030002	New York	Suffolk	76.8	78.4	0.20	0.02	0.00	11.07	0.09	16.82	0.36	0.13	2.34	0.47	0.01	8.77	0.00	0.08	0.08	0.34	0.72	0.09	0.00	1.53	0.02	0.98	0.25	0.24
390610006	Ohio	Hamilton	74.6	77.4	0.18	0.03	0.00	0.00	0.14	0.11	0.13	0.11	16.83	0.67	0.03	0.35	0.00	0.13	0.06	1.82	1.55	0.08	0.00	0.11	0.04	0.98	0.54	0.21
421010024	Pennsylvania	Philadelphia	73.6	76.9	0.12	0.02	0.00	1.39	0.18	0.19	0.46	0.04	3.70	0.40	0.01	20.14	0.00	0.18	0.04	1.04	0.99	0.08	0.00	2.35	0.01	3.03	0.16	0.17
480391004	Texas	Brazoria	79.9	80.8	0.25	0.08	0.00	0.00	0.12	0.00	0.08	0.06	0.04	0.73	0.05	0.02	0.00	0.08	0.08	0.38	37.06	0.14	0.00	0.04	0.05	0.03	0.33	0.30
481210034	Texas	Denton	75.0	77.4	0.17	0.06	0.00	0.00	0.14	0.00	0.08	0.02	0.10	1.28	0.00	0.03	0.00	0.09	0.03	0.19	32.33	0.15	0.00	0.03	0.02	0.04	0.06	0.27
482010024	Texas	Harris	75.4	77.9	0.07	0.05	0.00	0.00	0.05	0.00	0.23	0.02	0.05	0.21	0.03	0.03	0.00	0.30	0.02	0.09	30.98	0.10	0.00	0.07	0.02	0.05	0.02	0.18
482011034	Texas	Harris	75.7	76.6	0.27	0.04	0.00	0.00	0.05	0.00	0.21	0.06	0.04	1.02	0.02	0.02	0.00	0.26	0.07	0.12	29.80	0.08	0.00	0.07	0.03	0.05	0.24	0.22
482011039	Texas	Harris	76.9	78.8	0.21	0.04	0.00	0.00	0.05	0.01	0.06	0.05	0.03	0.79	0.03	0.02	0.00	0.05	0.05	0.32	32.53	0.07	0.00	0.03	0.03	0.02	0.28	0.21
484392003	Texas	Tarrant	77.3	79.7	0.35	0.05	0.00	0.00	0.15	0.02	0.10	0.04	0.16	2.24	0.03	0.09	0.00	0.11	0.07	0.12	31.46	0.16	0.00	0.05	0.03	0.07	0.13	0.33
484393009	Texas	Tarrant	76.4	76.4	0.15	0.05	0.00	0.00	0.14	0.02	0.18	0.02	0.12	0.86	0.02	0.07	0.00	0.15	0.03	0.23	33.69	0.14	0.00	0.08	0.02	0.07	0.05	0.25
551170006	Wisconsin	Sheboygan	76.2	78.7	0.09	0.02	0.00	0.00	0.21	0.02	0.06	0.04	0.72	1.59	0.01	0.19	0.00	0.04	0.02	0.50	2.18	0.07	0.00	0.07	0.01	0.29	12.44	0.11

Contributions to 2017 Nonattainment and Maintenance-Only Sites in the East (Part 3)

Monitor ID	State	County	2017 Average DV	2017 Maximum DV	Tribal	Canada & Mexico	Offshore	Fires	Initial & Boundary	Biogenics
90010017	Connecticut	Fairfield	74.1	76.6	0.01	0.95	0.73	0.16	15.73	3.21
90013007	Connecticut	Fairfield	75.5	79.7	0.02	1.20	1.28	0.19	16.38	3.92
90019003	Connecticut	Fairfield	76.5	79.5	0.02	1.19	1.18	0.19	16.17	3.93
90099002	Connecticut	New Haven	76.2	79.2	0.02	1.22	2.49	0.17	16.96	3.59
211110067	Kentucky	Jefferson	76.9	76.9	0.02	0.45	0.05	0.18	21.86	6.54
240251001	Maryland	Harford	78.8	81.4	0.03	0.55	0.28	0.31	15.55	5.45
260050003	Michigan	Allegan	74.7	77.7	0.04	0.27	0.31	0.69	11.20	8.46
360850067	New York	Richmond	75.8	77.4	0.03	1.40	0.86	0.26	17.14	4.86
361030002	New York	Suffolk	76.8	78.4	0.03	1.25	1.38	0.29	15.67	4.70
390610006	Ohio	Hamilton	74.6	77.4	0.03	0.64	0.18	0.49	16.97	6.89
421010024	Pennsylvania	Philadelphia	73.6	76.9	0.04	0.45	0.70	0.38	15.56	5.56
480391004	Texas	Brazoria	79.9	80.8	0.03	0.35	1.06	1.52	19.95	6.32
481210034	Texas	Denton	75.0	77.4	0.03	0.39	1.62	0.82	24.26	6.24
482010024	Texas	Harris	75.4	77.9	0.01	0.13	5.71	0.77	27.73	2.56
482011034	Texas	Harris	75.7	76.6	0.01	0.21	3.73	1.78	23.26	4.29
482011039	Texas	Harris	76.9	78.8	0.01	0.27	2.91	2.56	21.10	4.99
484392003	Texas	Tarrant	77.3	79.7	0.03	0.51	1.61	1.54	24.13	5.79
484393009	Texas	Tarrant	76.4	76.4	0.03	0.39	2.00	1.29	23.94	5.19
551170006	Wisconsin	Sheboygan	76.2	78.7	0.03	0.41	0.72	0.50	14.35	7.31

This page intentionally left blank

Appendix D

Analysis of Contributions from Florida

This page intentionally left blank

Reports by the CAMx model developer on the impact of modeling with the latest CAMx halogen chemistry indicates that the updated chemistry results in lower modeled ozone in air transported over saltwater marine environments for multiple days (Yarwood et al., 2012 and 2014). Specifically, the Ramboll Environ 2014 report notes that on days with multi-day transport across the Gulf of Mexico, modeling with the updated chemistry could lower 8-hour daily maximum ozone concentrations by up to 2 to 4 ppb in locations in eastern Texas, including Houston. To determine whether modeling with the updated chemistry could lower the contribution from Florida to these two receptors, we analyzed back trajectories from these receptors on those days when Florida was modeled to contribute at or above the 0.75 ppb threshold. The days analyzed were July 5 and 6 for Harris Co. receptor site 482010024 and June 2 and July 5 for Harris Co. receptor site 482011034. Specifically we created 4-day back trajectories based on the meteorological data used in the air quality modeling with separate trajectories starting at 8:00 am, 12:00 pm, and 3:00 pm LST for each of four vertical levels (250 m, 500 m, 750 m, and 1000 m). The back trajectories which crossed Florida upstream of these days are shown in Figures 4-1a and b. The results show that the paths of the air parcel trajectories for days with contributions at or above the threshold from Florida to the Houston receptors do indeed cross the Gulf of Mexico over multiple days before reaching the receptors in Houston.

In addition to Florida, Mississippi is the only other Gulf Coast state that is only linked to receptors in Houston. We therefore also looked at back trajectories for the linkages between Mississippi and receptors in the Houston area (i.e., receptors in Brazoria Co. site 480391004 and Harris Co., site 4802011039). Specifically, we examined back trajectories from Brazoria Co., TX on June 6 and Harris Co., TX on June 6 and September 11 which are the days that Mississippi contributed at or above the threshold to each of these receptors. The back trajectories for these days that passed over Mississippi upstream of the Houston area are shown in Figure 4-2a and b. These trajectories indicate that air parcels that crossed Mississippi did not traverse the Gulf of Mexico, but rather remained over land for most of the transport time between Mississippi and each of these receptors. Therefore, there is no reason to believe that the contributions from Mississippi to receptors in Brazoria Co., TX and Harris Co., TX would be lower if we had modeled using the updated halogen chemistry. Thus, we can conclude that the source-receptor transport pattern between Florida and Houston involving multi-day transport over the Gulf of

Mexico is unique such that modeling with the updated halogen chemistry would not be expected to affect linkages from other upwind states to receptors in Houston or any other linkages from upwind states to downwind nonattainment and maintenance receptors for the final rule.

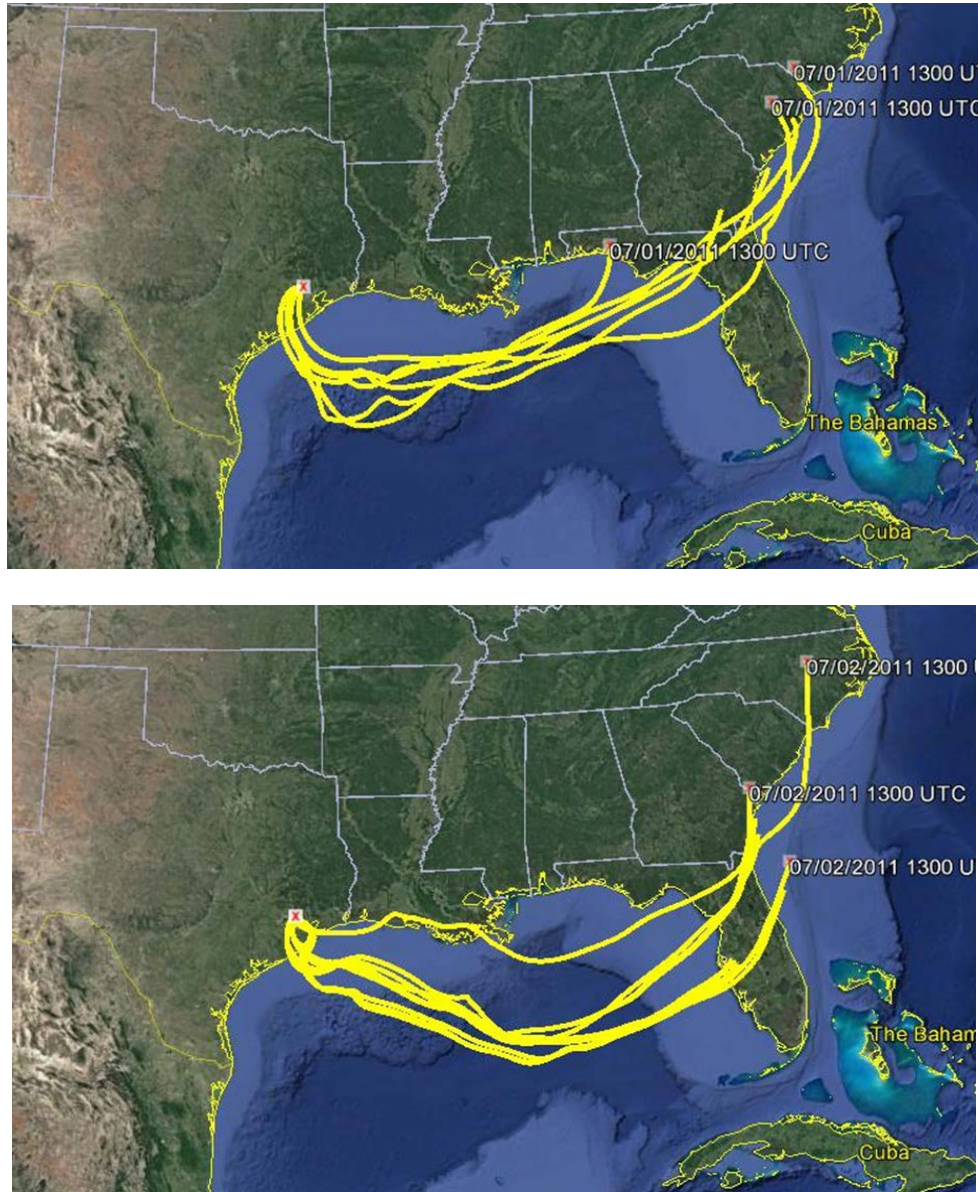


Figure D-1a. Back trajectories from Harris Co., TX site 482010024 on July 5 (top) and July 6 (bottom) when Florida was modeled to contribute at or above the 1 percent threshold to this site.

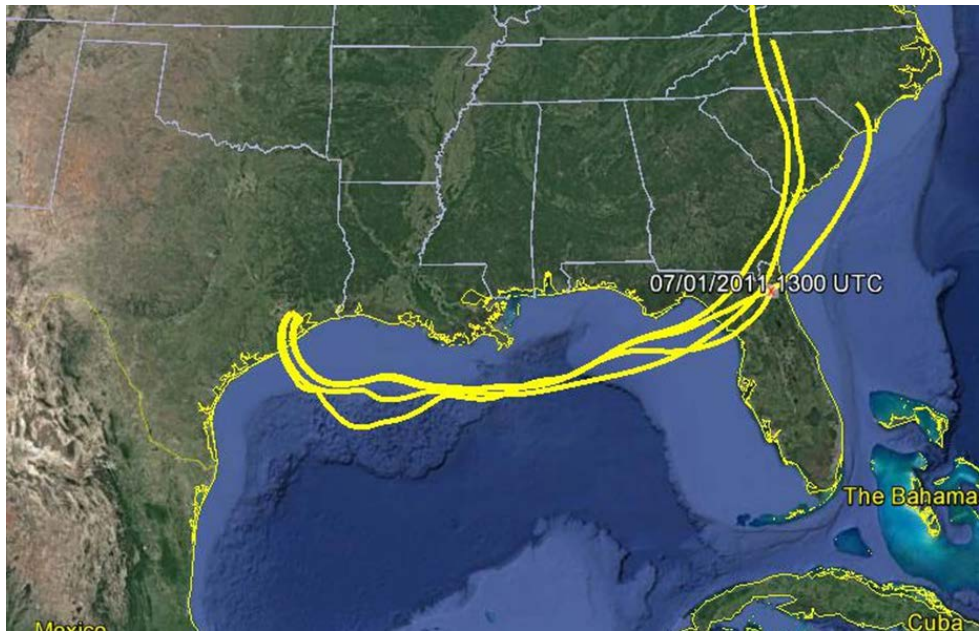
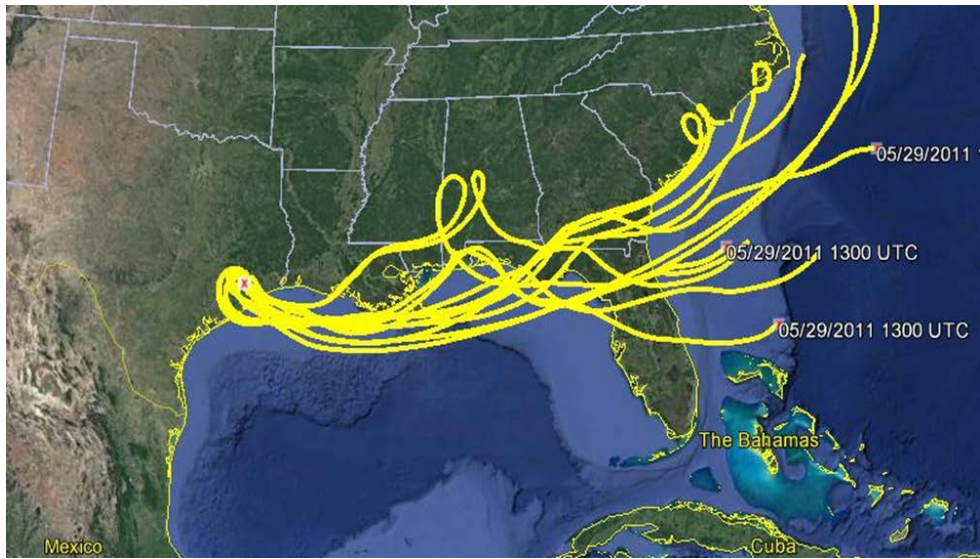


Figure D-1b. Back trajectories from Harris Co., TX site 482011034 on June 2 (top) and July 5 (bottom) when Florida was modeled to contribute at or above the 1 percent threshold to this site.

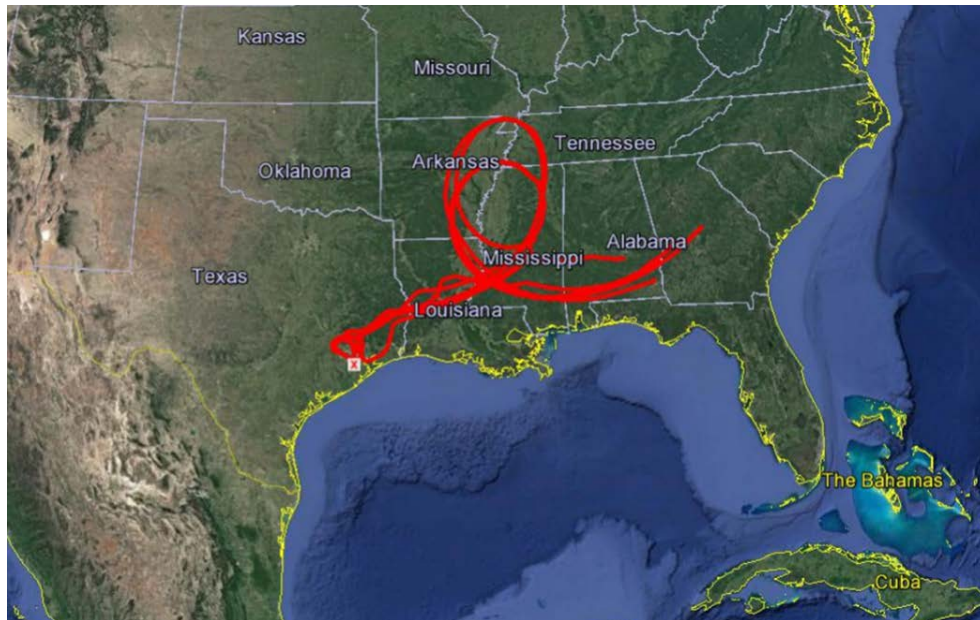


Figure D-2a. Back trajectories from Brazoria Co., TX site 480391004 on June 6 when Mississippi was modeled to contribute at or above the 1 percent threshold to this site.

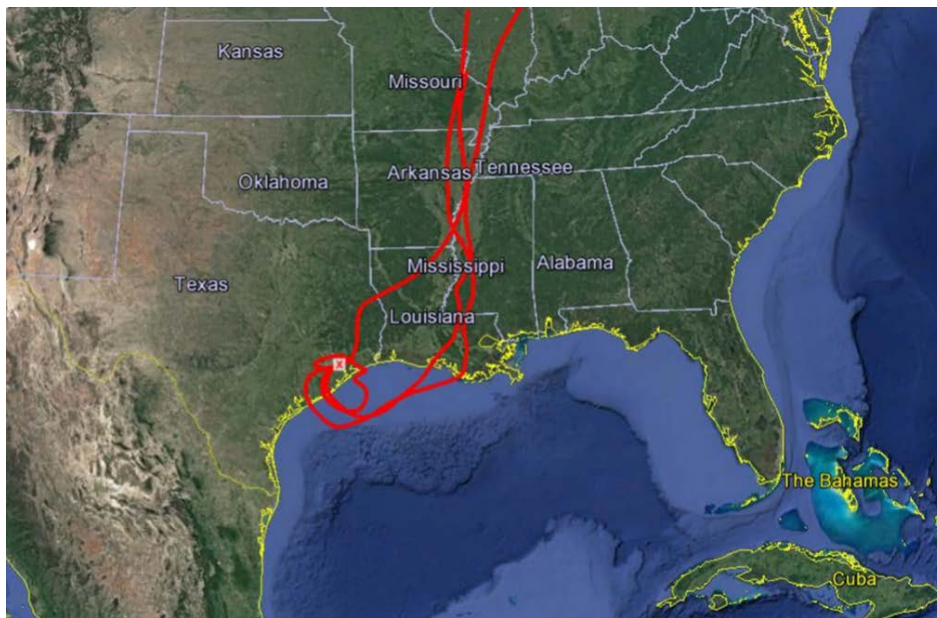
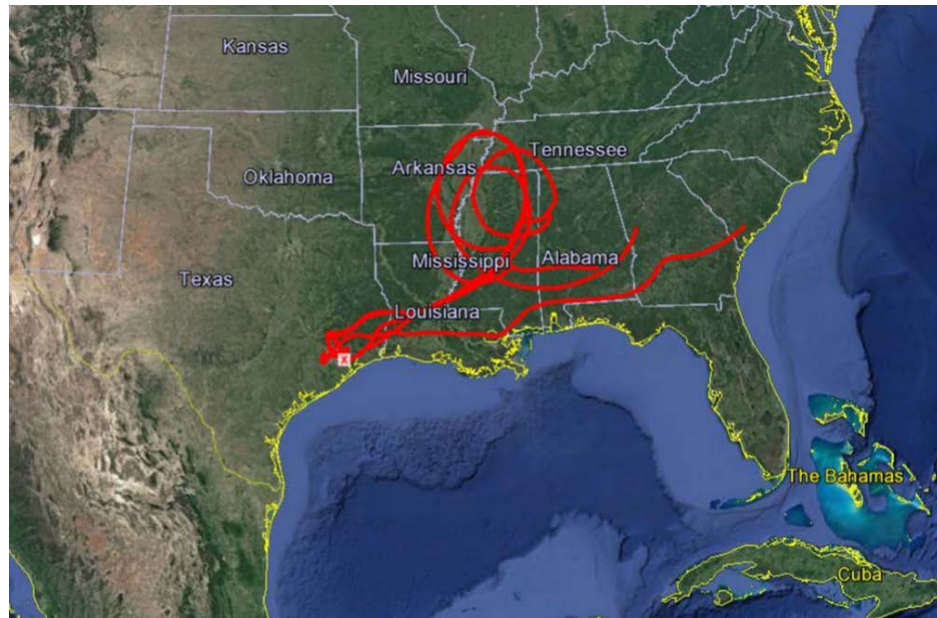


Figure D-2b. Back trajectories from Harris Co., TX site 482011039 on June 6 (top) and September 11 (bottom) when Mississippi was modeled to contribute at or above the 1 percent threshold to this site.

This page intentionally left blank

Appendix E
Back Trajectory Analysis of Transport Patterns

This page intentionally left blank

I. Introduction

This appendix describes the back trajectory analysis performed for each of the 19 nonattainment and maintenance receptors in the final CSAPR Update. The purpose of this analysis is to qualitatively compare the transport patterns, as indicated by back trajectories, to the upwind state-to-downwind receptor linkages identified based on detailed photochemical modeling performed as part of the final CSAPR Update. The modeled contributions of emissions from upwind states to ozone at downwind receptors are the result of the modeled transport meteorology and the emissions of precursor pollutants in combination with the chemical transformation and removal processes simulated by the model. In this analysis, we use back trajectories in a qualitative way to examine one of the factors, the transport patterns, on days with measured ozone exceedances. The back trajectories were calculated using meteorological fields determined based on observations that were constructed in a nearly independent manner from the simulated meteorological fields used in the photochemical modeling for this rule. Therefore, the general consistency between the transport patterns indicated by back trajectories and the upwind/downwind linkages corroborate and add confidence to the validity of the linkages for this rule.

II. Methodology

For the back trajectory EPA used a technique involving independent meteorological inputs to examine the general plausibility of these linkages. Using the HYSPLIT (HYbrid Single-Particle Lagrangian Integrated Trajectory) model along with observation-based meteorological wind fields, EPA created air flow back trajectories for each of the 19 nonattainment or maintenance-only receptors on days with a measured exceedance in 2011 and on exceedance days in several other recent high ozone years (i.e., 2005, 2007, 2010, and 2012). One focus of this analysis was on trajectories for exceedance days occurring in 2011, since this was the year of meteorology that was used for air quality modeling to support this rule. The trajectories during the four additional years were compared to the transport patterns in 2011 to examine whether common transport patterns are present.

The HYSPLIT model developed as a joint effort between NOAA and Australia's Bureau of Meteorology¹ is capable of computing the trajectory (i.e., path) of air parcels through a meteorological wind field. A "back trajectory" calculated by HYSPLIT is essentially the series of locations in the atmosphere that an air parcel occupied prior to arriving at a particular location of interest. Thus, the HYSPLIT model can be used to estimate the history of an air mass prior to arrival over a given air quality monitor at a given time.

Air parcels can follow highly complex, convoluted patterns as they move through the atmosphere. Circular pathways are common due to the clockwise air circulation around high-pressure systems and counter-clockwise circulation around low-pressure systems. A simple west-to-east trajectory could also occur for a parcel following the prevailing westerlies. Local meteorological effects due to land- and sea-breeze air circulations or terrain-induced flows can also influence air-parcel trajectories. Strong variations in wind speed and direction often occur in the vertical direction due to the diminishing impact of the Earth's surface on air motion with vertical distance from the ground. The Earth's surface impacts both

¹ (http://www.arl.noaa.gov/HYSPLIT_info.php)

wind speed and direction because the frictional effect of the surface opposes both the pressure-driven movement of air as well as the turning of the air due to large scale planetary motion. Thus, air masses may come from different directions at different heights. Highly complex air-parcel trajectories are common, because a given air parcel often experiences the combined effects of numerous interacting air flow systems. Pollutants emitted from sources in one area mix upward during the day and are transported with the wind flow at the surface and aloft. At night, the pollutants remaining aloft from emissions on the previous day can travel long distances due to the presence of phenomena such as the “nocturnal jet”, which is a ribbon of strong winds that forms at night just above the boundary layer under certain meteorological conditions.

Air-parcel trajectories were calculated based on meteorological fields obtained from the Eta Data Assimilation System (EDAS)². EDAS is an intermittent data assimilation system that uses successive three-hour model forecasts to generate gridded meteorological fields that reflect observations. The three-hour analysis updates allow for the assimilation of high-frequency observations, such as wind profiler data, Next Generation Weather Radar (NEXRAD) data, and aircraft-measured meteorological data. In this manner, the forecast wind fields are aligned to measured wind data.

For this analysis, site-specific backward air-parcel trajectories were calculated with the HYSPLIT model from heights at 250-m, 500-m, 750-m, 1000-m, and 1500 m above ground level on days with measured exceedances at the given receptor site. The trajectories were initialized at multiple elevations aloft in order to consider the effects of vertical variations in wind flows on transport patterns. Trajectories were tracked backward in time for 96 hours (i.e., 4 days) for each of several time periods (i.e., initialization times) on each exceedance day³. Back trajectories were initialized at 0800, 1200, and 1500 local Standard Time (LST). The morning initialization time roughly corresponds to the time when the morning boundary layer is rising and pollutants that were transported aloft overnight begin to mix down to the surface. The afternoon initialization times roughly span the time of the day with highest ozone concentrations.

Once the trajectories were created, they were converted to geographic files that can be read by programs such as Google Earth or ArcGIS. These files enable the characterization of the geographic location of each trajectory for every hour that was run. The point locations along the trajectory paths were used to create line densities that correlate to the number of times a trajectory passed through a geographic area. These line densities provide a general sense of the frequency at which an air parcel passed over given areas.

The back trajectories are considered to corroborate the upwind state-downwind receptor linkages if the density plots indicate that air parcels cross over some portion of each upwind state that is linked to that receptor, as determined from the final CSAPR Update modeling. Such a connection indicates that the observed wind patterns can transport pollutants from the upwind state to the downwind receptor and

² (EDAS; <http://ready.arl.noaa.gov/edas40.php>)

³ We selected 96 hours for calculating back trajectories to reveal multi-day interstate transport patterns while recognizing that the accuracy of the trajectory paths decreases with time.

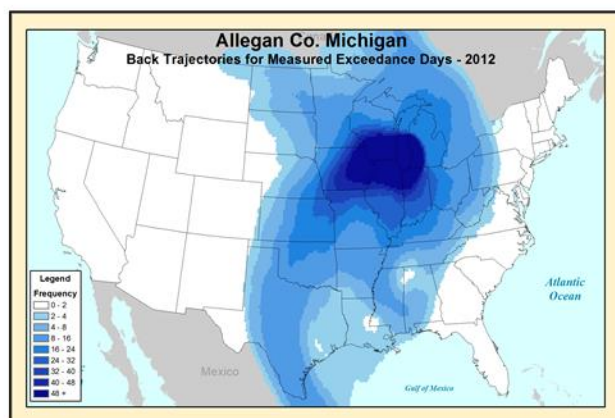
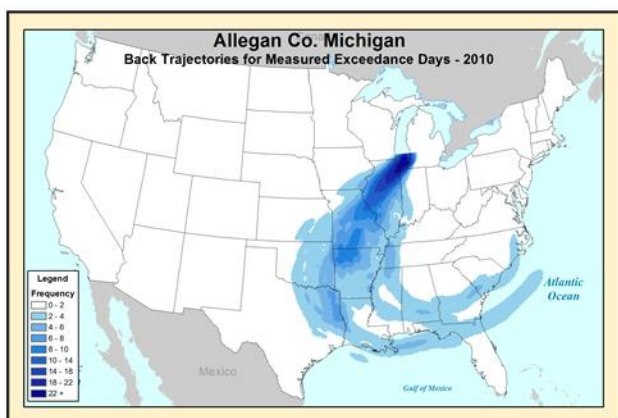
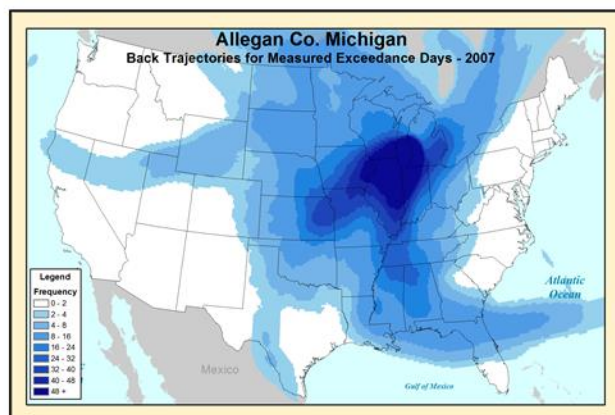
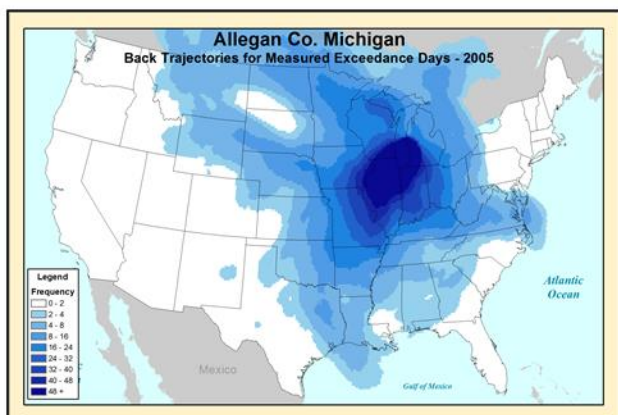
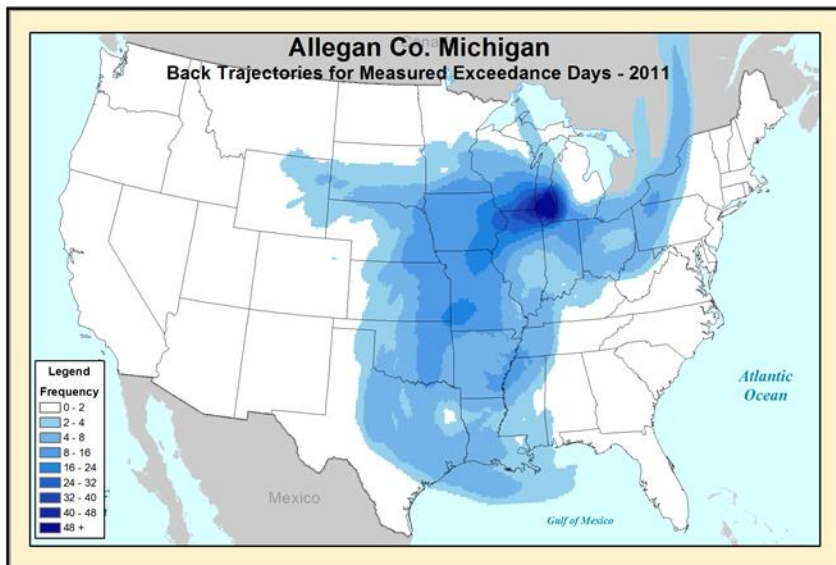
potentially impact ozone concentrations on exceedance days at the receptor. Due to vertical and temporal variations in wind speed and direction, not all trajectories from upwind states are expected to have traversed each upwind state at all vertical levels and times.

The photochemical modeling, which combines spatially refined hourly pollutant precursor emissions with hourly wind fields, and additional meteorological effects is specifically designed to treat time varying pollutant formation and transport. Thus, while a finding that the transport patterns based on the HYSPLIT back trajectories are consistent with the transport patterns evident from upwind state-downwind receptor linkages provides a means to corroborate the robustness of the linkages, the failure of backward trajectories to align precisely with any individual linkage does not undermine the credibility of that linkage.

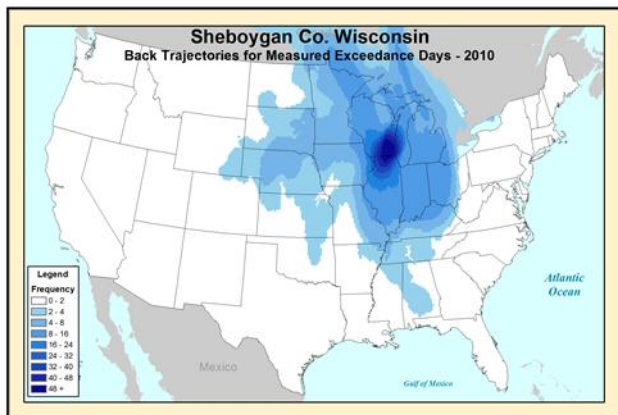
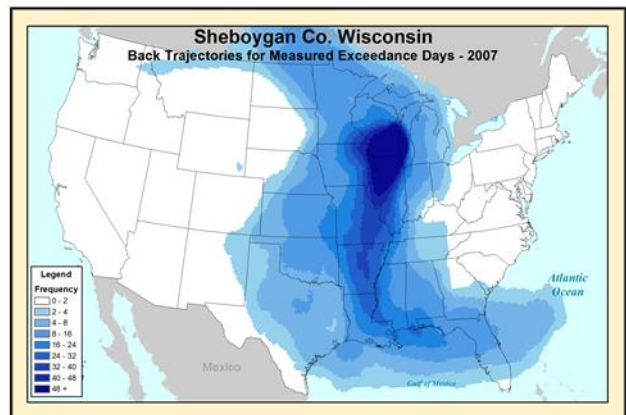
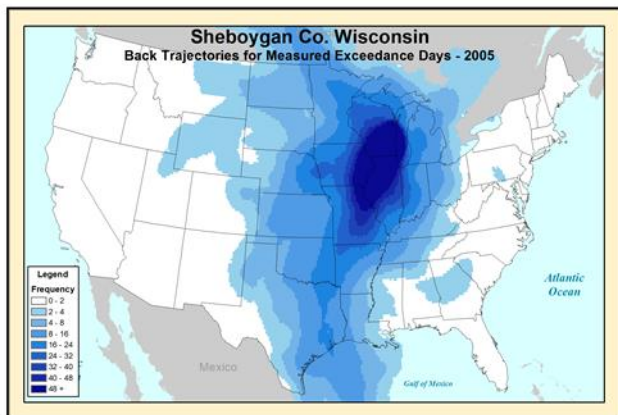
Furthermore, since the back trajectory calculations do not account for any air pollution formation, dispersion, transformation, or removal processes as influenced by emissions, chemistry, deposition, etc., the trajectories cannot be used to develop quantitative contributions and, thus, cannot be used to quantitatively evaluate the magnitude of the existing photochemical contributions from upwind states to downwind receptors. The intersection of upwind states by back trajectories from a particular receptor does not necessarily imply how much the upwind state contributes to ozone at that receptor. Also, there are cases in which the back trajectories from certain receptors cross other states that are not “linked” to that receptor. This is most likely due to the influence on pollution concentrations of meteorological conditions (e.g., temperature, clouds, and mixing) that are present when the air parcels cross these other states. In this regard, photochemical model simulations with chemistry and detailed source-apportionment tracking of pollutants, as used for the final CSAPR Update, are needed in order to quantify the magnitude of upwind state-to-downwind receptor contributions. However, if the transport patterns for observed exceedance days are consistent with the upwind/downwind relationships based on the modeled linkages then this provides important corroborative support for the modeled linkages because it indicates that the modeled transport patterns are consistent with transport patterns based on observed meteorological data.

Back trajectories for each of the 19 nonattainment and maintenance receptors on days with measured exceedances in 2005, 2007, 2010, 2011, and 2012 are provided in the remainder of this appendix. At the top of each page we identify the receptor and the upwind states that are linked to that receptor.

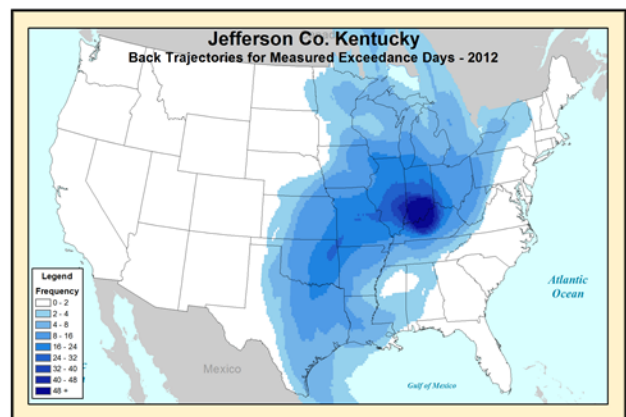
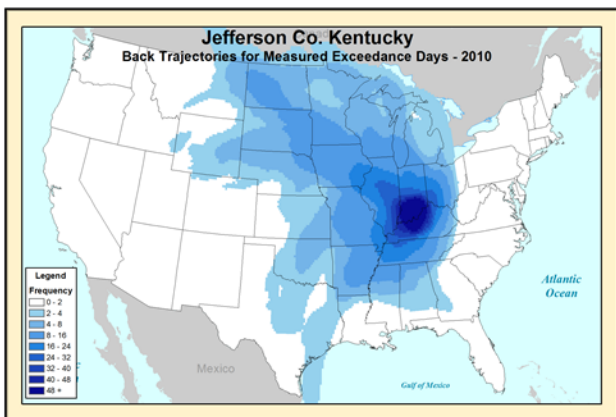
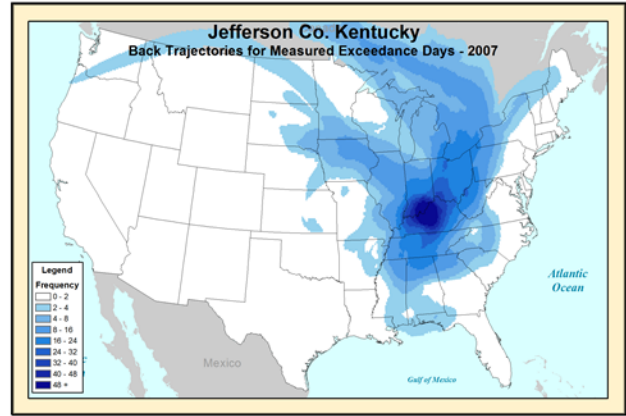
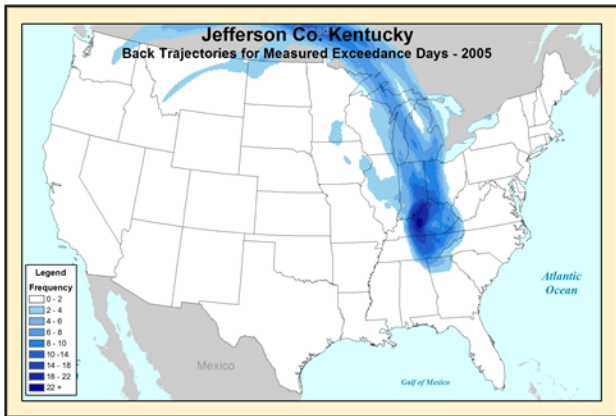
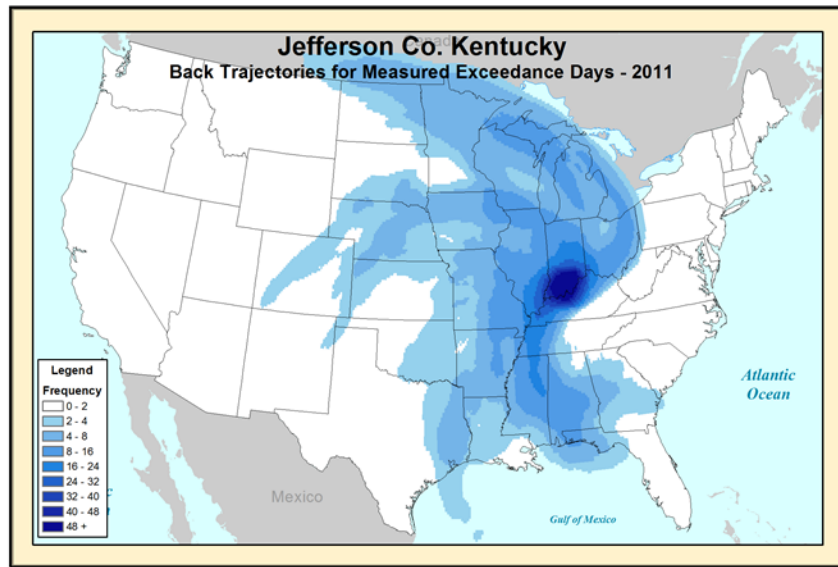
Upwind states linked to Allegan Co., MI site 260050003: AR, IL, IN, IA, KS, MO, OK, TX, and WI.



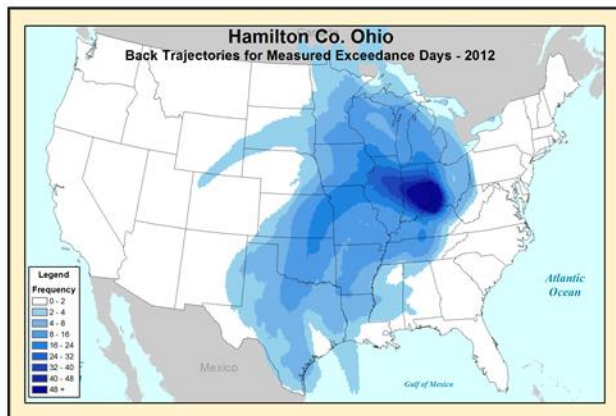
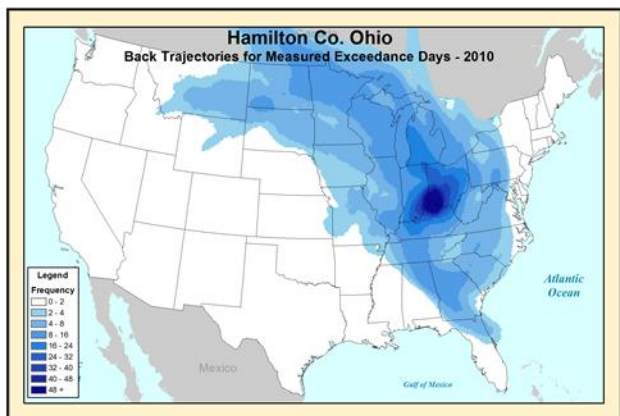
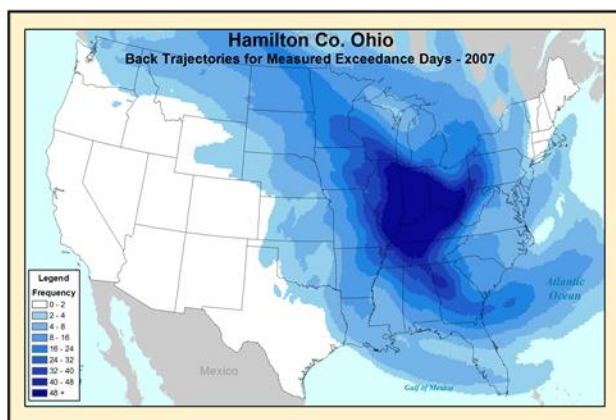
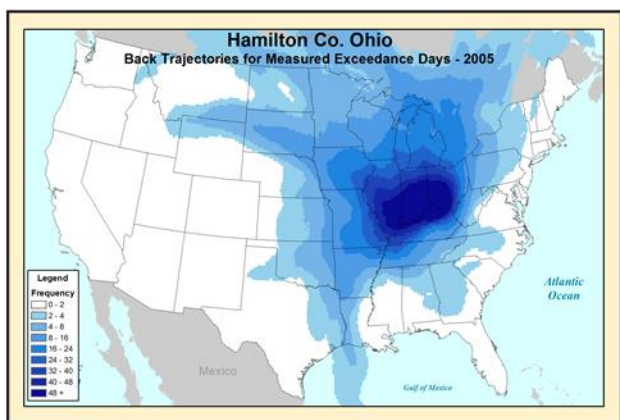
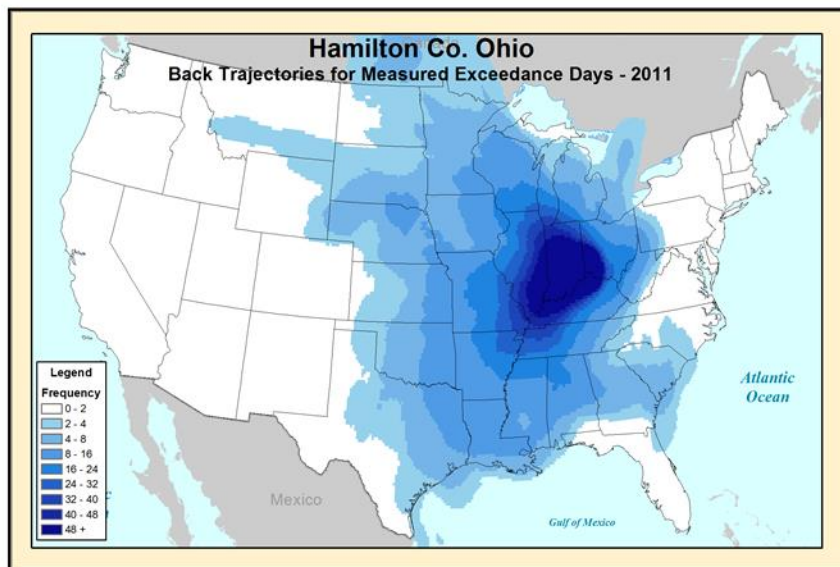
Upwind states linked to Sheboygan Co., WI site 551170006: IL, IN, KS, LA, MI, MO, OK, and TX.



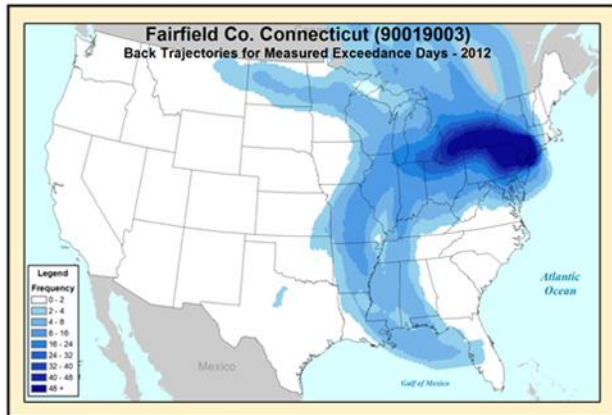
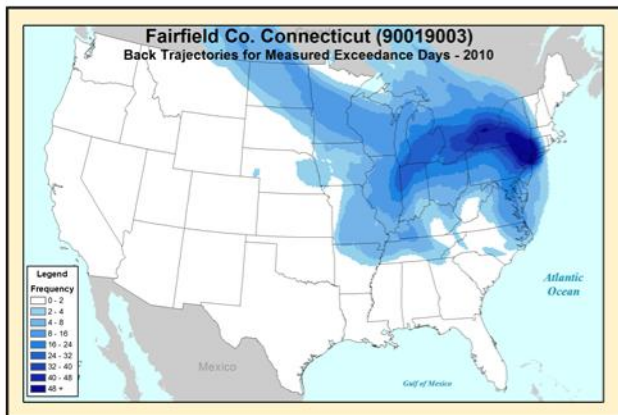
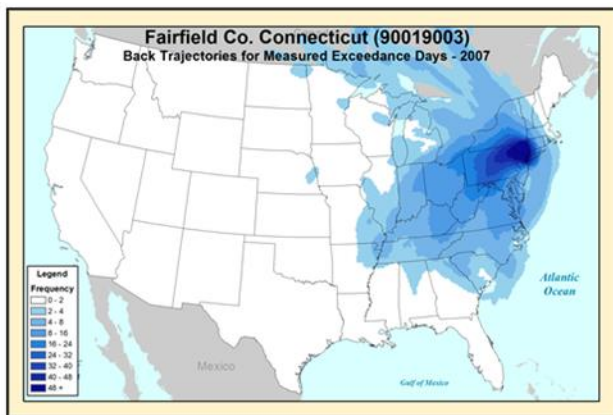
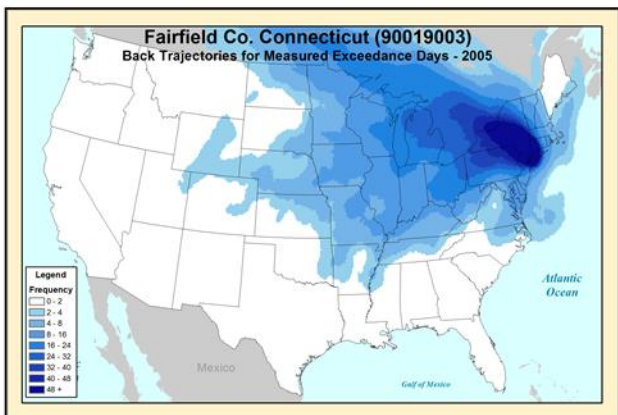
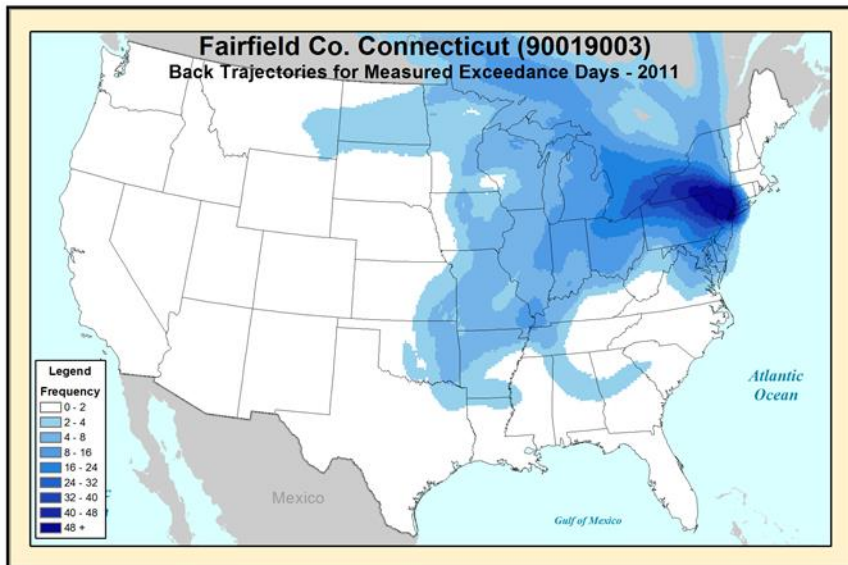
Upwind states linked to Jefferson Co., KY site 211110067: IL, IN, MI, and OH.



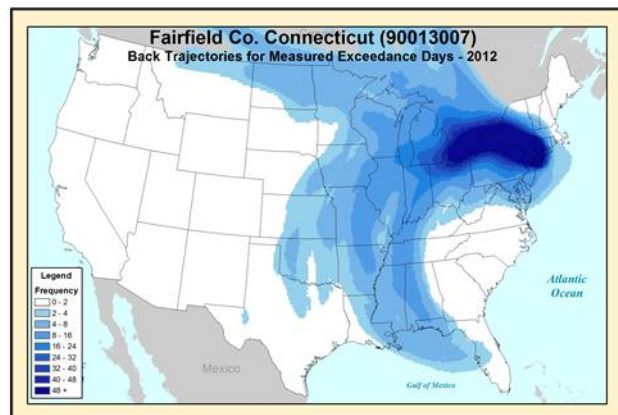
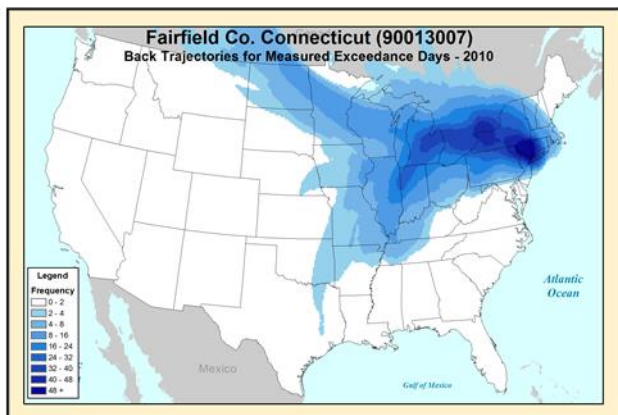
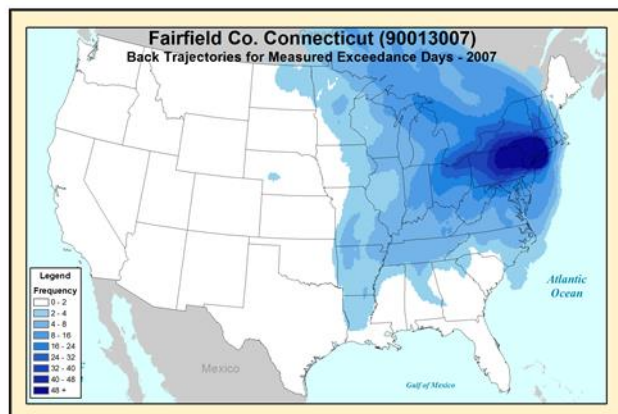
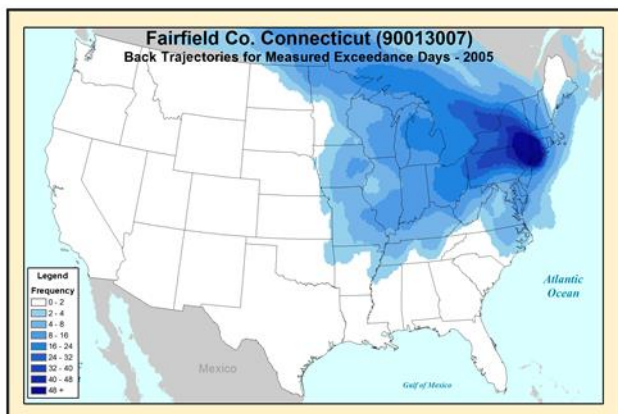
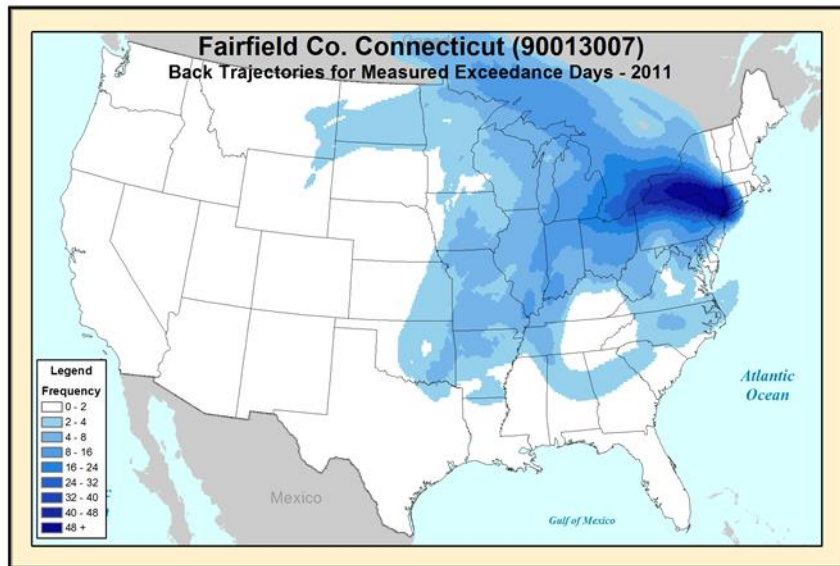
Upwind states linked to Hamilton Co., OH site390610006: IL, IN, KY, MI, MO, TN, TX, and WV.



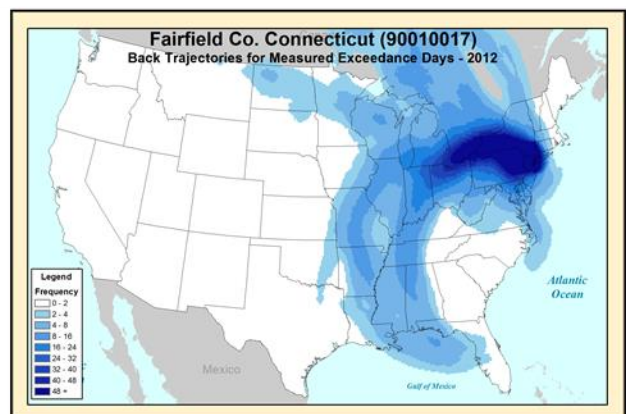
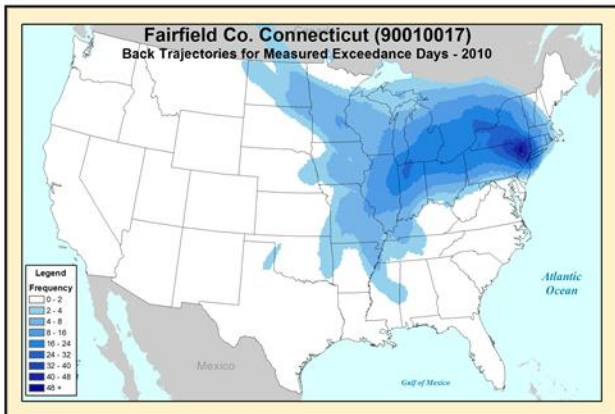
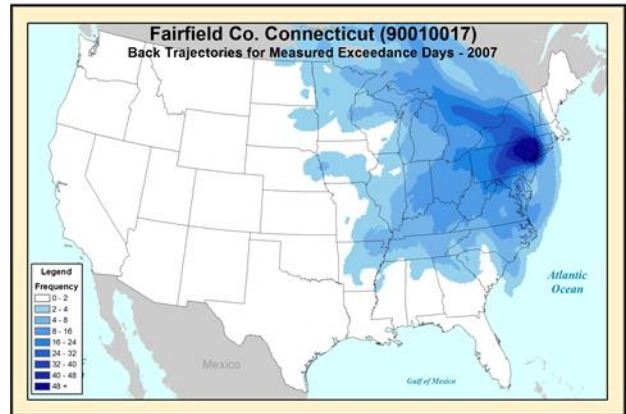
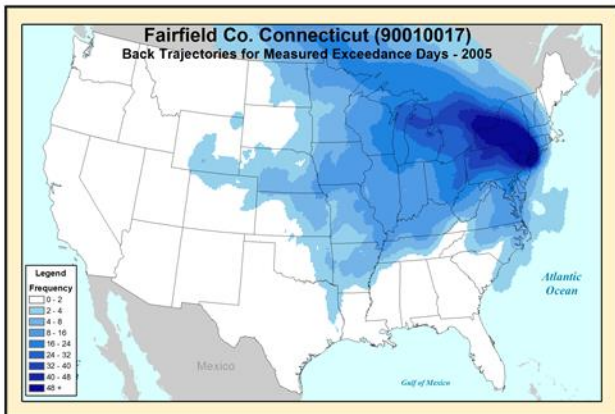
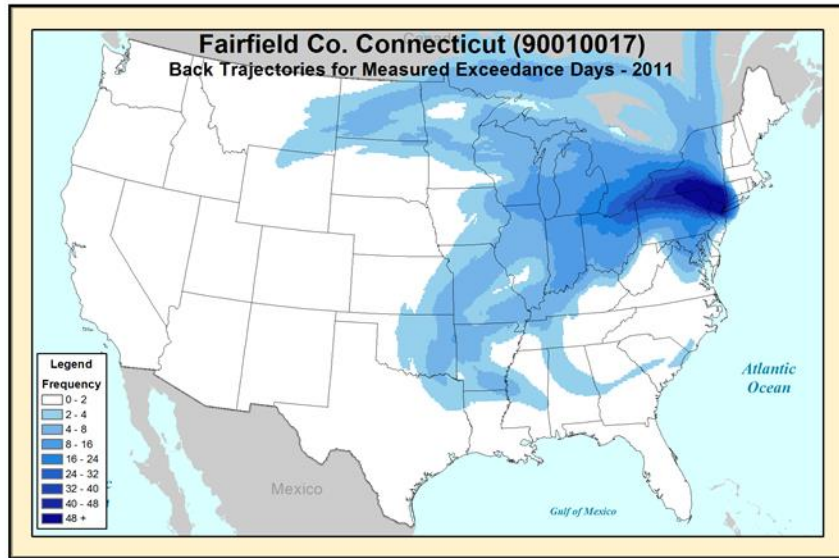
Upwind states linked to Fairfield Co., CT site 090019003: IN, MD, MI, NJ, NY, OH, PA, VA, and WV.



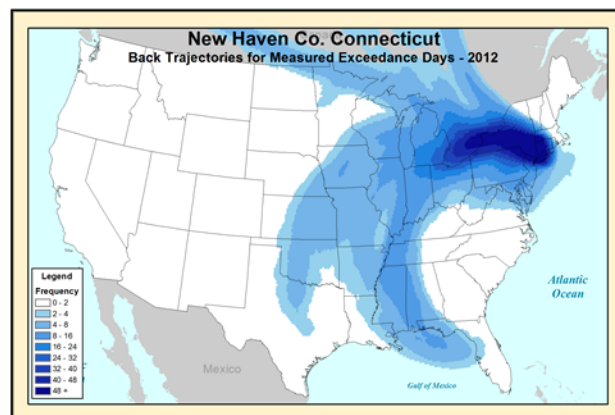
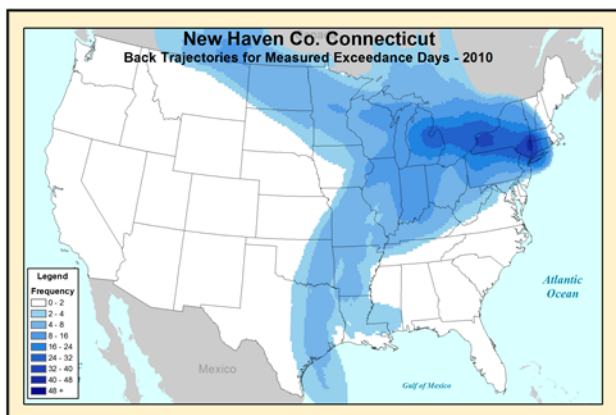
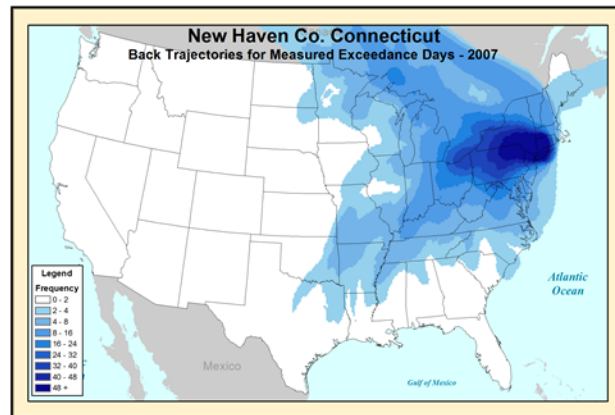
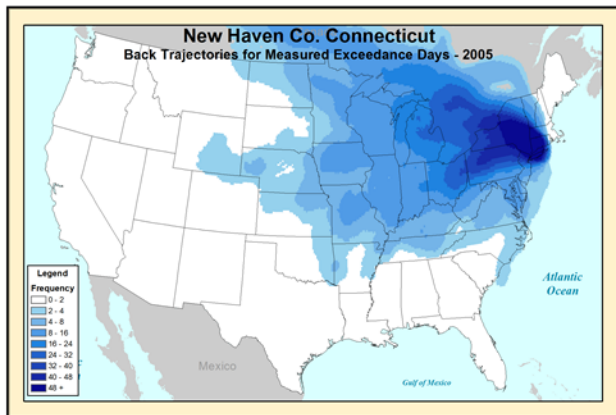
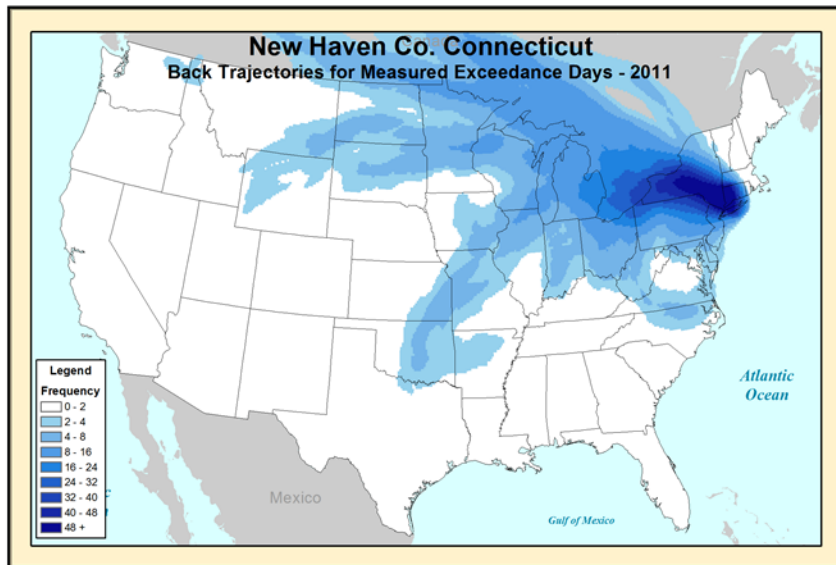
Upwind states linked to Fairfield Co., CT site 090013007: IN, MD, MI, NJ, NY, OH, PA, VA, and WV.



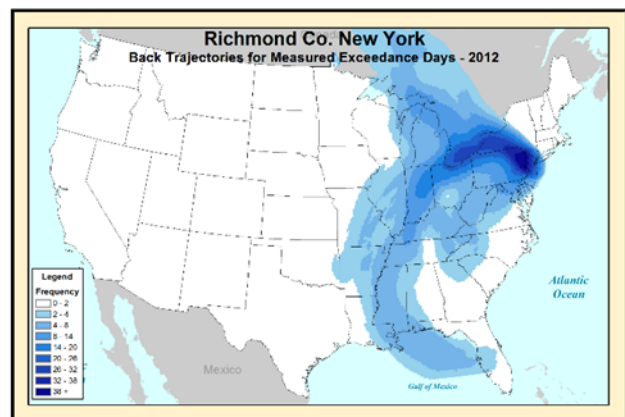
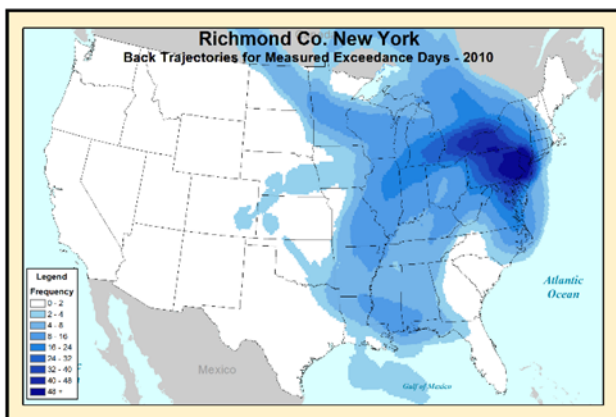
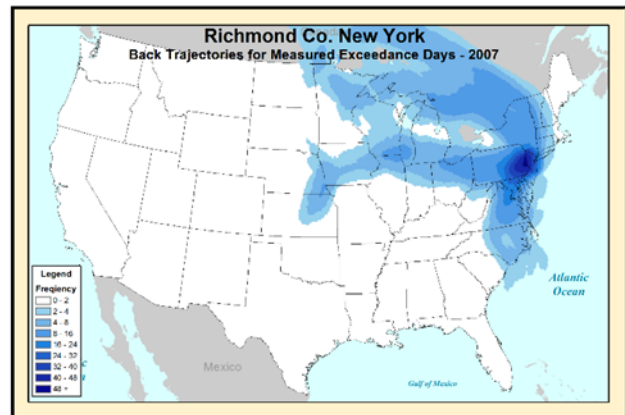
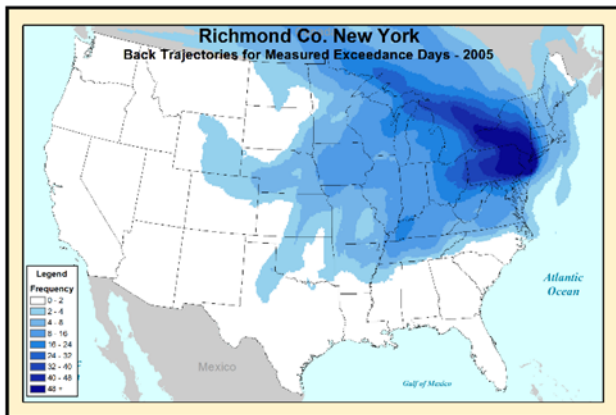
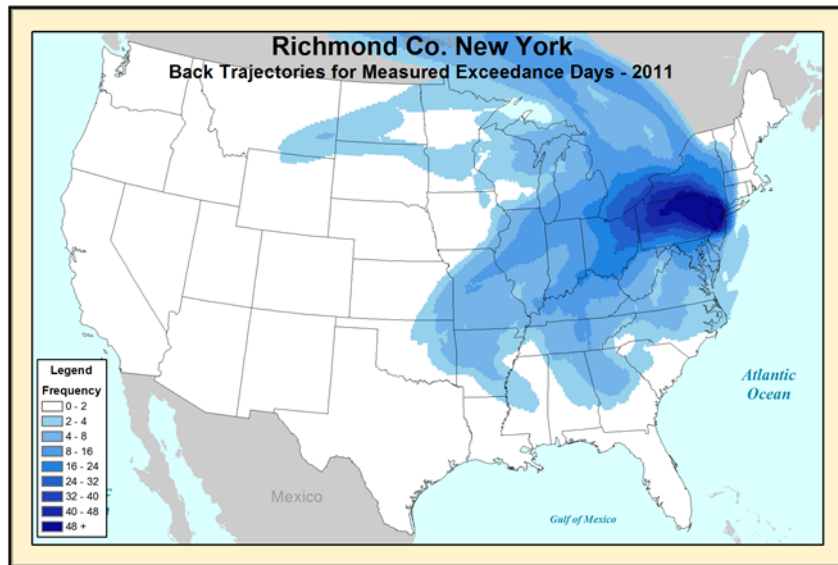
Upwind states linked to Fairfield Co., CT site 090010017: MD, NJ, NY, OH, PA, VA, and WV.



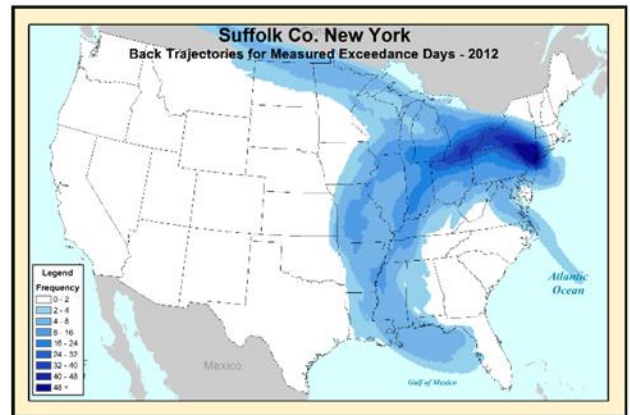
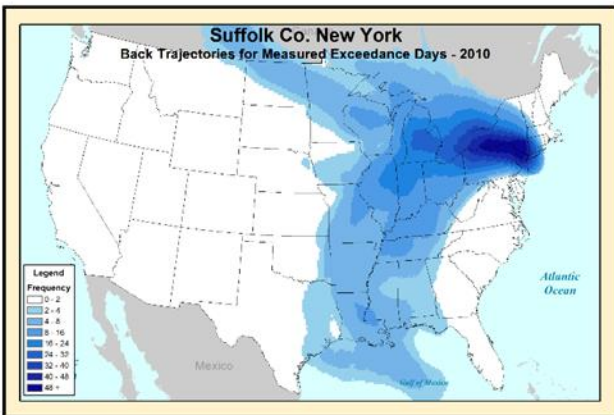
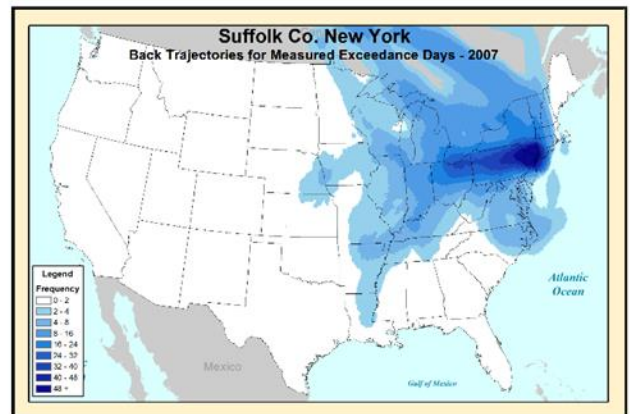
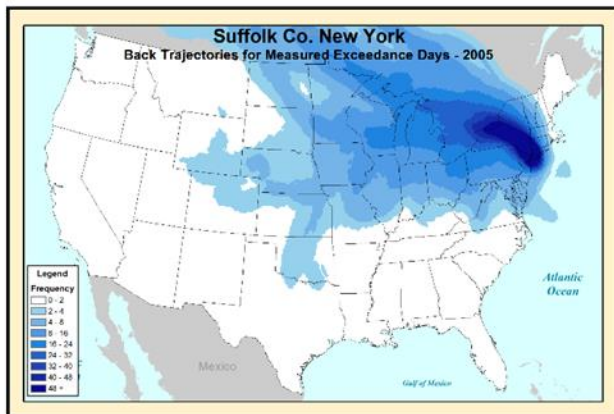
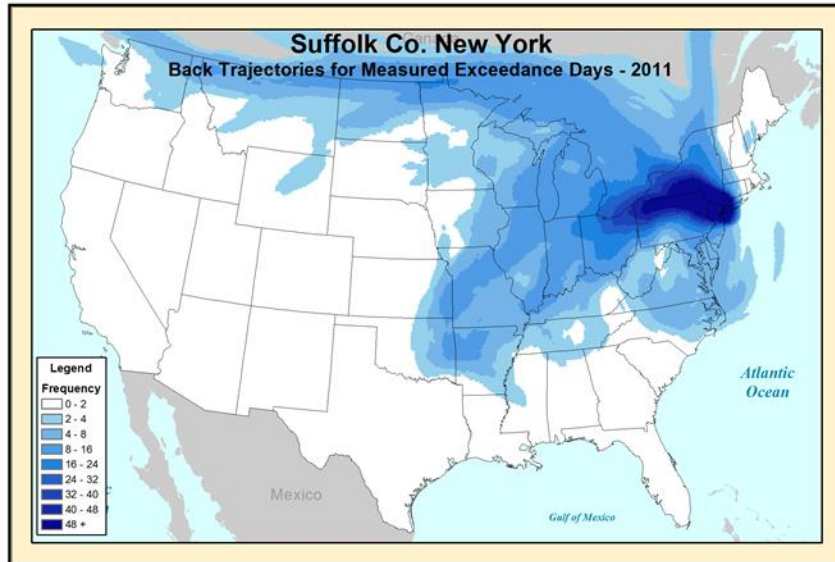
Upwind states linked to New Haven Co., CT site 090099002: MD, NJ, NY, OH, PA, and VA.



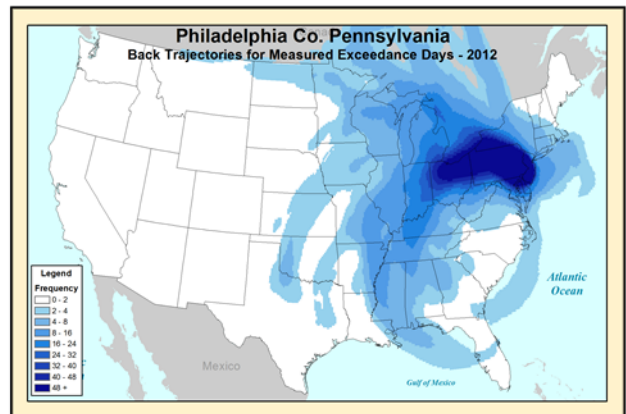
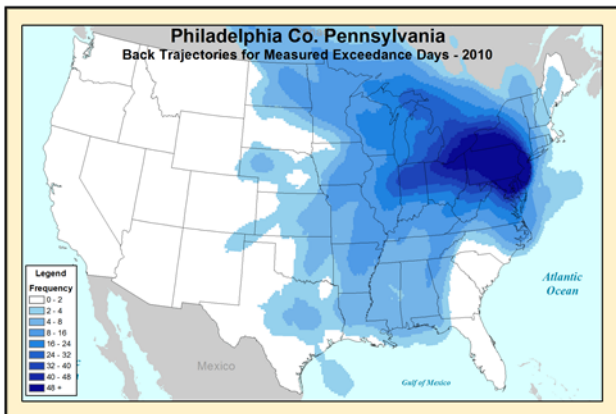
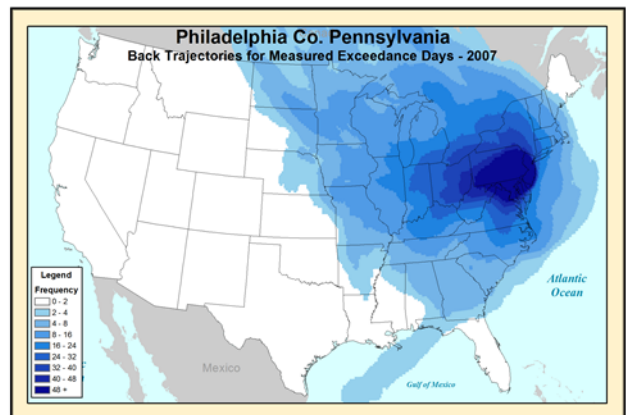
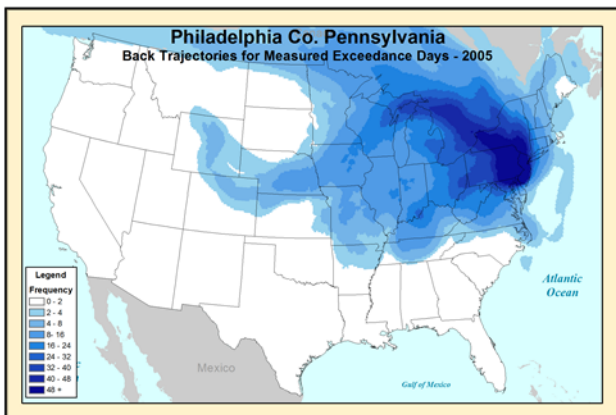
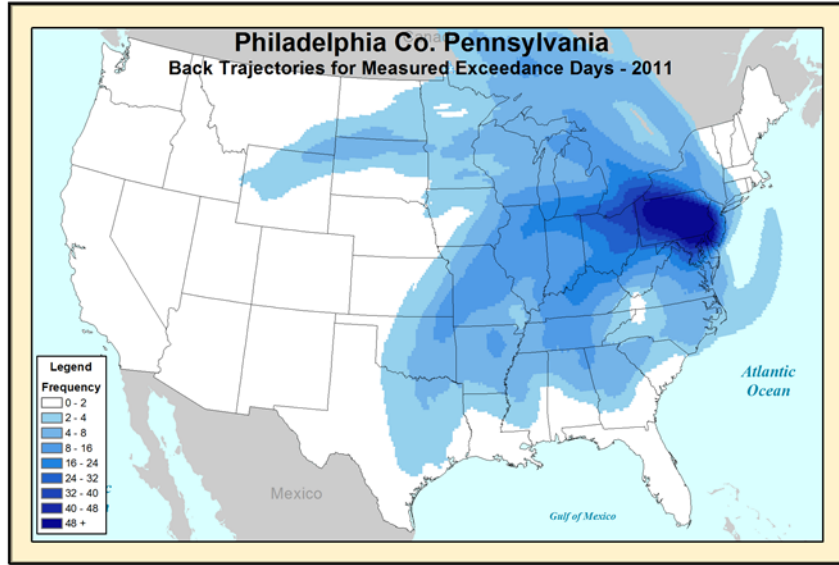
Upwind states linked to Richmond Co., NY site 360850067: IN, KY, MD, NJ, OH, PA, VA, and WV.



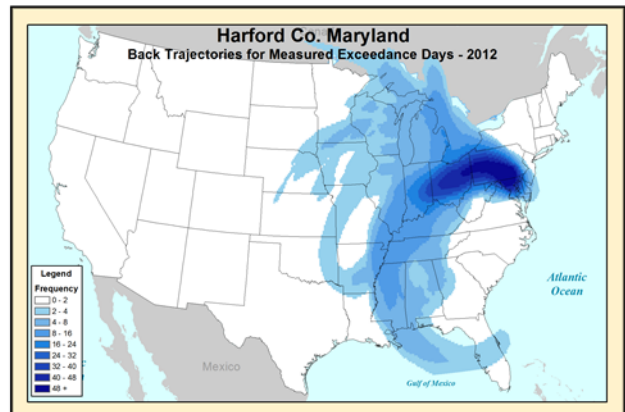
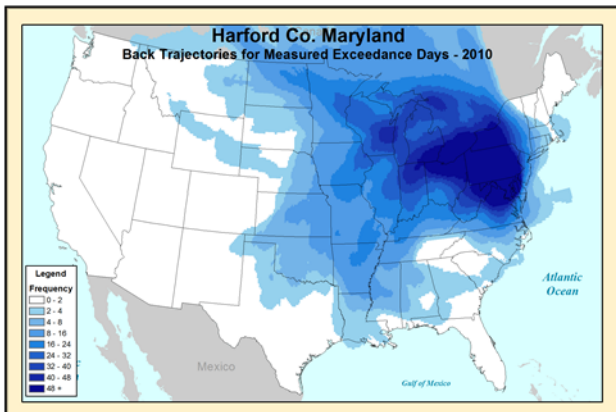
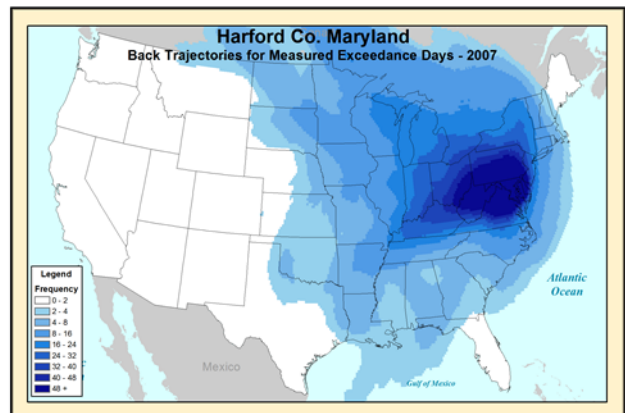
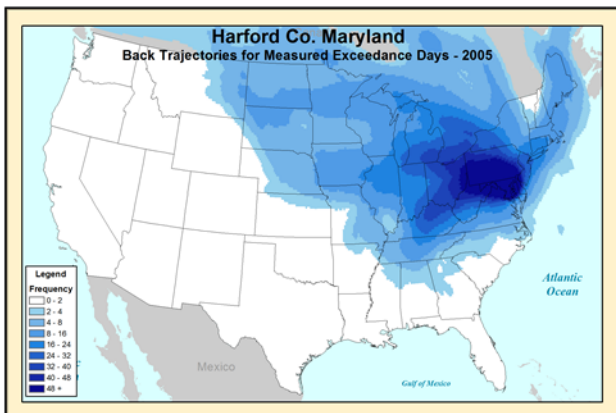
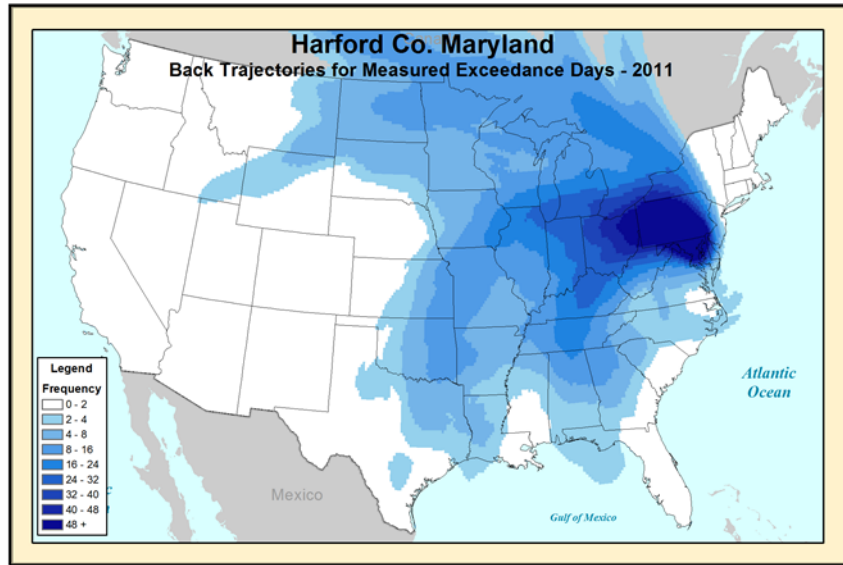
Upwind states linked to Suffolk Co., NY site 36030002: IL, IN, MD, MI, NJ, OH, PA, VA, and WV.



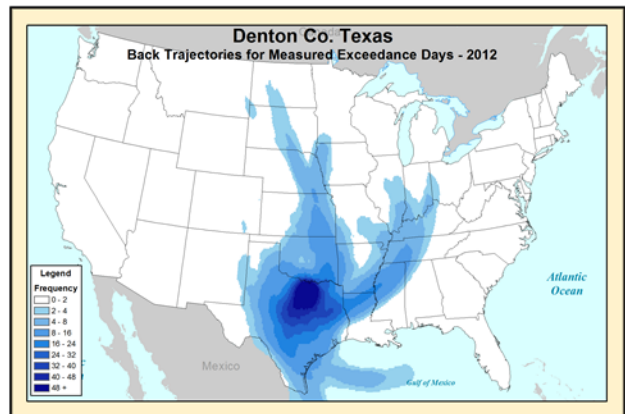
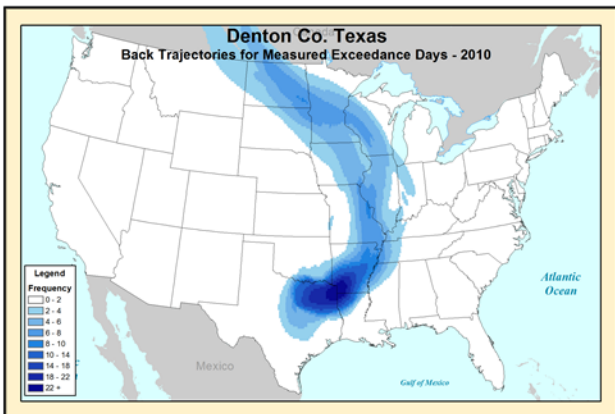
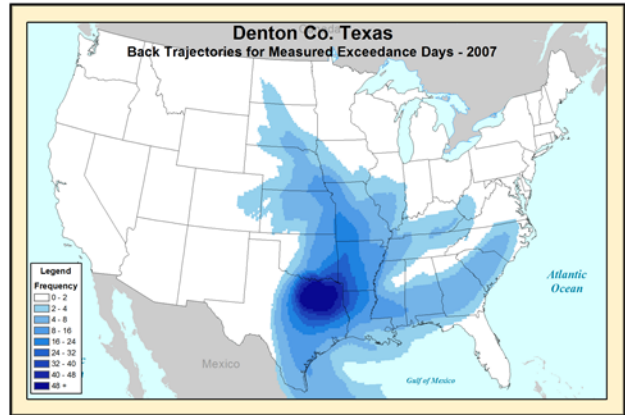
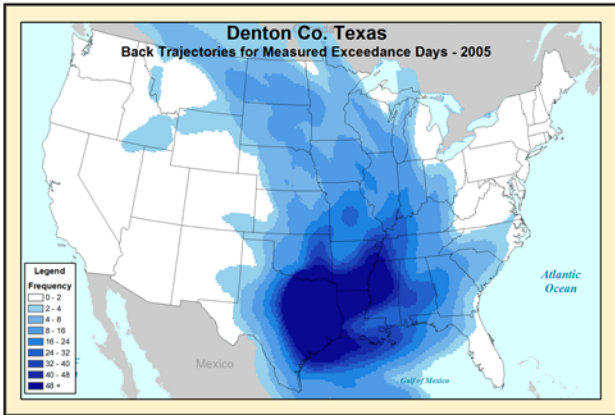
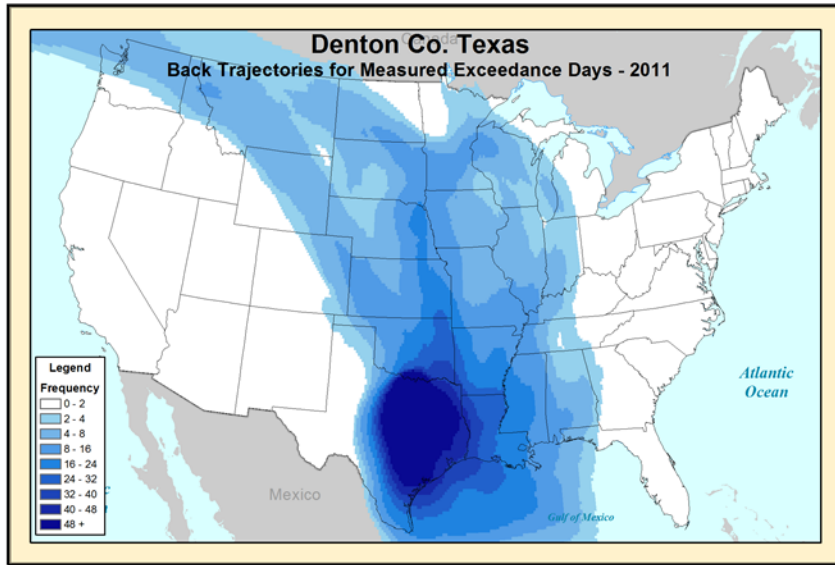
Upwind states linked to Philadelphia Co., PA site 421010024: DE, IL, IN, KY, MD, NJ, OH, TN, TX, VA, and WV.



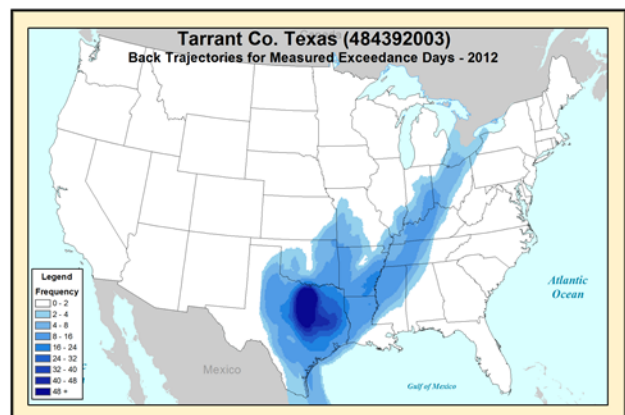
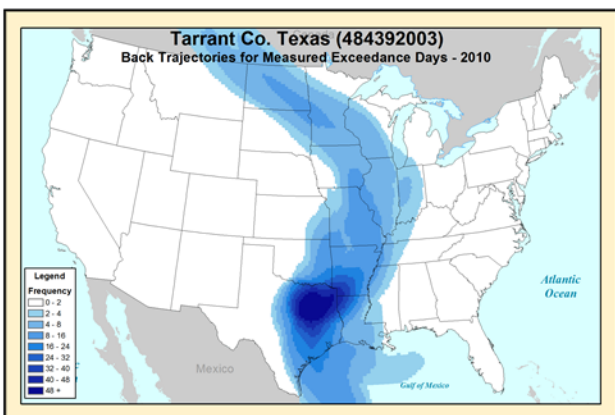
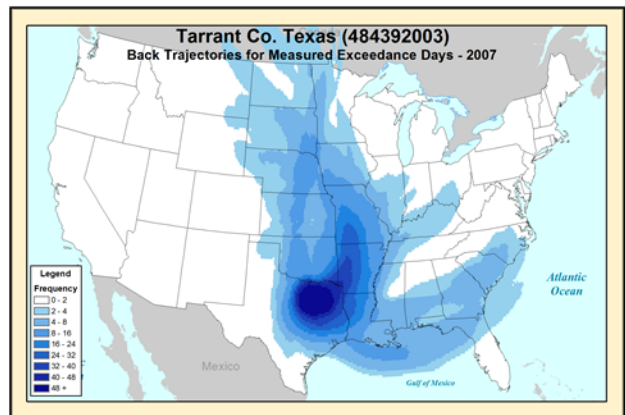
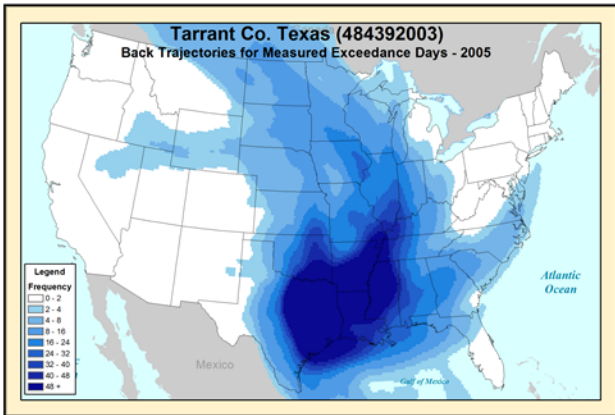
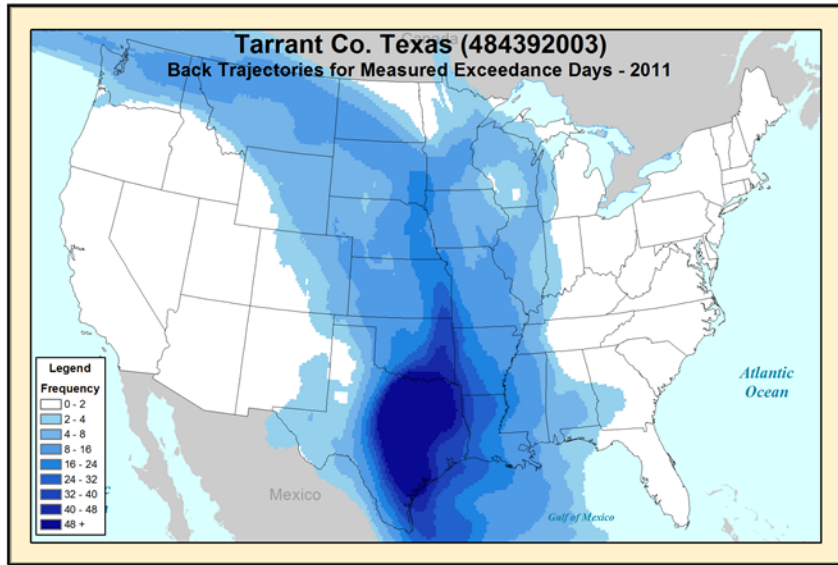
Upwind states linked to Harford Co., MD site 240251001: IL, IN, KY, MI, OH, PA, TX, VA, and WV. Washington, D.C. is also linked to this receptor.



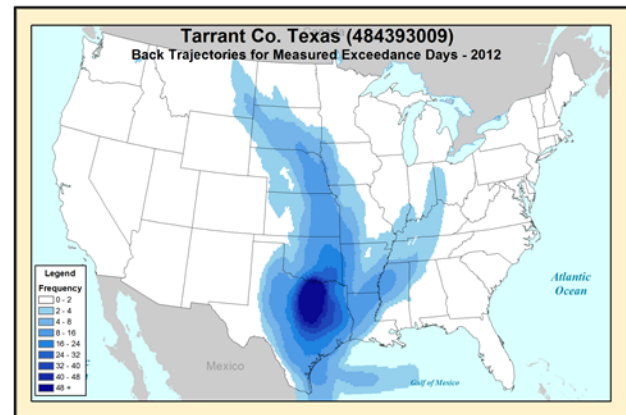
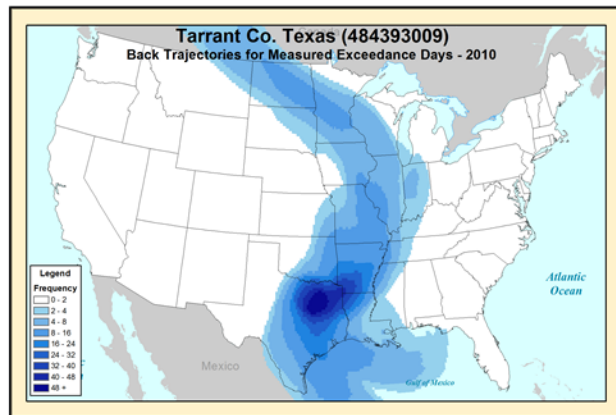
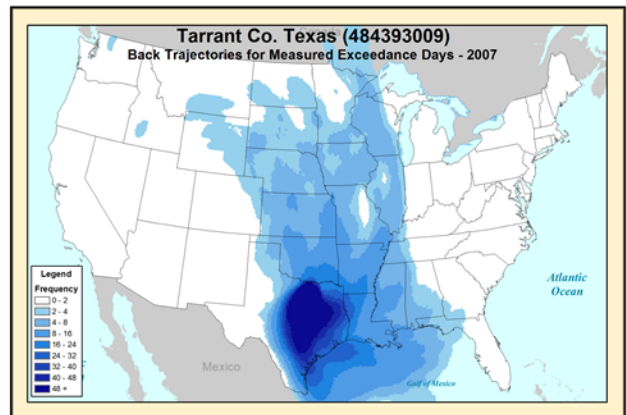
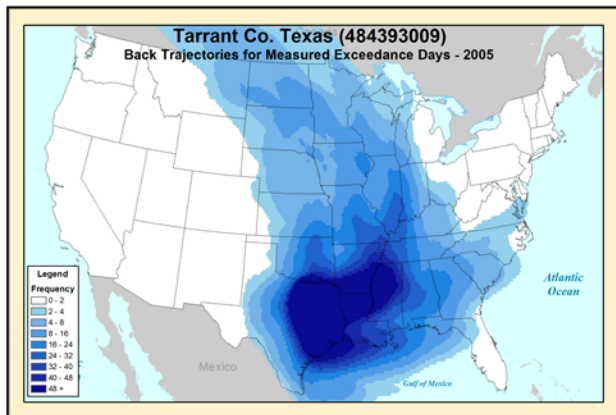
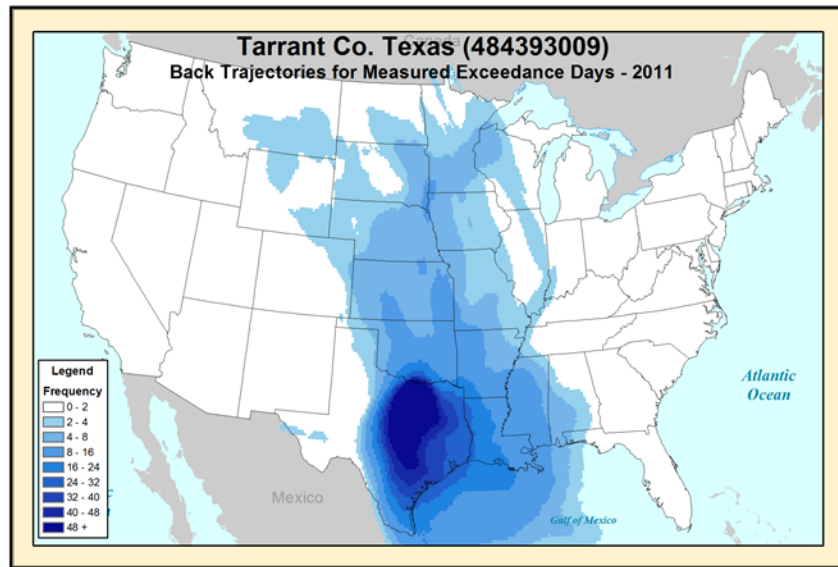
Upwind states linked to Denton Co., TX site 481210034: LA and OK.



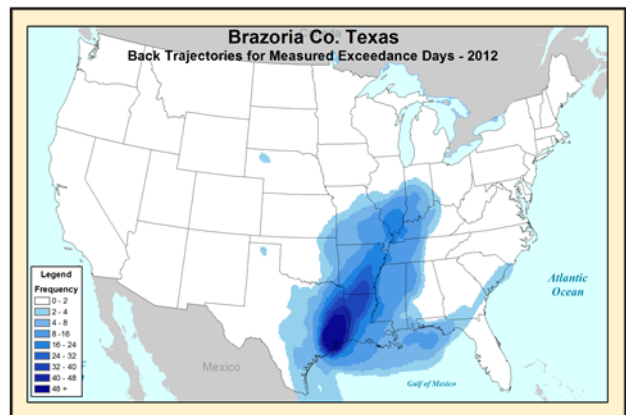
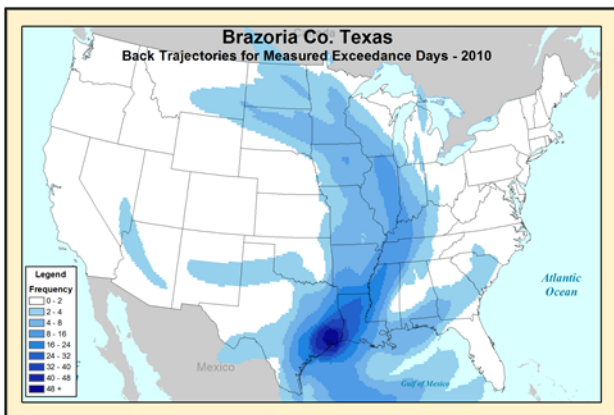
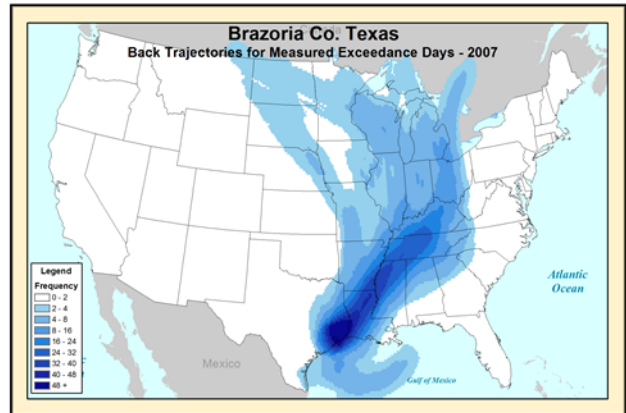
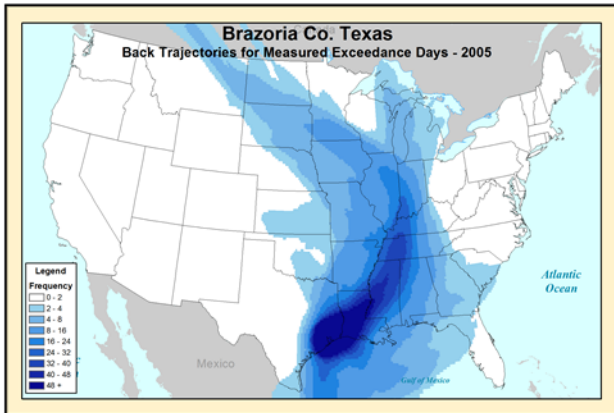
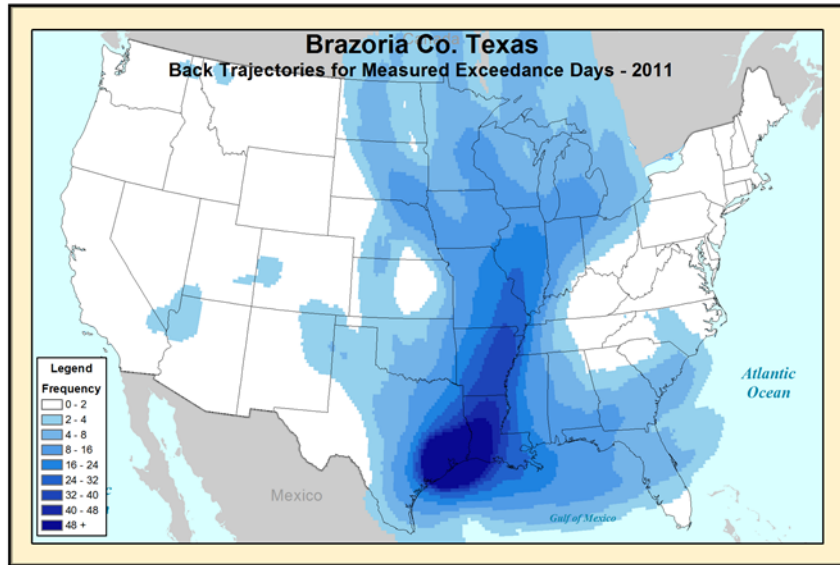
Upwind states linked to Tarrant Co., TX site 484392003: AL, KS, LA, and OK.



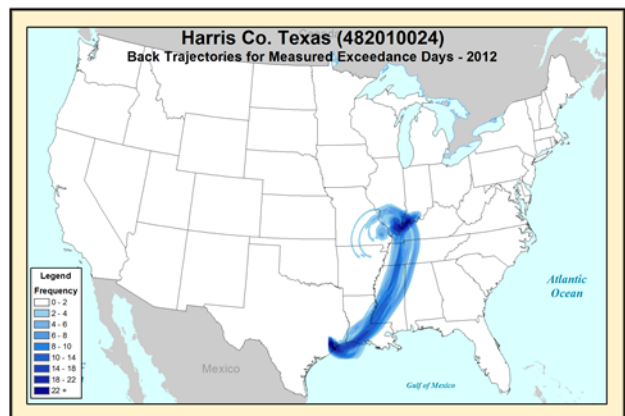
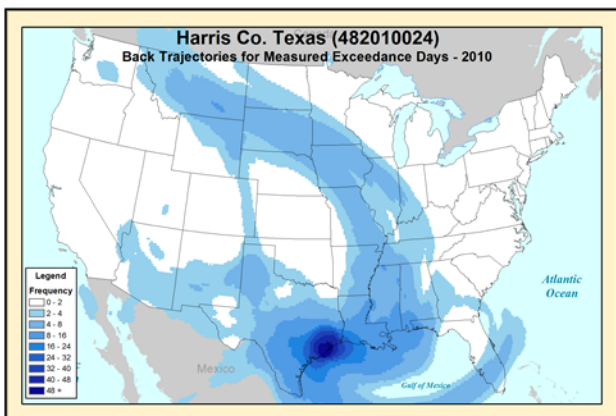
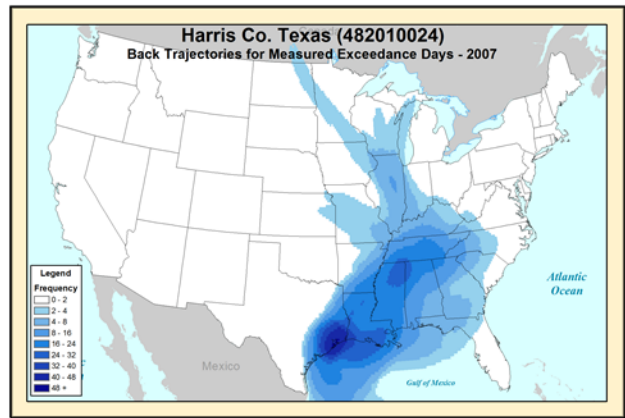
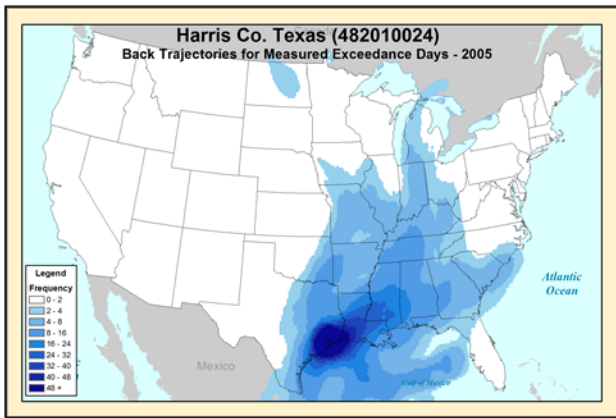
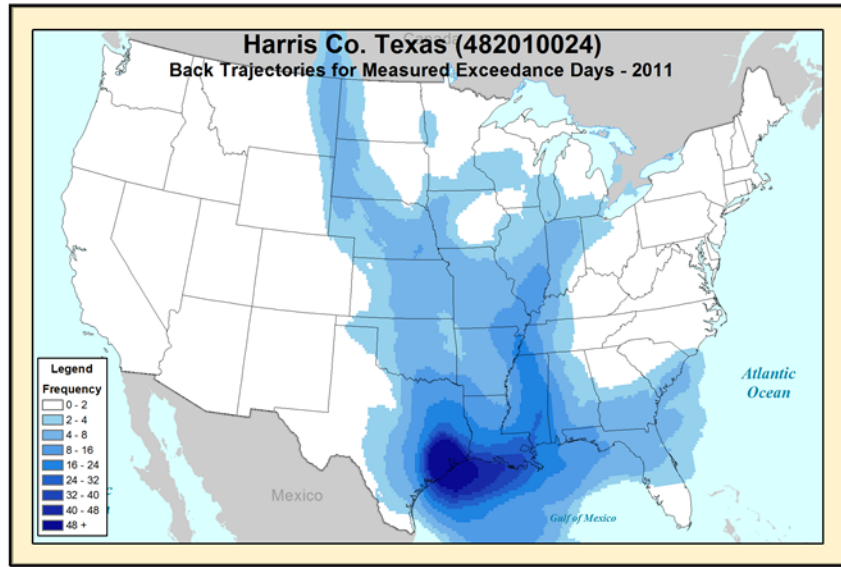
Upwind states linked to Tarrant Co., TX site 484393009: AL, LA, and OK.



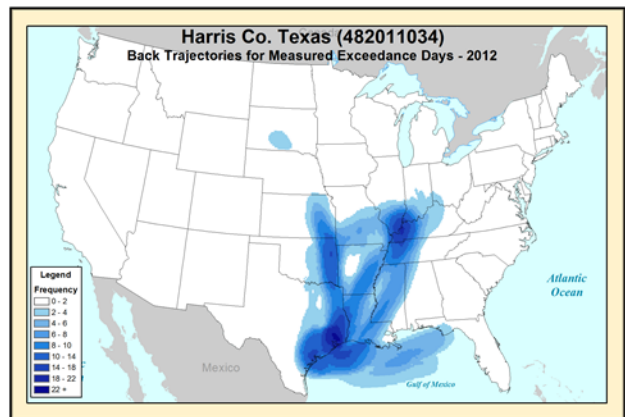
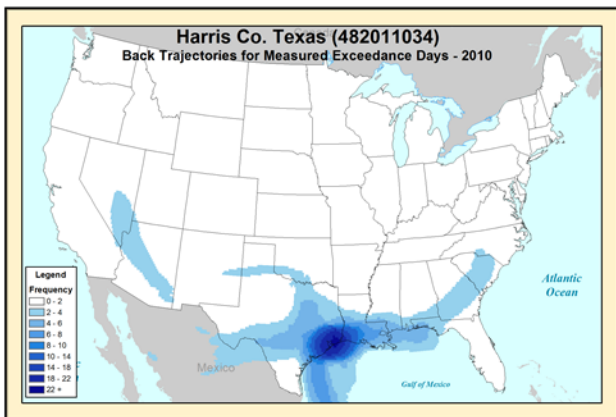
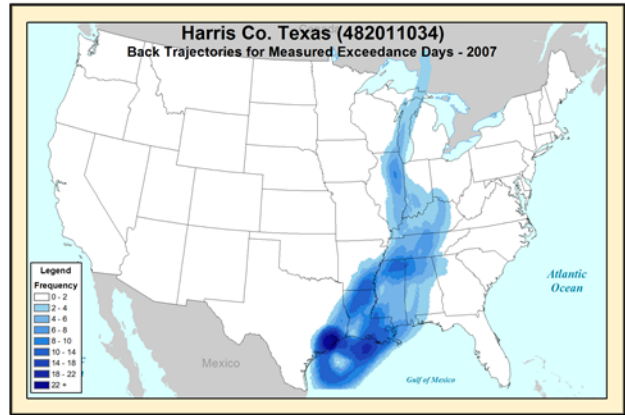
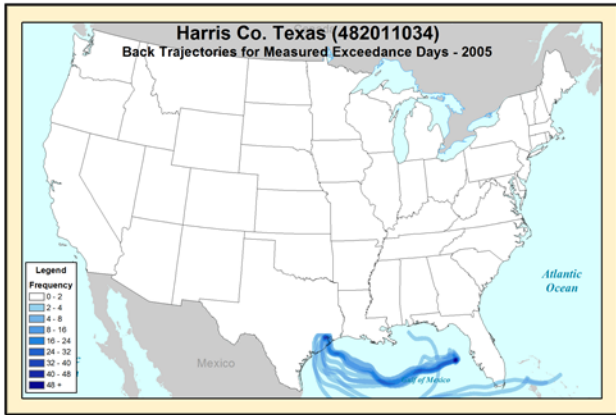
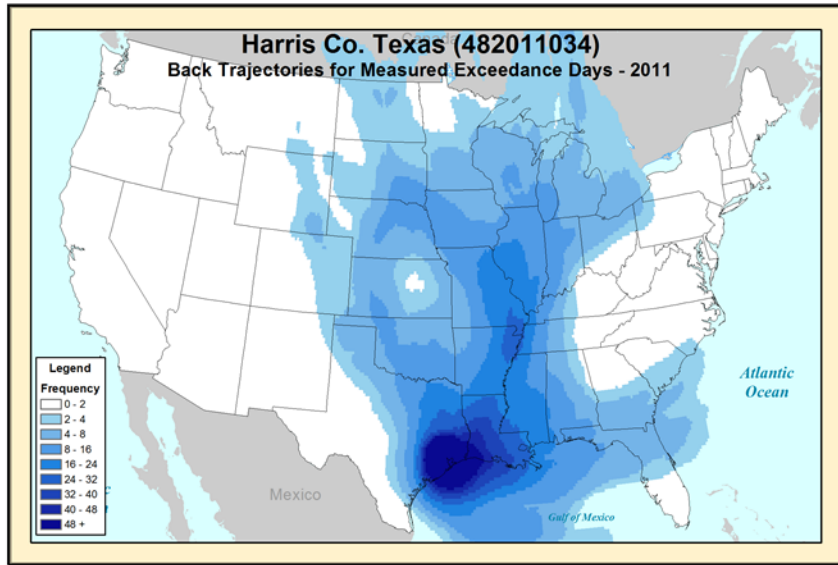
Upwind states linked to Brazoria Co., TX site 480391004: AR, IL, LA, MS, and MO.



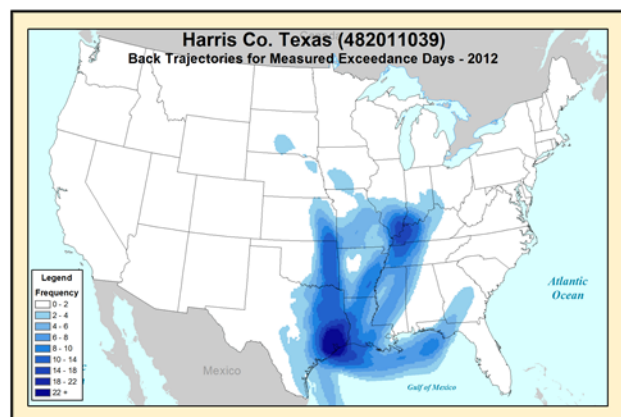
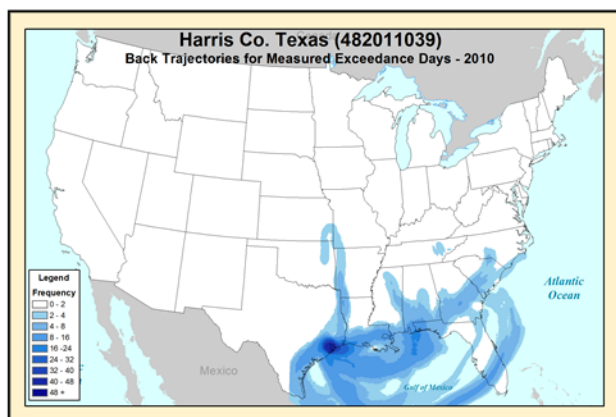
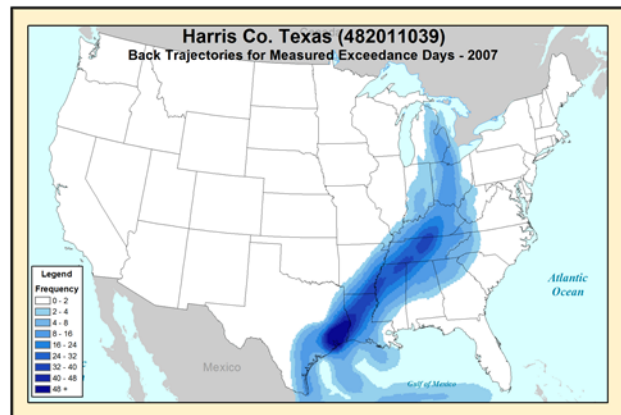
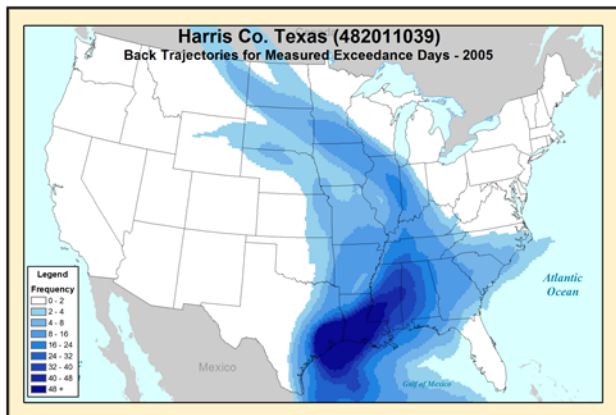
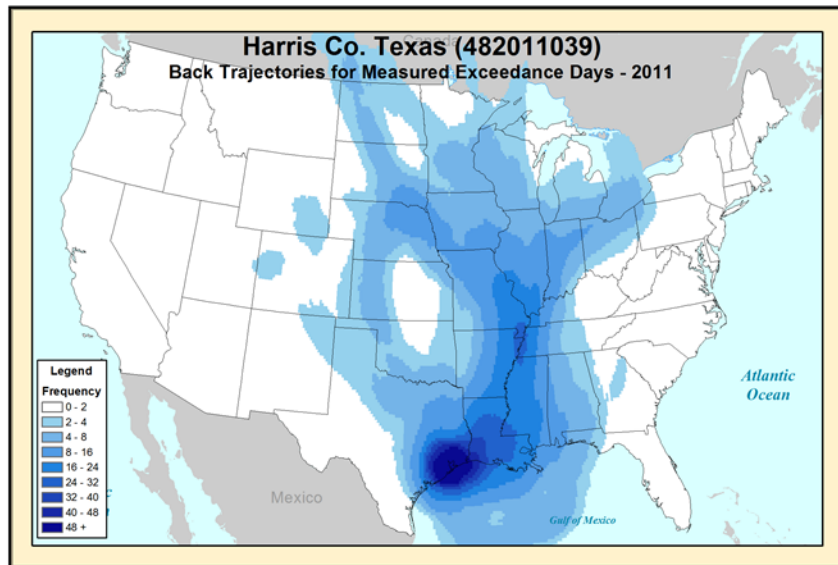
Upwind state linked to Harris Co., TX site 482010024: LA.



Upwind states linked to Harris Co., TX site 482011034: LA, MO, and OK.



Upwind states linked to Harris Co., TX site 482011039: AR, IL, LA, MS, MO, and OK.



Appendix F
Analysis of Contribution Thresholds

This page intentionally left blank

This appendix contains tables with data relevant for the analysis of alternative contribution thresholds, as described in section 5 of the main document.

Table F-1. Data for contribution metrics 1, 2, 3, and 4 for each nonattainment and maintenance receptor.

				Metric 1	Metric 2	Metric 3	Metric 4
Site	County	State	2017 Average Design Value (ppb)	In-State Contribution (ppb)	Total Contribution from All Upwind States (ppb)	Percent of 2017 Design Value from Upwind States	Percent of US Anthropogenic Ozone from Upwind States
90010017	Fairfield	CT	74.1	6.0	47.2	63.7%	88.7%
90013007	Fairfield	CT	75.5	5.1	47.3	62.6%	90.3%
90019003	Fairfield	CT	76.5	3.8	49.9	65.2%	92.9%
90099002	New Haven	CT	76.2	7.5	44.1	57.9%	85.5%
211110067	Jefferson	KY	76.9	23.5	24.2	31.5%	50.7%
240251001	Harford	MD	78.8	26.3	30.2	38.3%	53.5%
260050003	Allegan	MI	74.7	2.8	50.8	68.0%	94.8%
360850067	Richmond	NY	75.8	5.3	45.9	60.6%	89.6%
361030002	Suffolk	NY	76.8	16.8	36.6	47.7%	68.5%
390610006	Hamilton	OH	74.6	16.8	32.5	43.6%	65.9%
421010024	Philadelphia	PA	73.6	20.1	30.7	41.7%	60.4%
480391004	Brazoria	TX	79.9	37.0	13.6	17.0%	26.9%
481210034	Denton	TX	75	32.3	9.3	12.4%	22.4%
482010024	Harris	TX	75.4	30.9	7.4	9.8%	19.3%
482011034	Harris	TX	75.7	29.8	12.6	16.6%	29.7%
482011039	Harris	TX	76.9	32.5	12.5	16.3%	27.8%
484392003	Tarrant	TX	77.3	31.4	12.2	15.8%	28.0%
484393009	Tarrant	TX	76.4	33.6	9.8	12.8%	22.6%
551170006	Sheboygan	WI	76.2	12.4	40.4	53.0%	76.5%

Table F-2. Data for contribution metric 5 for each nonattainment and maintenance receptor.

			Metric 5: Number of States Contributing for the Given Threshold		
Site	County	State	0.5% Threshold (0.375 ppb)	1% Threshold (0.75 ppb)	5% Threshold (3.75 ppb)
90010017	Fairfield	CT	12	7	3
90013007	Fairfield	CT	13	9	3
90019003	Fairfield	CT	13	9	3
90099002	New Haven	CT	13	6	3
211110067	Jefferson	KY	8	4	2
240251001	Harford	MD	14	10	2
260050003	Allegan	MI	13	9	3
360850067	Richmond	NY	16	8	2
361030002	Suffolk	NY	14	9	2
390610006	Hamilton	OH	14	8	2
421010024	Philadelphia	PA	16	11	1
480391004	Brazoria	TX	11	5	0
481210034	Denton	TX	7	2	0
482010024	Harris	TX	3	2	0
482011034	Harris	TX	10	4	0
482011039	Harris	TX	8	6	0
484392003	Tarrant	TX	7	4	0
484393009	Tarrant	TX	7	3	0
551170006	Sheboygan	WI	14	8	2

Table F-3. Data for contribution metric 6 for each nonattainment and maintenance receptor.

			Metric 6: Total Contribution from All Upwind States		
Site	County	State	0.5% Threshold (0.375 ppb)	1% Threshold (0.75 ppb)	5% Threshold (3.75 ppb)
90010017	Fairfield	CT	44.0	41.6	36.0
90013007	Fairfield	CT	43.9	42.0	33.8
90019003	Fairfield	CT	46.4	44.6	36.0
90099002	New Haven	CT	41.1	37.4	33.2
211110067	Jefferson	KY	20.7	18.4	16.1
240251001	Harford	MD	26.5	24.4	9.9
260050003	Allegan	MI	48.8	46.6	35.7
360850067	Richmond	NY	42.1	37.7	26.5
361030002	Suffolk	NY	32.1	29.2	19.9
390610006	Hamilton	OH	29.1	25.5	18.1
421010024	Philadelphia	PA	27.0	24.3	5.2
480391004	Brazoria	TX	9.9	6.7	0.0
481210034	Denton	TX	5.9	3.2	0.0
482010024	Harris	TX	3.5	3.0	0.0
482011034	Harris	TX	9.1	5.8	0.0
482011039	Harris	TX	8.9	8.1	0.0
484392003	Tarrant	TX	7.5	5.9	0.0
484393009	Tarrant	TX	6.1	3.8	0.0
551170006	Sheboygan	WI	38.1	34.5	24.4

Table F-4. Data for contribution metric 7 for each nonattainment and maintenance receptor.

			Metric 7: Percent of Total Transport Captured		
Site	County	State	0.5% Threshold (0.375 ppb)	1% Threshold (0.75 ppb)	5% Threshold (3.75 ppb)
90010017	Fairfield	CT	93.1%	88.0%	76.2%
90013007	Fairfield	CT	92.7%	88.8%	71.3%
90019003	Fairfield	CT	93.0%	89.3%	72.2%
90099002	New Haven	CT	92.9%	84.6%	75.0%
211110067	Jefferson	KY	85.3%	76.0%	66.5%
240251001	Harford	MD	87.6%	80.5%	32.6%
260050003	Allegan	MI	95.9%	91.7%	70.2%
360850067	Richmond	NY	91.7%	82.0%	57.7%
361030002	Suffolk	NY	87.6%	79.6%	54.1%
390610006	Hamilton	OH	89.3%	78.3%	55.7%
421010024	Philadelphia	PA	87.7%	78.8%	17.0%
480391004	Brazoria	TX	72.9%	49.4%	0.0%
481210034	Denton	TX	62.9%	34.1%	0.0%
482010024	Harris	TX	46.0%	39.7%	0.0%
482011034	Harris	TX	72.5%	45.7%	0.0%
482011039	Harris	TX	71.3%	64.4%	0.0%
484392003	Tarrant	TX	61.4%	48.5%	0.0%
484393009	Tarrant	TX	62.2%	38.4%	0.0%
551170006	Sheboygan	WI	94.2%	85.3%	60.3%

Table F-5. Comparison of transport captured by a 0.5 percent threshold versus a 1 percent threshold.

Site	County	State	Percent of the total upwind transport captured by a 0.5 percent threshold that is captured by a 1 percent threshold.
90010017	Fairfield	CT	94.5%
90013007	Fairfield	CT	95.8%
90019003	Fairfield	CT	96.0%
90099002	New Haven	CT	91.1%
211110067	Jefferson	KY	89.1%
240251001	Harford	MD	91.9%
260050003	Allegan	MI	95.6%
360850067	Richmond	NY	89.4%
361030002	Suffolk	NY	90.9%
390610006	Hamilton	OH	87.7%
421010024	Philadelphia	PA	89.9%
480391004	Brazoria	TX	67.8%
481210034	Denton	TX	54.2%
482010024	Harris	TX	86.2%
482011034	Harris	TX	63.0%
482011039	Harris	TX	90.2%
484392003	Tarrant	TX	79.0%
484393009	Tarrant	TX	61.7%
551170006	Sheboygan	WI	90.5%